इंटरनेट मानक

Disclosure to Promote the Right To Information

Whereas the Parliament of India has set out to provide a practical regime of right to information for citizens to secure access to information under the control of public authorities, in order to promote transparency and accountability in the working of every public authority, and whereas the attached publication of the Bureau of Indian Standards is of particular interest to the public, particularly disadvantaged communities and those engaged in the pursuit of education and knowledge, the attached public safety standard is made available to promote the timely dissemination of this information in an accurate manner to the public.

"जानने का अधिकार, जीने का अधिकार"
Mazdoor Kisan Shakti Sangathan
"The Right to Information, The Right to Live"

"पुराने को छोड नये के तरफ"
Jawaharlal Nehru
"Step Out From the Old to the New"

IS/IEC 62209-1 (2005): Human Exposure to Radio Frequency Fields from Hand-held and Body-mounted Wireless Communication Devices Human Models, Instrumentation and Procedures, Part 1: SAR for Hand-held Devices used in Close Proximity to the Ear (300 MHz to 3GHz) [LITD 9: Electromagnetic Compatibility]

"ज्ञान से एक नये भारत का निर्माण"
Satyanarayan Gangaram Pitroda
"Invent a New India Using Knowledge"

Act Number 22 of 2005
The Indian Parliament
RIGHT TO INFORMATION

Made Available By
Public.Resource.Org

"ज्ञान एक ऐसा खजाना है जो कभी चुराया नहीं जा सकता है"
Bhartṛhari—Nītiśatakam
"Knowledge is such a treasure which cannot be stolen"

BLANK PAGE

BRUTUM FULMEN

IGNORANTIA JURIS NON EXCUSAT

PROTECTED BY COPYRIGHT

IS/IEC 62209-1 : 2005

भारतीय मानक

हस्त–स्थित व इंसानी शरीर आरोपित बेतार संचार युक्तियों से रेडियो आवृति के विकिरण का इंसान पर अनावरण — इंसानी मॉडल, मापयंत्रण, व प्रक्रियाऐं

भाग 1 कान के करीब इस्तेमाल होने वाली हस्त–स्थित युक्तियों के लिए (आवृति श्रंखला 300 मेगा हट्र्ज़ से 3 गीगा हट्र्ज़) विशिष्ट अनवेषण दर (एस ए आर) को निर्धारित करने की प्रक्रिया

Indian Standard

HUMAN EXPOSURE TO RADIO FREQUENCY FIELDS FROM HAND-HELD AND BODY-MOUNTED WIRELESS COMMUNICATION DEVICES — HUMAN MODELS, INSTRUMENTATION, AND PROCEDURES

PART 1 PROCEDURE TO DETERMINE THE SPECIFIC ABSORPTION RATE (SAR) FOR HAND-HELD DEVICES USED IN CLOSE PROXIMITY TO THE EAR (FREQUENCY RANGE OF 300 MHz TO 3 GHz)

ICS 33.050.10

© BIS 2012

BUREAU OF INDIAN STANDARDS
MANAK BHAVAN, 9 BAHADUR SHAH ZAFAR MARG
NEW DELHI 110002

March 2012 **Price Group 19**

CONTENTS

1 Scope 1
2 Normative references 1
3 Terms and definitions 1
4 Symbols and abbreviated terms 9
  4.1 Physical quantities 9
  4.2 Constants 10
  4.3 Abbreviations 10
5 Measurement system specifications 10
  5.1 General requirements 10
  5.2 Phantom specifications (shell and liquid) 11
  5.3 Specifications of the SAR measurement equipment 16
  5.4 Scanning system specifications 16
  5.5 Device holder specifications 16
  5.6 Measurement of liquid dielectric properties 17
6 Protocol for SAR assessment 17
  6.1 Measurement preparation 17
  6.2 Tests to be performed 23
  6.3 Measurement procedure 25
  6.4 Post-processing of SAR measurement data 26
7 Uncertainty estimation 27
  7.1 General considerations 27
  7.2 Components contributing to uncertainty 28
  7.3 Uncertainty estimation 40
8 Measurement report 42
  8.1 General 42
  8.2 Items to be recorded in the test report 42

Annex A (normative) Phantom specifications 44
Annex B (normative) Calibration (linearity, isotropy, sensitivity) of the measurement instrumentation and uncertainty estimation 50
Annex C (normative) Post-processing techniques and uncertainty estimation 65
Annex D (normative) SAR measurement system validation 70
Annex E (informative) Interlaboratory comparisons 77
Annex F (informative) Definition of a phantom coordinate system and a device under test coordinate system 79
Annex G (informative) Validation dipoles 81
Annex H (informative) Flat phantom 83
Annex I (informative) Recommended recipes for phantom head tissue-equivalent liquids 85
Annex J (informative) Measurement of the dielectric properties of liquids and uncertainty estimation 87

Bibliography 97

Figure 1 – Picture of the phantom showing ear reference points RE and LE, mouth reference point M, reference line N-F, and central strip 12
Figure 2 – Sagittally bisected phantom with extended perimeter (shown placed on its side as used for device SAR tests) 12
Figure 3 – Cross-sectional view of SAM at the reference plane containing B-M 14
Figure 4 – Side view of the phantom showing relevant markings 15
Figure 5 – Handset vertical and horizontal reference lines and reference points A, B on two example device types 20
Figure 6 – Cheek position of the wireless device on the left side of SAM 21
Figure 7 – Tilt position of the wireless device on the left side of SAM 22
Figure 8 – Block diagram of the tests to be performed 24
Figure 9 – Orientation of the probe with respect to the line normal to the surface, shown at two different locations 26
Figure 10 – Orientation and surface of the averaging volume relative to the phantom surface . 40
Figure A.1 – Illustration of dimensions in Table A.1 45
Figure A.2 –Close up side view of phantom showing the ear region......47
Figure A.3 – Side view of the phantom showing relevant markings 48
Figure B.1 – Experimental set-up for assessment of the sensitivity (conversion factor) using a vertically-oriented rectangular waveguide 54
Figure B.2 – Description of the antenna gain evaluation set-up 56
Figure B.3 – Set-up to assess spherical isotropy deviation in tissue-equivalent liquid 59
Figure B.4 – Alternative set-up to assess spherical isotropy deviation in tissue-equivalent liquid......60
Figure B.5 – Experimental set-up for the hemispherical isotropy assessment [11] 61
Figure B.6 – Conventions for dipole position (ξ) and polarization (θ) [11]......61
Figure B.7 – Measurement of axial isotropy with a reference antenna 63
Figure B.8 – Measurement of hemispherical isotropy with reference antenna 63
Figure C.1 – Methods of three points......66
Figure C.2 – Method of the tangential face 66
Figure C.3 – Method of averaging 67
Figure C.4 – Extrude method of averaging......67
Figure C.5 – Extrapolation of SAR data to the inner surface of the phantom based on a least-square polynomial fit of the measured data (squares)......69
Figure D.1 – Set-up for the *system check* 72
Figure F.1 – Example reference coordinate system for the SAM phantom 79
Figure F.2 – Example coordinate system on the device under test 80
Figure G.1 – Mechanical details of the reference dipole......82
Figure H.1 – Dimensions of the flat phantom set-up used for deriving the minimal dimensions for W and *L* 83
Figure H.2 – FDTD predicted uncertainty in the 10 g peak spatial-average SAR as a function of the dimensions of the flat phantom compared with an infinite flat phantom 84
Figure J.1 – Slotted line set-up......88
Figure J.2 – An open-ended coaxial probe with inner and outer radii *a* and *b*, respectively 90
Figure J.3 – TEM line dielectric test set-up [60] 92

Table 1 – Dielectric properties of the tissue-equivalent liquid 15

Table 2 – Reference SAR values in watts per kilogram used for estimating post-processing uncertainties 37

Table 3 – Measurement uncertainty evaluation template for handset SAR test 41

Table A.1 – Head dimensions relevant to phantom shape: SAM dimensions compared to 90th-percentile large male head from Gordon report [18] 46

Table A.2 – Specific guidelines for the design of SAM phantom and CAD file 47

Table B.1 – Uncertainty analysis for transfer calibration using temperature probes 53

Table B.2 – Uncertainty template for calibration using analytical field distribution inside waveguide 55

Table B.3 – Uncertainty template for evaluation of reference antenna gain 57

Table B.4 – Uncertainty template for calibration using reference antenna 58

Table D.1 – Numerical reference SAR values for reference dipole and flat phantom 76

Table G.1 – Mechanical dimensions of the reference dipoles 81

Table H.1 – Parameters used for calculation of reference SAR values in Table D.1 84

Table I.1 – Suggested recipes for achieving target dielectric parameters 86

Table J.1 – Parameters for calculating the dielectric properties of various reference liquids 94

Table J.2 – Dielectric properties of reference liquids at 20 °C 95

Table J.3 – Example uncertainty template and example numerical values for dielectric constant (ε_r') and conductivity (σ) measurement 96

Electromagnetic Compatibility Sectional Committee, LITD 9

NATIONAL FOREWORD

This Indian Standard (Part 1) which is identical with IEC 62209-1 : 2005 'Human exposure to radio frequency fields from hand-held and body-mounted wireless communication devices — Human models, instrumentation, and procedures — Part 1: Procedure to determine the specific absorption rate (SAR) for hand-held devices used in close proximity to the ear (frequency range of 300 MHz to 3 GHz)' issued by the International Electrotechnical Commission (IEC) was adopted by the Bureau of Indian Standards on the recommendation of the Electromagnetic Compatibility Sectional Committee and approval of the Electronics and Information Technology Division Council.

The text of IEC Standard has been approved as suitable for publication as an Indian Standard without deviations. Certain conventions are, however, not identical to those used in Indian Standards. Attention is particularly drawn to the following:

a) Wherever the words 'International Standard' appear referring to this standard, they should be read as 'Indian Standard'.

b) Comma (,) has been used as a decimal marker while in Indian Standards, the current practice is to use a point (.) as the decimal marker.

The technical committee has reviewed the provisions of the following International Standards referred in this adopted standard and has decided that they are acceptable for use in conjunction with this standard:

International Standard	*Title*
ISO/IEC Guide : 1995	Guide to the expression of uncertainty in measurement
ISO/IEC 17025 : 1999	General requirements for the competence of testing and calibration laboratories

Only the English language text of IEC Standard has been retained while adopting it in this Indian Standard and as such the page numbers given here are not the same as in the IEC Standard.

For the purpose of deciding whether a particular requirement of this standard is complied with, the final value, observed or calculated, expressing the result of a test or analysis, shall be rounded off in accordance with IS 2 : 1960 'Rules for rounding off numerical values (*revised*)'. The number of significant places retained in the rounded off value should be the same as that of the specified value in this standard.

INTRODUCTION

The international committees IEC TC 106, CENELEC Technical Committee TC 106x WG1, and IEEE Standards Coordinating Committee 34 (SCC34) worked together informally through common membership to achieve the goal of harmonization, specifically between IEC TC 106 Project Team 62209 for the document "Procedure to Measure the Specific Absorption Rate (SAR) for Hand-Held Mobile Telephones in the Frequency Range of 300 MHz to 3 GHz" and IEEE SCC34 for the IEEE Std 1528 "IEEE Recommended Practice for Determining the Peak Spatial-Average Specific Absorption Rate (SAR) in the Human Head from Wireless Communications Devices: Measurement Techniques" [22]1.

During the process a primary effort involved was to harmonize these two standards

---

1) Numbers in square brackets refer to the bibliography.

Indian Standard

HUMAN EXPOSURE TO RADIO FREQUENCY FIELDS FROM HAND-HELD AND BODY-MOUNTED WIRELESS COMMUNICATION DEVICES — HUMAN MODELS, INSTRUMENTATION, AND PROCEDURES

PART 1 PROCEDURE TO DETERMINE THE SPECIFIC ABSORPTION RATE (SAR) FOR HAND-HELD DEVICES USED IN CLOSE PROXIMITY TO THE EAR (FREQUENCY RANGE OF 300 MHz TO 3 GHz)

1 Scope

This International Standard applies to any electromagnetic field (EMF) transmitting device intended to be used with the radiating part of the device in close proximity to the human head and held against the ear, including mobile phones, cordless phones, etc. The frequency range is 300 MHz to 3 GHz.

The objective of this standard is to specify the measurement method for demonstration of compliance with the specific absorption rate (SAR) limits for such devices.

2 Normative references

The following referenced documents are indispensable for the application of this document. For dated references, only the edition cited applies. For undated references, the latest edition of the referenced document (including any amendments) applies.

ISO/IEC Guide:1995, *Guide to the Expression of Uncertainty in Measurement*

ISO/IEC 17025:1999, *General requirements for the competence of testing and calibration laboratories*

3 Terms and definitions

For the purposes of this document, the following terms and definitions apply.

3.1
attenuation coefficient
numerical factor intended to account for attenuation due to the human head or body tissue between the source and a specified point

3.2
average (temporal) absorbed power
value of the time-averaged rate of energy transfer given by

$$\overline{P}_{\mathrm{avg}} = \frac{1}{t_2 - t_1} \int_{t_1}^{t_2} P(t)\,\mathrm{d}t$$

where

t_1 is the start time of the exposure in seconds;

t_2 is the stop time of the exposure in seconds;

$t_2 - t_1$ is the exposure duration in seconds;

$P(t)$ is the instantaneous absorbed power in watts;

$\overline{P}_{\text{avg}}$ is the average power in watts.

3.3
axial isotropy

the maximum deviation of the SAR when rotating around the major axis of the probe cover/case while the probe is exposed to a reference wave impinging from a direction along the probe major axis

3.4
basic restriction

restrictions on human exposure to time-varying electric, magnetic, and electromagnetic fields that are based directly on established health effects

NOTE Within the frequency range of this standard, the physical quantity used as a basic restriction is the specific absorption rate (SAR).

3.5
boundary effect (probe)

a change in the sensitivity of an electric-field probe when the probe is located close to (less than one probe-tip diameter) media boundaries

3.6
complex permittivity

the ratio of the electric flux density in a medium to the electric field strength at a point. The permittivity of biological tissues is frequency dependent.

$$\varepsilon = \frac{|\vec{D}|}{|\vec{E}|} = \varepsilon_{\text{r}}\varepsilon_0$$

where

$\vec{D}$ is the electric flux density in coulombs per square metre;

$\vec{E}$ is electric field in volts per metre;

ε_0 is the permittivity of free space = 8,854 × 10^{-12} farads per metre;

ε_{r} is the complex relative permittivity: $\varepsilon_{\text{r}} = \varepsilon_{\text{r}}' - j\varepsilon_{\text{r}}'' = \varepsilon_{\text{r}}' + \dfrac{\sigma}{j\omega\varepsilon_0}$.

NOTE For an isotropic medium, the permittivity is a scalar quantity; for an anisotropic medium, it is a tensor quantity.

3.7
conducted output power

the average power supplied by a transmitter to the transmission line of an antenna during an interval of time sufficiently long compared with the period of the lowest frequency encountered in the modulation evaluated under normal operating conditions

3.8
conductivity
the ratio of the conduction-current density in a medium to the electric field strength

$$\sigma = \frac{|\vec{J}|}{|\vec{E}|}$$

where

$\vec{E}$ is the electric field in volts per metre;

$\vec{J}$ is the current density in amperes per metre squared;

σ is the conductivity of the medium in siemens per metre.

NOTE For an isotropic medium the conductivity is a scalar quantity; for an anisotropic medium it is a tensor quantity in which case the cross product of σ and $\vec{E}$ is implied.

3.9
detection limits
the lower (respectively upper) detection limit defined by the minimum (respectively maximum) quantifiable response of the measuring equipment

3.10
duty factor
the ratio of the pulse duration to the pulse period of a periodic pulse train

3.11
electric conductivity
See conductivity.

3.12
electric field
a vector field quantity $\vec{E}$ which exerts on any charged particle at rest a force $\vec{F}$ equal to the product of $\vec{E}$ and the electric charge q of the particle:

$$\vec{F} = q\vec{E}$$

where

$\vec{F}$ is the vector force acting on the particle in newtons;

q is the charge on the particle in coulombs;

$\vec{E}$ is the electric field in volts per metre.

3.13
electric flux density (displacement)
a vector quantity obtained at a given point by adding the electric polarization $\vec{P}$ to the product of the electric field $\vec{E}$ and the dielectric constant ε_0:

$$\vec{D} = \varepsilon_0\vec{E} + \vec{P}$$

where

$\vec{D}$ is the electric flux density in coulombs per square metre;

ε_0 is the permittivity of free space = 8,854 $\times$ 10^{-12} farads per metre;

$\vec{E}$ is the electric field in volts per metre;

$\vec{P}$ is the electric polarization of the medium in coulombs per square metre.

NOTE For purposes of this standard, the electric flux density at all points is equal to the product of the electric field and the dielectric constant:

$$\vec{D} = \varepsilon_r' \vec{E}$$

3.14
handset
a hand-held device intended to be operated close to the side of the head, consisting of an acoustic output or earphone and a microphone, and containing a radio transmitter and receiver

3.15
hemispherical isotropy
the maximum deviation of the SAR when rotating the probe around its major axis with the probe exposed to a reference wave, having varying incidence angles relative to the axis of the probe, incident from the half space in front of the probe

3.16
isotropy
See axial isotropy, hemispherical isotropy, probe isotropy.

3.17
linearity error
the maximum deviation of a measured quantity over the measurement range from the closest reference line defined over a given interval

3.18
loss tangent
the ratio of the imaginary and real parts of the complex relative permittivity of a material:

$$\tan\delta = \frac{\varepsilon_r''}{\varepsilon_r'} = \frac{\sigma}{\omega\varepsilon_r'\varepsilon_0}$$

where

$\tan\delta$ is the loss tangent (dimensionless);

ε_r'' is the imaginary part of the complex relative permittivity;

ε_r' is the real part of the complex relative permittivity;

ε_0 is the permittivity of free space = $8{,}854 \times 10^{-12}$ farads per metre;

ω is the angular frequency ($\omega = 2\pi f$) in radians per second;

σ is the conductivity of the medium in siemens per metre.

3.19
magnetic field
a vector quantity obtained at a given point by subtracting the magnetization $\vec{M}$ from the magnetic flux density $\vec{B}$ divided by the magnetic constant (permeability) μ:

$$\vec{H} = \frac{\vec{B}}{\mu} - \vec{M}$$

where

$\vec{H}$ is the magnetic field in amperes per metre;

$\vec{B}$ is the magnetic flux density in teslas;

μ is the magnetic constant (permeability) of the vacuum in henries per metre;

$\vec{M}$ is the magnetization in amperes per metre.

NOTE For the purposes of this standard, $\vec{M} = 0$ at all points.

3.20
magnetic flux density

a vector field quantity $\vec{B}$ which exerts on any charged particle having velocity $\vec{v}$ a force $\vec{F}$ equal to the product of the vector product $\vec{v} \times \vec{B}$ and the electric charge q of the particle:

$$\vec{F} = q\vec{v} \times \vec{B}$$

where

$\vec{F}$ is the vector force acting on the particle in newtons;

q is the charge on the particle in coulombs;

$\vec{v}$ is the velocity of the particle in metres per second;

$\vec{B}$ is the magnetic flux density in teslas.

3.21
magnetic permeability

a scalar or tensor quantity μ the product of which by the magnetic field $\vec{H}$ in a medium is equal to the magnetic flux density $\vec{B}$:

$$\vec{B} = \mu\vec{H}$$

where

$\vec{H}$ is the magnetic field in amperes per metre;

μ is the magnetic constant (permeability) of the vacuum in henries per metre;

$\vec{B}$ is the magnetic flux density in teslas.

NOTE For an isotropic medium, the permeability is a scalar; for an anisotropic medium, it is a tensor.

3.22
measurement range

the interval of operation of the measurement system, which is bounded by the lower and the upper detection limits

3.23
mobile (wireless) device

for this standard only, a wireless communication device which is used when held in proximity of the head against the ear.

NOTE The terms “mobile” and “portable” have specific but generic meanings in IEC 60050 [21] – mobile: capable of operating while being moved (IEV 151-16-46); portable: capable to be carried by one person (IEV 151-16-47). The term “portable” often implies the ability to operate when carried. These definitions are used interchangeably in various wireless regulations and industry specifications, in some cases referring to types of wireless devices and in other cases to intended use.

3.24
multi-band (wireless device)
a wireless device capable of operating in more than one frequency band

3.25
multi-mode (wireless device)
a wireless device capable of operating in more than one mode of transmitting signals, e.g., analogue, TDMA and CDMA

3.26
peak spatial-average SAR
the maximal value of averaged SAR within a specific mass

3.27
penetration depth
See skin depth.

3.28
permittivity
See complex permittivity, relative permittivity.

3.29
phantom (head)
in this context, a simplified representation or a model similar in appearance to the human anatomy and composed of materials with electrical properties similar to the corresponding tissues

3.30
pinna
auricle
the largely cartilaginous projecting portion of the outer ear consisting of the helix, lobule and anti-helix

3.31
power
See average (temporal) absorbed power, conducted output power.

3.32
probe isotropy
the degree to which the response of an electric field or magnetic field probe is independent of the polarization and direction of propagation of the incident wave

3.33
relative permittivity
the ratio of the complex permittivity to the permittivity of free space. The complex relative permittivity,

$$\varepsilon_\mathrm{r} = \frac{\varepsilon}{\varepsilon_0}$$

of an isotropic, linear lossy dielectric medium is given by

$$\varepsilon_\mathrm{r} = \varepsilon_\mathrm{r}' - j\varepsilon_\mathrm{r}'' = \varepsilon_\mathrm{r}' + \frac{\sigma}{j\omega\varepsilon_0} = \varepsilon_\mathrm{r}'\left(1 - j\frac{\varepsilon_\mathrm{r}''}{\varepsilon_\mathrm{r}'}\right) = \varepsilon_\mathrm{r}'(1 - j\tan\delta)$$

where

ε_0 is the free-space permittivity ($8{,}854 \times 10^{-12}$ F/m) or dielectric constant, in farads per metre;

ε is the complex permittivity in farads per metre;

ε_r is the complex relative permittivity;

ε_r' is the real part of the complex relative permittivity, also known as dielectric constant;

ε_r'' is the part of the complex relative permittivity (dielectric loss index), which represents dielectric losses;

σ is the conductivity in siemens per metre;

ω is the angular frequency in radians per second;

tan δ is the loss tangent.

3.34

response time

the time required by the measuring equipment to reach 90 % of its final value after a step variation of the input signal

3.35

scanning system

an automatic positioning system capable of placing the measurement probe at specified positions

3.36

sensitivity (of a measurement system)

the ratio of the magnitude of the system response (e.g., voltage) to the magnitude of the quantity being measured (e.g., electric field strength squared)

3.37

skin depth

the distance from the boundary of a medium to the point at which the field strength or induced current density have been reduced to 1/*e* of their values at the boundary

The skin depth δ of a medium depends on the propagation constant, γ, of the electromagnetic wave, along the propagation direction [56]. The propagation constant depends on the dielectric properties of the material and on the characteristics of the propagating mode.

The skin depth is defined as:

$$\delta = \frac{1}{\mathrm{Re}[\gamma]}$$

where the factor $\gamma = \alpha + j\beta$, α is the attenuation constant and β is the phase constant of the propagating wave, and

$$\gamma^2 = -\omega^2 \mu \varepsilon + k_c^2$$

where μ and ε are the magnetic permeability and the complex relative permittivity of the medium respectively, and k_c^2 is the transverse propagation constant of the mode. Thus

$$\delta = \frac{1}{\mathrm{Re}\{\sqrt{-\omega^2 \mu \varepsilon + k_c^2}\}}.$$

In case of free space propagation $k_{\mathrm{c}}^{2}=0$, then the equation for the skin depth is:

$$\delta=\frac{1}{\omega}\left[\left(\frac{\mu_0\varepsilon_{\mathrm{r}}'\varepsilon_0}{2}\right)\left(\sqrt{1+\left(\frac{\sigma}{\omega\varepsilon_{\mathrm{r}}'\varepsilon_0}\right)^2}-1\right)\right]^{-1/2}$$

where

δ is the skin depth in metres;

ω is the angular frequency in radians per second;

$\varepsilon_{\mathrm{r}}'$ is the real part of the complex relative permittivity;

ε_0 is the permittivity of free space in farads per metre;

μ_0 is the permeability of free space in henries per metre;

σ is the conductivity of the medium in siemens per metre.

NOTE In case of TE_{10} mode propagation in a rectangular waveguide, with largest cross-sectional dimension *a*:

$$k_{\mathrm{c}}^{2}=\left(\frac{\pi}{a}\right)^2$$

3.38
specific absorption rate (SAR)

the time derivative of the incremental electromagnetic energy (d*W*) absorbed by (dissipated in) an incremental mass (d*m*) contained in a volume element (d*V*) of given mass density (ρ)

$$\mathrm{SAR}=\frac{\mathrm{d}}{\mathrm{d}t}\left(\frac{\mathrm{d}W}{\mathrm{d}m}\right)=\frac{\mathrm{d}}{\mathrm{d}t}\left(\frac{\mathrm{d}W}{\rho\mathrm{d}V}\right)$$

SAR can be obtained using either of the following equations:

$$\mathrm{SAR}=\frac{\sigma E^2}{\rho}$$

$$\mathrm{SAR}=c_{\mathrm{h}}\left.\frac{\mathrm{d}T}{\mathrm{d}t}\right|_{t=0}$$

where

SAR is the specific absorption rate in watts per kilogram;

E is the r.m.s. value of the electric field strength in the tissue in volts per metre;

σ is the conductivity of the tissue in siemens per metre;

ρ is the density of the tissue in kilograms per cubic metre;

c_{h} is the heat capacity of the tissue in joules per kilogram and kelvin;

$\left.\frac{\mathrm{d}T}{\mathrm{d}t}\right|_{t=0}$ is the initial time derivative of temperature in the tissue in kelvins per second.

3.39
uncertainty (combined)
standard uncertainty of the result of a measurement when that result is obtained from the values of a number of other quantities, equal to the positive square root of a sum of terms, the terms being the variances and/or covariances of the values of these other quantities weighted according to how the measurement result varies with changes in these quantities

3.40
uncertainty (expanded)
a quantity defining an interval about the result of a measurement that may be expected to encompass a large fraction of the distribution of values that could reasonably be attributed to the measurand

3.41
uncertainty (standard)
the estimated standard deviation of a measurement result, equal to the positive square root of the estimated variance

3.42
wavelength
the distance between two points of equivalent phase of two consecutive cycles of a wave in the direction of propagation. The wavelength λ is related to the magnitude of the phase velocity v_p and the frequency f by the equation:

$$\lambda = \frac{v_\mathrm{p}}{f}$$

The wavelength λ of an electromagnetic wave is related to the frequency and speed of light in the medium by the expression

$$c = f\lambda$$

where

f is the frequency in hertz;
c is the speed of light in metres per second;
v_p is the magnitude of the phase velocity;
λ is the wavelength in metres.

NOTE In free space the velocity of an electromagnetic wave is equal to the speed of light.

4 Symbols and abbreviated terms

4.1 Physical quantities

The internationally accepted SI-units are used throughout the standard.

Symbol	Quantity	Unit	Dimensions
α	Attenuation coefficient	reciprocal metre	1/m
B	Magnetic flux density	tesla	T, Vs/m^2
D	Electric flux density	coulomb per square metre	C/m^2
c_h	Specific heat capacity	joule per kilogram kelvin	J/(kg K)
E	Electric field strength	volt per metre	V/m
f	Frequency	hertz	Hz
H	Magnetic field strength	ampere per metre	A/m

J	Current density	ampere per square metre	A/m^2
$\overline{P}_{\text{avg}}$	Average (temporal) absorbed power	watt	W
SAR	Specific absorption rate	watt per kilogram	W/kg
T	Temperature	kelvin	K
ε	Permittivity	farad per metre	F/m
λ	Wavelength	metre	m
μ	Permeability	henry per metre	H/m
ρ	Mass density	kilogram per cubic metre	kg/m^3
σ	Electric conductivity	siemens per metre	S/m

NOTE In this standard, temperature is quantified in degrees Celsius, as defined by: T (°C) = T (K) – 273,16.

4.2 Constants

Symbol	Physical constant	Magnitude
c	Speed of light in vacuum	$2{,}998 \times 10^8$ m/s
η	Impedance of free space	$120\ \pi$ or $377\ \Omega$
ε_0	Permittivity of free space	$8{,}854 \times 10^{-12}$ F/m
μ_0	Permeability of free space	$4\ \pi \times 10^{-7}$ H/m

4.3 Abbreviations

CAD = Computer aided design; commonly used file formats are IGES and DXF
DXF = Digital exchange file
ERP = Ear reference point
DUT = Device under test
IGES = International graphics exchange standard
RF = Radio frequency
RSS = Root sum square
SAM = Specific anthropomorphic mannequin

5 Measurement system specifications

5.1 General requirements

A SAR measurement system is composed of a phantom, electronic measurement instrumentation, a scanning system and a device holder.

The test shall be performed using a miniature probe that is automatically positioned to measure the internal *E*-field distribution in a phantom model representing the human head exposed to the electromagnetic fields produced by wireless devices. From the measured *E*–field values, the SAR distribution and the peak spatial-average SAR value shall be calculated.

The test shall be performed in a laboratory conforming to the following environmental conditions:

- the ambient temperature shall be in the range of 18 °C to 25 °C and the variation of the liquid temperature shall not exceed ±2 °C during the test;
- the ambient noise shall be within 0,012 W/kg (3 % of the lower detection limit 0,4 W/kg);
- the wireless device shall not connect to local wireless networks;
- the effects of reflections, secondary RF transmitters, etc., shall be smaller than 3 % of the measured SAR.

Validation of a system according to the protocol defined in Annex D shall be done at least once per year, when a new system is put into operation, or whenever modifications have been made to the system, such as a new software version, different readout electronics or different types of probes. The manufacturer of the measurement equipment should declare conformity of their product with this standard.

5.2 Phantom specifications (shell and liquid)

5.2.1 General requirements

Scanning of an E-field probe is carried out within two bisected phantom halves or a full-head phantom with an opening on the top. The physical characteristics of the phantom model (size and shape) for handset testing simulate the head of a user because head shape is a dominant parameter for exposure evaluations. The phantom model shall use materials with dielectric properties similar to those of head tissues. To enable field scanning within, the head material shall consist of a liquid contained in a shell. The shell material shall be as unobtrusive as possible to device radiation, as prescribed below. At least three reference points on the phantom shall be defined by the phantom manufacturer for use in correlating the scanning system with the phantom. These points shall be visible to the user and spaced no less than 10 cm apart. A hand holding the device shall not be modelled (see Annex A).

5.2.2 Standard phantom shape and size

The standard phantom shape is derived from the size and dimensions of the 90th-percentile large adult male head reported in an anthropometric study [18], with the ears adapted to represent the flattened ears of a handset user (see Annex A). Figure 1 shows the realization of these requirements.

The Specific Anthropomorphic Mannequin (SAM) standard phantom as shown in Figure 2 shall be used for the handset SAR measurements of this standard. CAD files for the inner (*SAM_in*) and outer (*SAM_out*) surfaces of the standard phantom are publicly available on CD-ROM in 3D-CAD formats (3D-IGES and DXF). The manufacturer of the phantom shall document conformity of their product with the shape and thickness specifications of this standard.

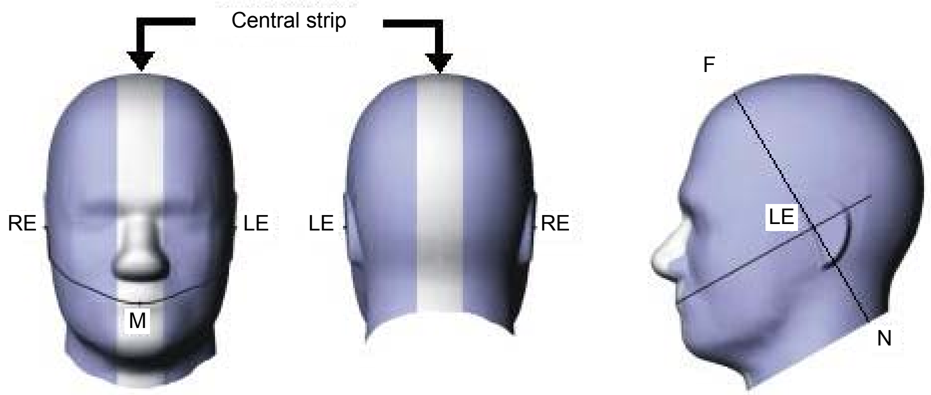

Key

RE	Right ear reference point (ERP)
LE	Left ear reference point (ERP)
M	Mouth reference point
F	Line N-F front endpoint (information only – mark on phantom not required)
N	Line N-F neck endpoint (information only – mark on phantom not required)

NOTE Full-head model is for illustration purposes only–procedures in this standard were derived primarily for the phantom set-up of Figure 2. The central strip region including the nose has a larger thickness tolerance.

Figure 1 – Picture of the phantom showing ear reference points RE and LE, mouth reference point M, reference line N-F, and central strip

5.2.3 Phantom shell

The phantom shell material shall be resistant to all ingredients used in the tissue-equivalent liquid recipes. The shell of the phantom including ear spacers shall be constructed from low permittivity and low loss material, with a relative permittivity ≤5 and a loss tangent ≤0,05. The shape of the phantom shall have a tolerance of less than ±0,2 mm with respect to the CAD file of the SAM phantom. In any area within the projection of the handset, the shell thickness shall be (2 ± 0,2) mm, except for the ears and the extended perimeter walls (as shown in Figure 2). The low-loss ear spacers (same material as the head shell) shall provide a 6 mm spacing from the tissue-equivalent liquid boundary at the ear reference points (ERPs), within a tolerance of less than ±0,2 mm. In the central strip region within ±1,0 cm of the central sagittal plane (Figure 1), the tolerance shall be ±1,0 mm.

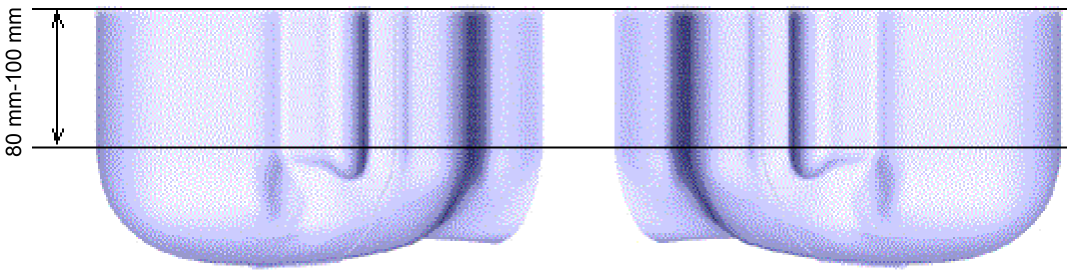

Figure 2 – Sagittally bisected phantom with extended perimeter (shown placed on its side as used for device SAR tests)

In Figure 1 the point “M” is the mouth reference point, “LE” is the left ear reference point (ERP), and “RE” is the right ERP. These points shall be marked on the exterior of the phantom to support reproducible positioning of the wireless device in relation to the phantom. The plane passing through the two ear reference points and M is defined as the reference plane, and contains the line B-M (back-mouth). The CAD file cross section for the reference plane is given in Figure 3. This view is scaled down by a factor of 1,3 from the 26 cm × 18 cm actual size. To facilitate placement of the device, the line N-F (neck-front) shall be a straight line drawn through each ERP, along the front truncated edge of the ear on each side. The projection of both the line B-M and the line N-F shall be indicated on the exterior of the phantom shell, to facilitate device positioning (see Figure 4). The position of the centre of the acoustic output side of the handset shall be located against the ERP of the phantom. All reference point locations are specified in the CAD files.

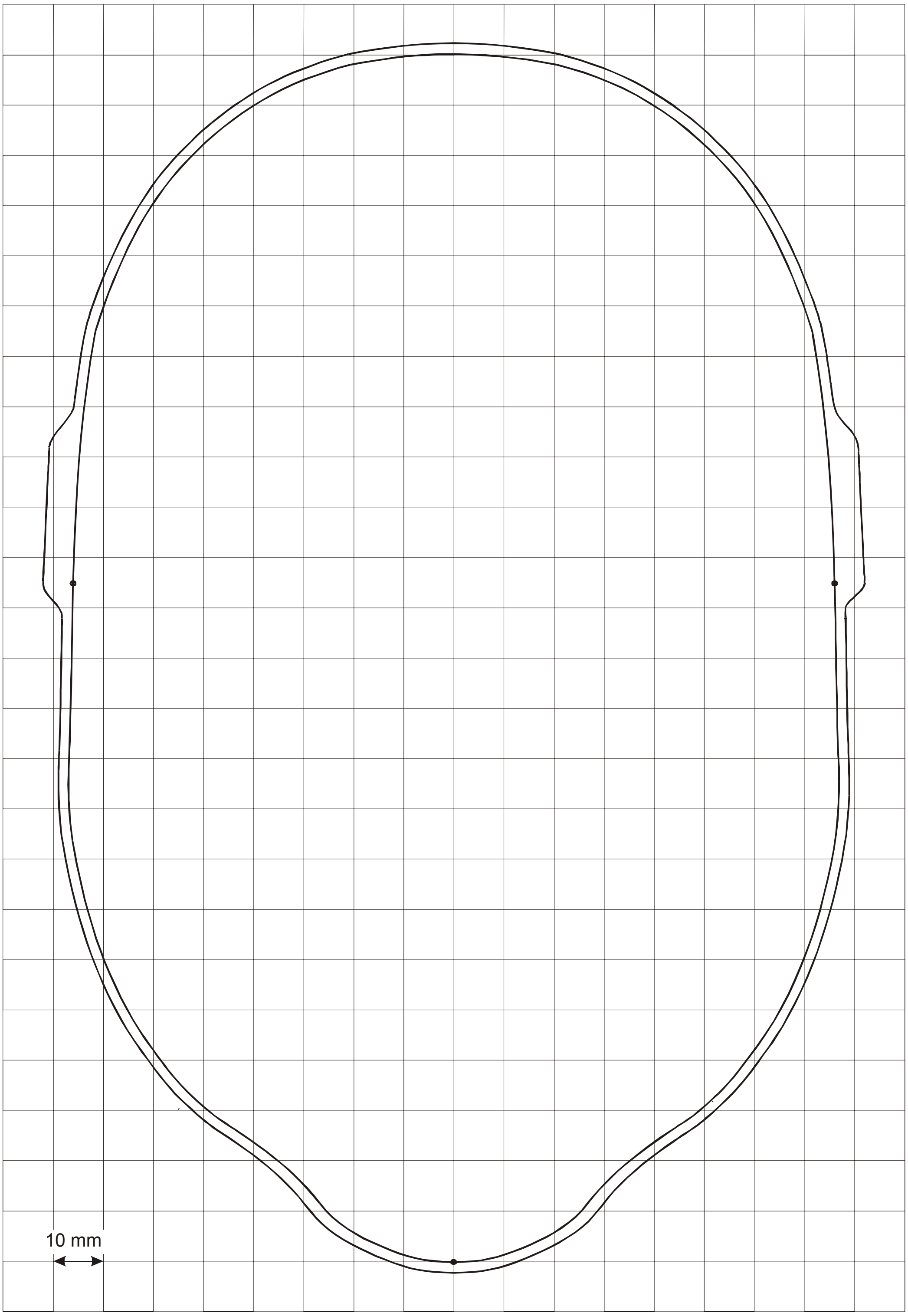

Figure 3 – Cross-sectional view of SAM at the reference plane containing B-M

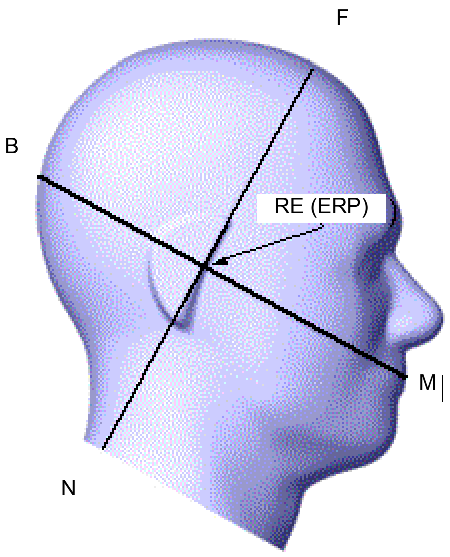

Key

B	Line B-M back endpoint (information only – mark on phantom not required)
F	Line N-F front endpoint (information only – mark on phantom not required)
N	Line N-F neck endpoint (information only – mark on phantom not required)
M	Mouth reference point
RE	Right ear reference point (ERP)

NOTE Full-head model is for illustration purposes only–procedures in this standard were derived primarily for the phantom set-up of Figure 2.

Figure 4 – Side view of the phantom showing relevant markings

5.2.4 Tissue-equivalent liquid properties

The dielectric properties of the liquid used in the phantom shall be those listed in Table 1. For dielectric properties of head tissue-equivalent liquid at other frequencies within the frequency range, a linear interpolation method shall be used. Examples of recipes for liquids having parameters as defined in Table 1 are given in Annex I.

Table 1 – Dielectric properties of the tissue-equivalent liquid

Frequency MHz	**Relative dielectric constant (ε_r)**	**Conductivity (σ)** S/m
300	45,3	0,87
450	43,5	0,87
835	41,5	0,90
900	41,5	0,97
1 450	40,5	1,20
1 800	40,0	1,40
1 900	40,0	1,40
1 950	40,0	1,40
2 000	40,0	1,40
2 450	39,2	1,80
3 000	38,5	2,40

5.3 Specifications of the SAR measurement equipment

The measurement equipment shall be calibrated as a complete system. The probe shall be calibrated together with an identical or technically equivalent type of amplifier, measurement device and data acquisition system. The measurement equipment shall be calibrated in each tissue-equivalent liquid at the appropriate operating frequency and temperature, according to the methodology described in Annex B. Calibration of the probe separately from the system is allowed, provided the loading conditions at the probe connector are specified and implemented during measurements.

The minimum detection limit shall be lower than 0,02 W/kg, and the maximum detection limit shall be higher than 100 W/kg. The linearity shall be within ±0,5 dB over the SAR range from 0,01 W/kg to 100 W/kg. Sensitivity and isotropy shall be determined in the tissue-equivalent liquid. The response time shall be specified. It is recommended that the outside dimension (diameter) of the probe cover/case should not exceed 8 mm in the vicinity of the dipole elements.

5.4 Scanning system specifications

5.4.1 General requirements

The scanning system holding the probe shall be able to scan the whole exposed volume of the phantom in order to evaluate the three-dimensional SAR distribution. The mechanical structure of the scanning system shall not interfere with the SAR measurements. The scanning system shall be correlated with the phantom using at least three reference points on the phantom, with these points defined by the user or system manufacturer.

5.4.2 Technical requirements

5.4.2.1 Accuracy

The accuracy of the probe tip positioning over the measurement area shall be better than ±0,2 mm.

5.4.2.2 Positioning resolution

The positioning resolution is the increment at which the measurement system is able to perform measurements. The positioning resolution shall be 1 mm or less.

5.5 Device holder specifications

Care shall be taken to avoid significant influence on SAR measurements by any reflection and absorption from the environment (such as floor, device holder, surface of the liquid).

The device holder shall permit the device to be positioned according to the definitions given in 6.1.4 with a tolerance of ±1° in the tilt angle. It shall be made of low loss and low permittivity material(s): loss tangent $\leq 0,05$ and relative permittivity ≤ 5. The positioning uncertainties shall be estimated following the procedures described in 7.2.2.4.2.

To verify that the holder does not perturb SAR, a substitution test should be done by replacing the holder with low relative permittivity and low loss foam blocks, or adhering the handset to the phantom using tape or string, for example (see 7.2.2.4.1).

5.6 Measurement of liquid dielectric properties

The dielectric properties of the tissue-equivalent liquid shall be measured at the relevant temperature and relevant frequency. The dielectric parameters should be evaluated and compared with the values given in Table 1 using linear interpolation. The measured dielectric properties, not the values of Table 1, shall be used in the SAR calculations. This measurement can be performed using the equipment and procedures described in Annex J.

NOTE See 6.1.1 for the allowable variations between the measured and the Table 1 dielectric parameters, as defined for the purposes of this standard.

6 Protocol for SAR assessment

6.1 Measurement preparation

6.1.1 General preparation

The dielectric properties of the tissue-equivalent liquids shall be measured within 24 h before the SAR measurements, unless the laboratory can prove compliance for longer intervals, e.g., weekly measurements. The dielectric properties of the tissue-equivalent liquids shall be measured at the same liquid temperature as that during the SAR measurements within ±2 °C.

Until verified recipes are available for head tissue-equivalent liquid in the range of 2 GHz to 3 GHz that give both measured dielectric parameters within ±5 % of the values in Table 1, the following is recommended.

a) For frequencies above 300 MHz but less than 2 GHz, the measured conductivity and dielectric constant shall be within ±5 % of the target values in Table 1 (measurement uncertainty of liquid parameters is addressed separately – see 7.2.3),
b) For frequencies in the range of 2 GHz to 3 GHz, the measured conductivity shall be within ±5 % of the target values in Table 1. The tolerance of measured relative permittivity can be relaxed to no more than ±10 %, but shall be as close as possible to the values in Table 1 using available recipes. Effects on the SAR due to the deviation of the dielectric constant from the target values shall be included in the uncertainty estimation.

The phantom shell shall be filled with the tissue-equivalent liquid to a depth of at least 15 cm above the ERP for the horizontal phantom configuration. The liquid shall be carefully stirred before the measurement, and should be free of air bubbles. Care shall be taken to avoid reflections from the liquid surface, which is accomplished with 15 cm depth in the frequency range 300 MHz to 3 GHz. The viscosity of the liquid shall not impede probe movement.

6.1.2 *System check*

A *system check* according to the procedures of Annex D shall be executed before doing handset SAR measurements. The purpose of the *system check* is to verify that the system operates within its specifications. The *system check* is a test of repeatability to ensure that the system works correctly during the compliance test. The *system check* shall be performed in order to detect possible drift over short time periods and other uncertainties in the system, such as:

- changes in the liquid parameters, e.g., due to water evaporation or temperature changes,
- component failures,

- component drift,
- operator errors in the set-up or the software parameters,
- adverse conditions in the system, e.g., RF interference.

The *system check* is a complete 1 g or 10 g average SAR measurement. The measured 1 g or 10 g average SAR value is normalized to the target input power of the standard source and compared with the previously recorded target 1 g or 10 g value corresponding to the measurement frequency, the standard source and specific flat phantom. The acceptable tolerance must be determined for each *system check* and shall be within ±10 % of previously recorded *system check* target values. The *system check* shall be performed at a frequency that is within ±10 % of the DUT mid-band frequency.

NOTE The terms *system validation* and *system check* are italicised because they refer to specific test protocols described for the purposes of this standard.

6.1.3 Preparation of the wireless device under test

The tested wireless device shall use its internal transmitter. The antenna(s), battery and accessories shall be those specified by the manufacturer. The battery shall be fully charged before each measurement, without external connections or cables.

The device output power and frequency (channel) shall be controlled using an internal test program or by the use of appropriate test equipment (base station simulator with antenna). The wireless device shall be set to transmit at its highest power level for the conditions of use next to the ear. The exposure tests shall be based on the functional and exposure characteristics of the test devices, e.g., operating modes, antenna configurations, etc.

Whenever possible, final commercial product versions shall be tested using all normal operational configurations, e.g., without any cables attached. Cables attached to a product are very likely to alter the transmitter RF current distribution on metallic and conducting portions of the product. Additionally, if tests are performed using prototypes, it shall be verified that the commercial version has exactly the same mechanical and electrical characteristics as the tested prototype. If this cannot be guaranteed, testing shall be repeated by sampling of unmodified commercial product versions.

NOTE If operation of the DUT at the highest time-averaged power level is not possible, the test may be performed at lower power and results then scaled to the maximum output power, provided that the DUT SAR response is linear.

6.1.4 Position of the wireless device in relation to the phantom

6.1.4.1 General considerations

This standard specifies two handset test positions against the head phantom – the “cheek” position and the “tilt” position. These two test positions are defined in the following subclauses. The handset should be tested in both of these positions on left and right sides of the SAM phantom. If handset construction is such that the handset positioning procedures described in 6.1.4.2 and 6.1.4.3 to represent normal-use conditions cannot be used, e.g., some asymmetric handsets, alternative alignment procedures should be adapted with all details provided in the test report. These alternative procedures should replicate intended use conditions as closely as possible, according to the intent of the procedures described in this clause.

6.1.4.2 Definition of the cheek position

The cheek position is established in points a) to i) as follows.

a) Ready the handset for talk operation, if necessary. For example, for handsets with a cover piece (flip cover), open the cover. If the device can also be used with the cover closed, both configurations shall be tested.

b) Define two imaginary lines on the handset, the vertical centreline and the horizontal line, for the handset in vertical orientation as shown in Figures 5a and 5b. The vertical centreline passes through two points on the front side of the handset: the midpoint of the width w_t of the handset at the level of the acoustic output (point A in Figures 5a and 5b), and the midpoint of the width w_b of the bottom of the handset (point B). The horizontal line is perpendicular to the vertical centreline and passes through the centre of the acoustic output (see Figures 5a and 5b). The two lines intersect at point A. Note that for many handsets, point A coincides with the centre of the acoustic output. However, the acoustic output may be located elsewhere on the horizontal line. Also note that the vertical centreline is not necessarily parallel to the front face of the handset (see Figure 5b), especially for clam-shell handsets, handsets with flip cover pieces, and other irregularly shaped handsets.

c) Position the handset close to the surface of the phantom such that point A is on the (virtual) extension of the line passing through points RE and LE on the phantom (see Figure 6). The plane defined by the vertical centreline and the horizontal line of the device must be parallel to the sagittal plane of the phantom.

d) Translate the handset towards the phantom along the line passing through RE and LE until the handset touches the ear.

e) Rotate the handset around the (virtual) LE-RE Line until the DUT vertical centreline is in the reference plane.

f) Rotate the device around its vertical centreline until the plane defined by the DUT vertical centreline and horizontal line is parallel to the N-F Line, then translate the handset towards the phantom along the LE-RE line until DUT point A touches the ear at the ERP.

g) While keeping point A on the line passing through RE and LE and maintaining the handset in contact with the pinna, rotate the handset about the line N-F until any point on the handset is in contact with a phantom point below the pinna (cheek) (see Figure 6). The physical angles of rotation shall be documented.

h) While keeping DUT point A in contact with the ERP, rotate the handset around a line perpendicular to the plane defined by the DUT vertical centreline and horizontal line and passing through DUT point A, until the DUT vertical centreline is in the reference plane.

i) Verify that the cheek position is correct as follows:
   - the N-F line is in the plane defined by the DUT vertical centreline and horizontal line,
   - DUT point A touches the pinna at the ERP, and
   - the DUT vertical centreline is in the reference plane.

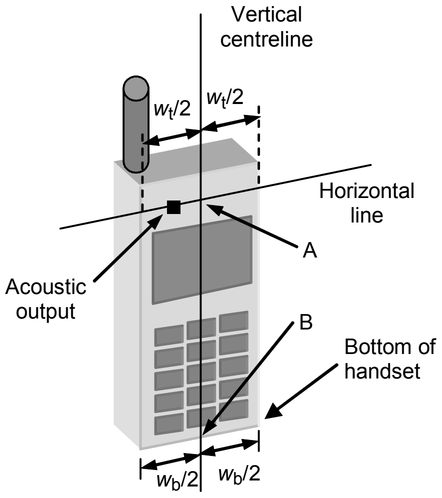

Key

w_t	Width of the handset at the level of the acoustic output
w_b	Width of the bottom of the handset
A	Midpoint of the width w_t of the handset at the level of the acoustic output
B	Midpoint of the width w_b of the bottom of the handset

Figure 5a –Typical “fixed” case handset

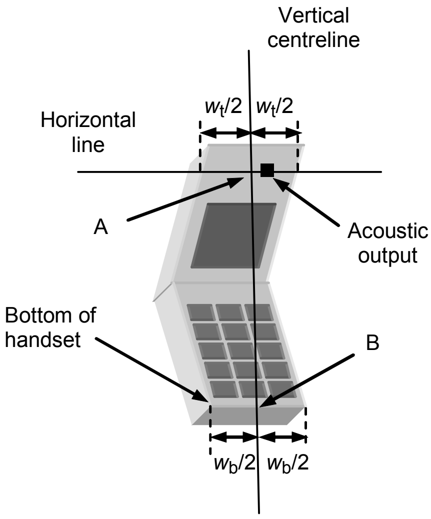

Key

w_t	Width of the handset at the level of the acoustic output
w_b	Width of the bottom of the handset
A	Midpoint of the width w_t of the handset at the level of the acoustic output
B	Midpoint of the width w_b of the bottom of the handset

Figure 5b – Typical “clam-shell” case handset

Figure 5 – Handset vertical and horizontal reference lines and reference points A, B on two example device types

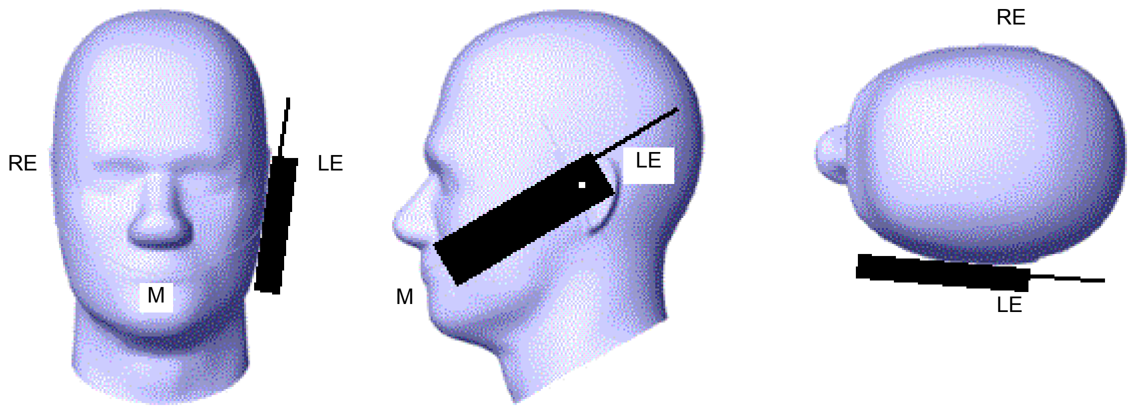

Key

M	Mouth reference point
LE	Left ear reference point (ERP)
RE	Right ear reference point (ERP)

NOTE This device position must be maintained for the phantom test set-up shown in Figure 2.

Figure 6 – Cheek position of the wireless device on the left side of SAM

6.1.4.3 Definition of the tilt position

The tilt position is established in points a) to d) as follows.

a) Repeat steps a) to i) of 6.1.4.2 to place the device in the cheek position (see Figure 6).

b) While maintaining the orientation of the device, retract the device parallel to the reference plane far enough away from the phantom to enable a rotation of the device by 15°.

c) Rotate the device around the horizontal line by 15° (see Figure 7).

d) While maintaining the orientation of the handset, move the handset towards the phantom on a line passing through RE and LE until any part of the handset touches the ear. The tilt position is obtained when the contact is on the pinna. If the contact is at any location other than the pinna, e.g., the antenna with the back of the phantom head, the angle of the handset shall be reduced. In this case, the tilt position is obtained if any part of the handset is in contact with the pinna as well as a second part of the handset is in contact with the phantom, e.g., the antenna with the back of the head.

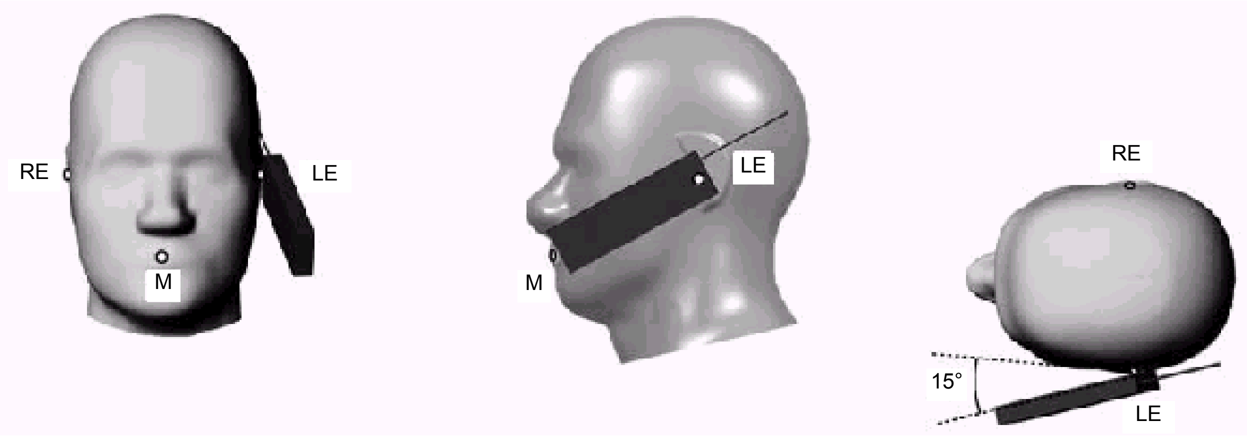

Key

M	Mouth reference point
LE	Left ear reference point (ERP)
RE	Right ear reference point (ERP)

NOTE This device position must be maintained for the phantom test set-up shown in Figure 2.

Figure 7 – Tilt position of the wireless device on the left side of SAM

6.1.5 Test frequencies

A device should be compatible with applicable exposure standards at all channels transmitted by the device. However, testing at every channel is impractical and unnecessary. The purpose of this subclause is to define a practical subset of channels where SAR measurements are to be performed. This subset of channels is chosen so as to give a characterization of compatibility of a handset with any applicable exposure standards.

For each operational mode of the handset, tests should be performed at the channel that is closest to the centre of each transmit frequency band. If the width of the transmit frequency band, ($\Delta f = f_{high} - f_{low}$,) exceeds 1 % of its centre frequency f_c, then the channels at the lowest and highest frequencies of the transmit band should also be tested. Furthermore, if the width of the transmit band exceeds 10 % of its centre frequency, the following formula should be used to determine the number of channels, N_c, to be tested:

$$N_c = 2 * \text{roundup}\ [10* (f_{high} - f_{low})/f_c] + 1,$$

where

f_c	is the centre frequency of the band in hertz;
f_{high}	is the highest frequency in the band in hertz;
f_{low}	is the lowest frequency in the band in hertz;
N_c	is the number of channels;
Δf	is the width of the transmit frequency band in hertz.

NOTE The function roundup (x) rounds its argument x to the next highest integer. Thus, the number of channels, N_c, will always be an odd number. The channels tested should be equally spaced apart in frequency (as much as possible) and should include the channels at the lowest and highest frequencies.

6.2 Tests to be performed

In order to determine the highest value of the peak spatial-average SAR of a handset, all device positions, configurations and operational modes shall be tested for each frequency band according to steps 1 to 3 below. A flowchart of the test process is shown in Figure 8.

Step 1: The tests described in 6.3 shall be performed at the channel that is closest to the centre of the transmit frequency band (f_c) for:

a) all device positions (cheek and tilt, for both left and right sides of the SAM phantom, as described in 6.1.4),

b) all configurations for each device position in a), e.g., antenna extended and retracted, and

c) all operational modes, e.g., analogue and digital, for each device position in a) and configuration in b) in each frequency band.

If more than three frequencies need to be tested according to 6.1.5 (i.e., $N_c > 3$), then all frequencies, configurations and modes shall be tested for all of the above test conditions.

Step 2: For the condition providing highest peak spatial-average SAR determined in Step 1, perform all tests described in 6.3 at all other test frequencies, i.e., lowest and highest frequencies (see 6.1.5). In addition, for all other conditions (device position, configuration and operational mode) where the peak spatial-average SAR value determined in Step 1 is within 3 dB of the applicable SAR limit, it is recommended that all other test frequencies shall be tested as well.

Step 3: Examine all data to determine the highest value of the peak spatial-average SAR found in Steps 1 to 2.

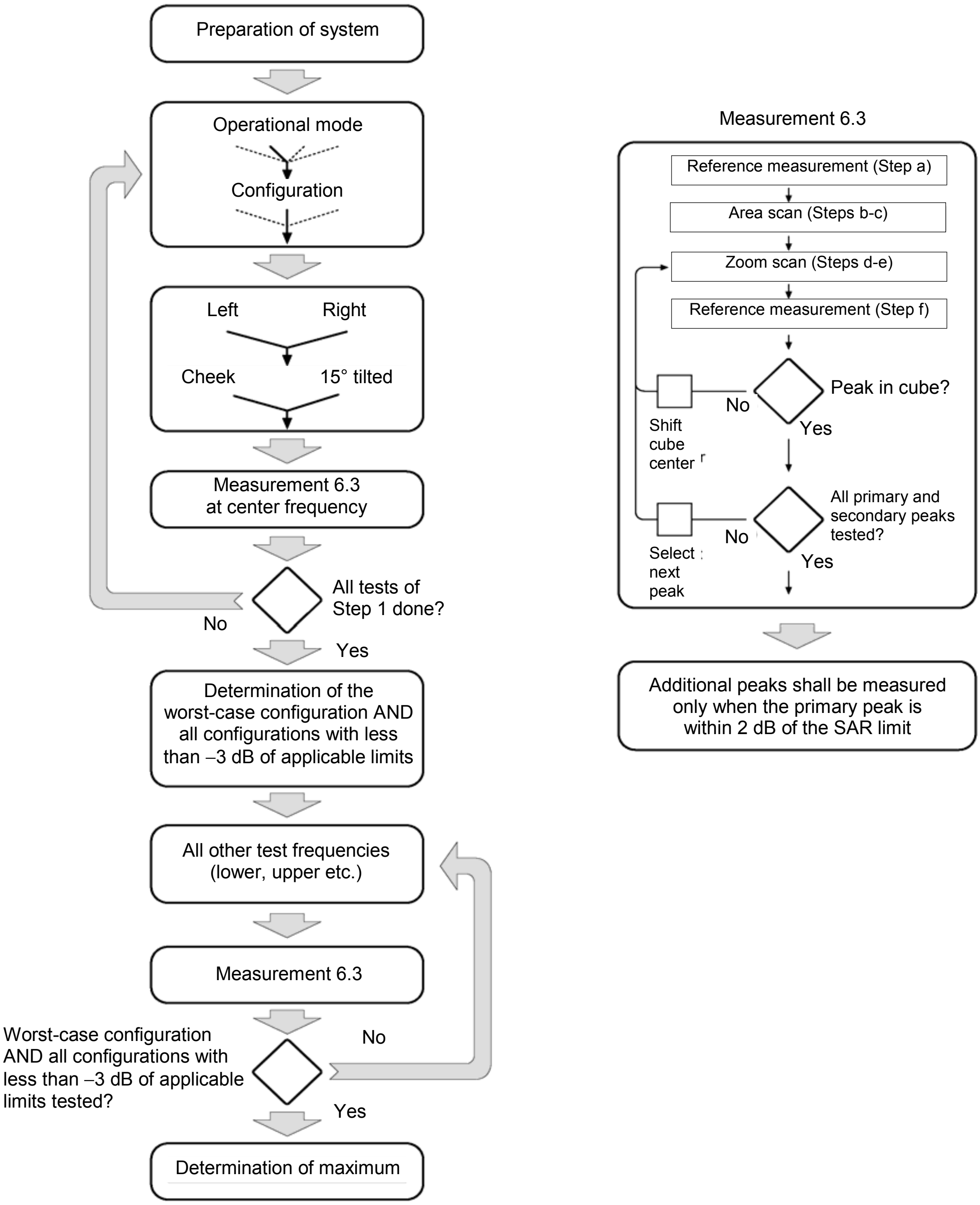

Figure 8 – Block diagram of the tests to be performed

6.3 Measurement procedure

The following procedure shall be performed for each of the test conditions (see Figure 8) described in 6.2:

a) measure the local SAR at a test point within 10 mm or less in the normal direction from the inner surface of the phantom. The test point can be close to the ear;

b) measure the SAR distribution within the phantom (*area scan* procedure). The SAR distribution is scanned along the inside surface of one side of the phantom head, at least for an area larger than the projection of the handset and antenna. The spatial grid step shall be less than 20 mm. The resolution accuracy can also be tested using the reference functions of 7.2.4. If surface scanning is used, then the distance between the geometrical centre of the probe dipoles and the inner surface of the phantom shall be 8,0 mm or less (±1,0 mm). At all measurement points, the angle of the probe with respect to the line normal to the surface is recommended but not required to be less than 30° (see Figure 9);

   NOTE If the angle is larger than 30° and the measurement distance closer than one probe-tip diameter, the boundary effect may become larger and polarization dependent. This additional uncertainty needs to be analysed and taken into account.

c) from the scanned SAR distribution, identify the position of the maximum SAR value, as well as the positions of any local maxima with SAR values within 2 dB of the maximum value that are not within the *zoom-scan* volume; Additional peaks shall be measured only when the primary peak is within 2 dB of the SAR limit (i.e., 1 W/kg for a 1,6 W/kg 1 g limit, or 1,26 W/kg for a 2 W/kg 10 g limit). This is consistent with the 2 dB threshold already stated;

d) measure SAR with a grid step of 8 mm or less in a volume with a minimum size of 30 mm by 30 mm and 30 mm in depth (*zoom scan* procedure). The grid step in the vertical direction shall be 5 mm or less (see C.3.3). Separate grids shall be centred on each of the local SAR maxima found in step c). Uncertainties due to field distortion between the media boundary and the dielectric cover/case of the probe should also be minimized, which is achieved if the distance between the phantom surface and physical tip of the probe is larger than half of the probe tip diameter. Other methods may utilize correction procedures for these boundary effects that enable high precision measurements closer than half the probe diameter [51]. At all measurement points, the angle of the probe with respect to the line normal to the surface is recommended but not required to be less than 30°;

   NOTE If the angle is larger than 30° and the measurement distance closer than one probe diameter, the boundary effect may become larger and polarization dependent. This additional uncertainty needs to be analysed and taken into account.

e) use interpolation and extrapolation procedures defined described in Annex C to determine the local SAR values at the spatial resolution needed for mass averaging;

f) the local SAR should be measured at exactly the same location as used in a). The absolute value of the measurement drift, i.e., the difference between the SAR measured in f) and a), shall be recorded in the uncertainty budget (Table 3). It is recommended that the drift be kept within ±5 %. If this is not possible, even with repeat testing, additional information, e.g., data for local SAR versus time, should be used to demonstrate that the output power applied during the test is appropriate for testing the device. Power reference measurements can be taken after each *zoom scan*, if more than one *zoom scan* is needed. However, the drift should always be recorded as the difference between the device initial state with fully charged battery and all subsequent measurements using that battery.

NOTE The terms *area scan* and *zoom scan* are italicised because they refer to specific test protocols described for the purposes of this standard.

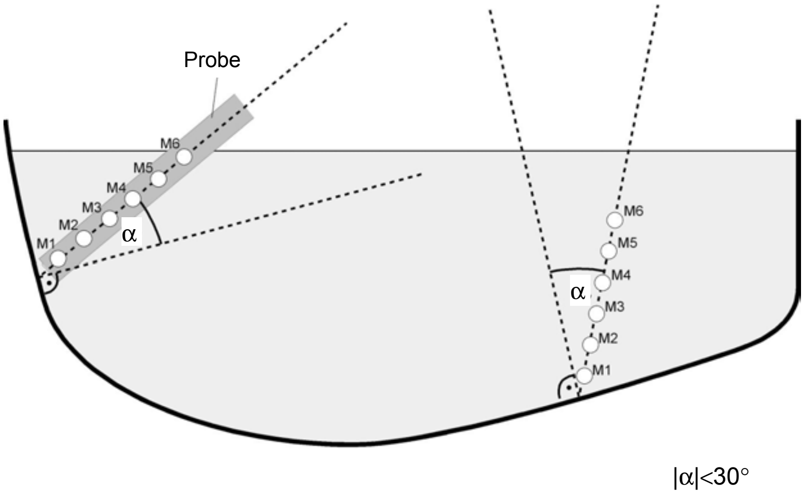

Key

M1, …, M6	Example measurement points used for extrapolation to the surface
α	Angle of the probe with respect to the line normal to the surface

Figure 9 – Orientation of the probe with respect to the line normal to the surface, shown at two different locations

6.4 Post-processing of SAR measurement data

6.4.1 Interpolation

If the resolution of measurement grid is not as fine as required to compute the average SAR over a given mass, interpolation shall be carried out between the measurement points. Examples of interpolation schemes are given in Annex C.

6.4.2 Extrapolation

The electric field probes used to measure SAR usually contain three orthogonal dipoles in close proximity and embedded in a protective cover/case. The measurement (calibration) point is situated a few millimetres from the tip of the probe and this offset shall be taken into account when identifying the position of the measured SAR. Examples of extrapolation schemes are given in Annex C.

6.4.3 Definition of the averaging volume

The averaging volume shall be in the shape of a cube with side dimension that establishes a 1 g or 10 g mass. A density of 1 000 kg/m^3 shall be used to represent the head tissue density (actual phantom liquid density shall not be used). The side length of the 1 g cube shall be 10 mm, and the side length of the 10 g cube shall be 21,5 mm.

If the cube intersects the surface of the phantom, it shall be oriented such that three vertices touch the surface of the shell (C.2.2.1), or one face tangent to the surface at its centre (C.2.2.2). The face of the cube closest to the surface shall be modified to conform to the surface and the added volume shall be subtracted from the opposite face of the cube. Schemes for averaging over a cubical volume are given in Annex C. Descriptions of methods for the estimation of SAR averaged over the mass previously defined are given in Annex C.

6.4.4 Searching for the maxima

The cubical averaging volume shall be shifted throughout the *zoom-scan* volume near the inner surface of the phantom in the vicinity of the local maximum SAR, using considerations such as those given in Annex C. The cube with the highest local maximum SAR shall not be at the edge/perimeter of the *zoom-scan* volume. In case it is, the *zoom-scan* volume shall be shifted and the measurements shall be repeated.

7 Uncertainty estimation

7.1 General considerations

7.1.1 Concept of uncertainty estimation

The concepts of uncertainty estimation in the measurement of the SAR values produced by wireless devices is based on the general rules provided by the ISO/IEC Guide to the Expression of Uncertainty in Measurement [25]. Nevertheless, uncertainty estimation for complex measurements remains as a difficult task and requires high-level and specialized engineering knowledge. In order to facilitate this task, guidelines and approximation formulas are provided in this clause, enabling the estimation of each individual uncertainty component. The concept is designed to provide the system uncertainty for the entire frequency range of 300 MHz to 3 GHz and for any device under test. This has the disadvantage that the uncertainty might be overestimated for some cases but enables the usage of approximations as provided in this clause. In addition, an advantage is that the uncertainty estimation can be performed by third parties, i.e., Table 3 could be provided by the manufacturer of the system after installation. Band-specific uncertainty assessments are possible but should be avoided. In this case, if the standard allows *X* % deviation from the target values for some influence quantity, then the maximum *X* % and not the site-specific deviation shall be used for Table 3. It should be noted that it is not sufficient to provide only Table 3 without the availability of a detailed documentation of the estimation of each influence quantity including methodology, assessment of data for each component, as well as how the uncertainty was derived from the data set.

7.1.2 Type A and Type B evaluations

Both Type A and Type B evaluations of the standard uncertainty shall be used. When a Type A analysis is performed, the standard uncertainty u_i shall be derived using the estimated standard deviation from statistical observations. When a Type B analysis is performed, u_i comes from the upper a_+ and lower a_- limits of the quantity in question, depending on the probability distribution function defining $a = (a_+ - a_-)/2$, then:

- rectangular distribution: $u_i = a/\sqrt{3}$
- triangular distribution: $u_i = a/\sqrt{6}$
- normal distribution: $u_i = a/k$
- U-shaped (asymmetric) distribution: $u_i = a/\sqrt{2}$

where

a is the half-length of the interval set by limits of the influence quantity;

k is a coverage factor;

u_i is the standard uncertainty.

For n repeat measurements of the same specific device or quantity in the same test set-up, the standard deviation of the mean (= $s/\sqrt{n}$) can be used for the standard uncertainty, where s is the standard deviation obtained from a larger set of previous readings for the same test conditions. Predetermined standard deviations based on a larger number of repeat tests can be used to estimate uncertainty components in cases where the system, method, configuration and conditions, etc., are representative of the specific device test [62]. Predetermination does not include the contributions of the particular EUT. For a specific device, the value of n used for the standard deviation of the mean is the number of tests with the specific device, not the tests used in the predetermination.

7.1.3 Degrees of freedom and coverage factor

When the degrees of freedom are less than 30, a coverage factor of two is not the appropriate multiplier to be used to achieve a 95 % confidence level [7]. A simple but only approximately correct method is to use t in place of the coverage factor k, where t is the Student's-t factor. Standard deviations of t-distributions are narrower than normal (Gaussian) distributions, but the curves approach the Gaussian shape for large numbers of degrees of freedom. The degrees of freedom for most standard uncertainties based on Type B evaluations can be assumed to be infinite [62]. Then the effective degrees of freedom of the combined standard uncertainty, u_c, will most strongly depend on the degrees of freedom of the Type A contributions and their magnitude relative to the Type B contributions.

The coverage factor (k_p) for small sample populations should be determined as

$$k_p = t_\mathrm{p}(\nu_\mathrm{eff}),$$

where

k_p is the coverage factor for a given probability p;

$t_p(\nu_\mathrm{eff})$ is the t-distribution;

ν_eff is the effective degrees of freedom estimated using the Welch-Satterthwaite formula:

$$\nu_\mathrm{eff} = \frac{u_\mathrm{c}^4}{\sum\limits_{i=1}^{m} \frac{c_i^4 u_i^4}{\nu_i}} .$$

The subscript p refers to the approximate confidence level, e.g., 95 %. Tabulated values of $t_p(\nu_\mathrm{eff})$ are available, for example in NIST TN1297 [46].

NOTE As an example, assume that the combined standard uncertainty calculated from all the influence quantities in Table 3 with an assumed positioning uncertainty of 7 % is ν_c = 14,5 %. Assume also that the number of samples or tests is equal to 5, so ν_i = 4 and the degrees of freedom for all of the other components are $\nu_i = \infty$. From the equation $\nu_\mathrm{eff} = u_\mathrm{c}^4 \Big/ \sum\limits_{i=1}^{m} \frac{c_i^4 u_i^4}{\nu_i}$, the effective degrees of freedom for the combined standard uncertainty is ν_eff = 74, so k = 2 does apply in this case, and the expanded uncertainty is U = 29 %. If the standard uncertainty for positioning variations goes to 9 % and the number of tests is reduced to 4 (ν_i = 3), then ν_c = 15,6 %, ν_eff = 27, $k = k_\mathrm{p} = k_{95} = t = t_{95}$ = 2,11, and the expanded uncertainty becomes U = 2,11 × 15,6 = 32,9 %.

7.2 Components contributing to uncertainty

7.2.1 Contribution of the measurement system

7.2.1.1 Calibration of the measurement equipment

A protocol for the evaluation of the sensitivity (calibration) is given in Annex B, including an approach to the uncertainty estimation. The uncertainty in the sensitivity shall be estimated assuming a normal probability distribution.

7.2.1.2 Probe isotropy

The isotropy of the probe shall be measured according to the protocol defined in Annex B. The uncertainty due to isotropy shall be estimated with a rectangular probability distribution.

$$\text{Total Isotropy Uncertainty} = \sqrt{(1-w_i)\times[\text{Axial isotropy}]^2 + w_i \times [\text{Hemispherical isotropy}]^2}\ ,$$

where w_i is a weighting factor to account for field incidence angles around an imaginary sphere enclosing the probe tip.

If the probe orientation is essentially normal to the surface (within ±30°) during the measurement, then $w_i = 0{,}5$, otherwise $w_i = 1$.

7.2.1.3 Probe linearity

The probe linearity shall be assessed for the square of the measured electric field strength according to the protocol defined in Annex B. A correction shall then be performed to establish linearity. The uncertainty is considered after this correction. Since diode sensors can become peak detectors in pulsed fields, linearity shall be assessed with two signals – a CW signal, and a pulsed signal at 10 % duty factor with a repetition rate of 500 Hz (more conservative uncertainty than 11 Hz or 217 Hz, for example). The assessment should be in the range of 0,4 W/kg to 100 W/kg in steps of 3 dB or less. The SAR uncertainty is estimated as the maximum deviation in the square of the measured and actual field strengths for the entire assessment. The uncertainty shall be estimated assuming a rectangular probability distribution.

7.2.1.4 Detection limits

Detection limits shall be evaluated according to the protocol defined in Annex B. The linearity test in 7.2.1.3 provides the uncertainty estimate for a lower detection limit of 0,4 W/kg and an upper detection limit of 100 W/kg, provided the duty factor is within 10 % and 100 %. If measurements are taken outside this range, the same assessment as described in 7.2.1.3 shall be extended correspondingly. The uncertainty shall be estimated assuming a rectangular probability distribution.

7.2.1.5 Boundary effect

The probe boundary effect occurs due to coupling effects between the probe dipoles and the medium boundary at the shell. Boundary effect characteristics can be evaluated using the waveguide setup as described in Annex B of this document. The probe boundary effect uncertainty is derived from the first-order-approximation of an exponential decay combined with a linear function representing the boundary effect and is estimated as:

$$\text{SAR}_{\text{uncertainty}}[\%] = \delta\text{SAR}_{\text{be}} \frac{\left(d_{\text{be}} + d_{\text{step}}\right)^2}{2d_{\text{step}}} \frac{\left(e^{-d_{\text{be}}/(\delta/2)}\right)}{\delta/2} \quad \text{for } \left(d_{\text{be}} + d_{\text{step}}\right) < 10\ \text{mm}$$

where

$\text{SAR}_{\text{uncertainty}}$	is the uncertainty in percent of the probe boundary effect
d_{be}	is the distance between the surface and the closest *zoom-scan* measurement point, in millimetre;
d_{step}	is the separation distance between the first and second measurement points that are closest to the phantom surface, in millimetre, assuming the boundary effect at the second location is negligible;

δ	is the minimum penetration depth in millimetres of the head tissue-equivalent liquids defined in this standard, i.e., $\delta \approx$ 14 mm at 3 GHz;
$\delta \mathrm{SAR}_{\mathrm{be}}$	in percent of SAR is the deviation between the measured SAR value, at the distance d_{be} from the boundary, and the analytical SAR value.

Enter the uncertainty of the probe boundary effect in the appropriate row and column in the uncertainty table, using a rectangular distribution.

7.2.1.6 Readout electronics

The uncertainty components of the field probe readout electronics, including amplification, linearity, loading of the probe and evaluation algorithm uncertainties shall be assessed under worst-case conditions. If the readout electronics components have tolerances of the same magnitude, each tolerance shall be converted to a standard uncertainty using the normal probability distribution. The root sum squared value of these uncertainties shall then be used to get the overall readout electronics uncertainty.

7.2.1.7 Response time

The probe shall be exposed to a well-defined electric field producing at least 2 W/kg at the boundary of phantom and the tissue-equivalent liquid. The signal response time is evaluated as the time required by the measurement equipment (probe and readout electronics) to reach 90 % of the expected final value after a step variation or switch on/off of the power source. The SAR uncertainty resulting from this response time may be neglected if the probe is spatially stationary for a period of time greater than twice the response time while a SAR value is measured. In this case, enter a zero in column 3 in Table 3. If the probe is not spatially stationary for twice the response time or more, enter the actual uncertainty of the response time in column 3.

7.2.1.8 Integration time

The integration time applied to measure the electric field at a specific point may introduce additional uncertainties due to discretization if the handset does not emit a continuous wave (CW) signal or the readout system is not locked to the signal. This uncertainty is dependent on the signal characteristics and shall be estimated prior to all SAR measurements. If a non-CW signal is used, the uncertainty due to integration time uncertainties shall be accounted for in the total uncertainty estimation. A rectangular probability distribution is assumed for evaluating integration time uncertainties.

NOTE For a TDMA signal (t_{frame} = period of frame), the maximum uncertainty for a defined integration time (t_{int}) is given by:

$$\mathrm{SAR}_{\mathrm{uncertainty}}\,[\%] = 100 \times \sum_{\text{all sub-frames}} \frac{t_{\mathrm{frame}}}{t_{\mathrm{int}}} \frac{slot_{\mathrm{idle}}}{slot_{\mathrm{total}}}$$

for $t_{\mathrm{int}} > t_{\mathrm{frame}}$, where

$\mathrm{SAR}_{\mathrm{uncertainty}}$	is the uncertainty for the integration time in percent
t_{frame}	is the frame duration;
$slot_{\mathrm{idle}}$	is the number of idle slots in a frame;
$slot_{\mathrm{total}}$	is the total number of slots in a frame.

Enter this value in the uncertainty table, and a rectangular distribution can be assumed.

7.2.2 Contribution of mechanical constraints

7.2.2.1 Scanning system

The mechanical restrictions of the field probe positioner can introduce deviations in the accuracy and repeatability of probe positioning which add to the uncertainty of the measured SAR. The uncertainty may be estimated with respect to the specifications of the probe positioner relative to the position required by the actual measurement location defined by the geometrical centre of the field probe sensors and is expressed as maximum deviation d_{ss}. By assuming a rectangular probability distribution, the peak spatial-average SAR uncertainty contributions due to mechanical restrictions of the probe positioner, d_{ss}, may be calculated using a first-order error approximation:

$$\mathrm{SAR}_{\mathrm{uncertainty}}[\%] = \frac{d_{\mathrm{ss}}}{\delta/2} \times 100$$

where

$\mathrm{SAR}_{\mathrm{uncertainty}}$	is the uncertainty in percent
d_{ss}	is the maximum position uncertainty between the calculated position of the centre of the probe sensors and the actual position with respect to a reference point defined by the system manufacturer;
δ	is the minimum penetration depth in millimetre of the head tissue-equivalent liquid defined in this standard, i.e., $\delta \approx$ 14 mm at 3 GHz.

If the manufacturer of the positioner does not specify the mechanical restrictions of the probe positioner, this must be evaluated to determine the contribution to SAR measurement uncertainty. This can be simply performed by evaluating the relative accuracy of movement in the area of the coarse scan and converting differences in positions specified by the software to that actually achieved into an uncertainty. The SAR tolerance shall be entered in column 3 of Table 3 using an assumed rectangular distribution.

7.2.2.2 Phantom shell

The phantom uncertainty is defined as the uncertainty of the induced peak spatial-average SAR due to phantom production tolerances, and uncertainties of the dielectric parameters of the tissue-equivalent liquid within the phantom (see 7.2.3.3, 7.2.3.4). Phantom production tolerances include:

- deviations in the inner and outer shapes of the phantom shell from that defined by the CAD file used for this standard;
- deviations in phantom shell thickness from that defined by the CAD file.

The uncertainty is estimated according to the worst-case dependence of SAR on distance from a source, i.e., dependence on the square of the distance and assuming a distance of a = 10 mm between the head tissue-equivalent liquid and the location of the source equivalent filament current density (the equivalent current density does not correspond to the closest current source but to a current density approximating the local *H*-field distributions).

$$\mathrm{SAR}_{\mathrm{uncertainty}}[\%] = 100 \times \left(\frac{(a+d)^2}{a^2} - 1 \right)$$

$$\mathrm{SAR}_{\mathrm{uncertainty}}[\%] = 100 \times \frac{2d}{a} \qquad \text{if } d \ll a$$

where

$\text{SAR}_{\text{uncertainty}}$ is the uncertainty in percent

d is the maximum tolerance of the shell thickness and phantom shape;

a is the distance between the head tissue-equivalent liquid and the location of the source equivalent filament current density.

Enter the uncertainty value in the corresponding row of Table 3, with a rectangular distribution assumed.

7.2.2.3 Probe position with respect to phantom shell surface

The uncertainty of the probe positioner with respect to the phantom shell d_{ph} shall be estimated. By assuming a rectangular probability distribution, the peak spatial-average SAR uncertainty contribution is calculated using a first-order error approximation:

$$\text{SAR}_{\text{uncertainty}}[\%] = \frac{d_{\text{ph}}}{\delta/2} \times 100$$

where

$\text{SAR}_{\text{uncertainty}}$ is the uncertainty in percent;

d_{ph} is the uncertainty for determining the distance between probe tip and phantom shell, i.e., the uncertainty of determining the phantom location with respect to the probe tip;

δ is the minimum penetration depth in millimetres of the head tissue-equivalent liquid defined in this standard, i.e., $\delta \approx$ 14 mm at 3 GHz.

The SAR uncertainty shall be entered in column 3 of Table 3 in the uncertainty table assuming a rectangular distribution.

7.2.2.4 Device positioning and holder uncertainties

A device holder is used to maintain the test position of a handset against the phantom during a SAR measurement. Because a device holder may influence the characteristics of a handset under test, the SAR uncertainty due to device holder perturbation shall be estimated using the procedures in 7.2.2.4.1. Procedures for SAR uncertainties due to positioning variations resulting from mechanical tolerances of the device holder are discussed in 7.2.2.4.2. Both clauses include procedures for device-specific and predetermined uncertainties. If predetermined uncertainties are used, in most cases multiple repeats of device-specific tests can be done to reduce the predetermined standard deviations further.

7.2.2.4.1 Device holder perturbation uncertainty

The device holder shall be made of low-loss dielectric material with a dielectric constant of less than 5 and loss tangent of less than 0,05 (these material parameters can be determined for example using the coaxial contact probe method). Nevertheless, some holders may still affect the source, so the uncertainty resulting from the holder (i.e., the deviation from a set-up without the holder) should be estimated. The uncertainty for a specific test device should be estimated according to the method described in 7.2.2.4.1.1, which is a type B method. The method described in 7.2.2.4.1.2 provides a Type A method to assess the uncertainty for a group of handsets having similar SAR characteristics and tested with the same device holder.

7.2.2.4.1.1 Device holder perturbation uncertainty for a specific test device: Type B

The uncertainty for a specific handset operating in a specific configuration shall be estimated by performing the following two tests using a flat phantom.

a) assessment of the peak spatial-average SAR ($\mathrm{SAR}_{\text{w/ holder}}$) by placing the device in the holder in the same way it would be held when tested against the head, then positioning the handset in direct contact with a flat phantom (horizontal and vertical centre line of the handset parallel to the bottom of the flat phantom);

b) assessment of the peak spatial-average SAR ($\mathrm{SAR}_{\text{w/o holder}}$) by placing the device in the same position but held in place using foamed polystyrene or equivalent low-loss and non-reflective material (permittivity no greater than 1,2 and loss tangent no greater than 10^{-5}).

The SAR tolerance to be used in Table 3 is:

$$\mathrm{SAR}_{\text{uncertainty}}\,[\%] = \left(\frac{\mathrm{SAR}_{\text{w/ holder}} - \mathrm{SAR}_{\text{w/o holder}}}{\mathrm{SAR}_{\text{w/o holder}}} \right) \times 100$$

where

$\mathrm{SAR}_{\text{uncertainty}}$	is the uncertainty in percent
$\mathrm{SAR}_{\text{w/ holder}}$	is the SAR with device holder in watts per kilogram
$\mathrm{SAR}_{\text{w/o holder}}$	is the SAR without device holder in watts per kilogram

This uncertainty has an assumed rectangular probability distribution and $v_i = \infty$ degrees of freedom.

7.2.2.4.1.2 Device holder perturbation uncertainty for a specific test device: Type A

A Type A uncertainty analysis can be applied for a group of handsets having similar shapes and SAR distributions. The uncertainty arising from this analysis can apply to other handsets having similar SAR characteristics and tested with the same device holder, such that the specific tests described in 7.2.2.4.1.1 can be avoided. The effect of the device holder for *N* different models of handsets in the different configurations shall be estimated by performing the tests of 7.2.2.4.1.1 for each model (*N* shall be at least six), where for each configuration

$$\mathrm{SAR}_{\text{uncertainty}}\,[\%] = \left(\frac{\mathrm{SAR}_{\text{w/ holder}} - \mathrm{SAR}_{\text{w/o holder}}}{\mathrm{SAR}_{\text{w/o holder}}} \right) \times 100$$

where

$\mathrm{SAR}_{\text{uncertainty}}$	is the uncertainty in percent
$\mathrm{SAR}_{\text{w/ holder}}$	is the SAR with device holder in watts per kilogram
$\mathrm{SAR}_{\text{w/o holder}}$	is the SAR without device holder in watts per kilogram

The corresponding uncertainty for Table 3 shall be estimated by using the root-mean-square of the individual uncertainties, with degrees of freedom of $v_i = N - 1$. It is recommended that the database be updated yearly in order to account for handset design changes.

7.2.2.4.2 Handset positioning uncertainty with a specific test device holder: Type A

The deviation of the actual handset position from the positions described in the standard depends on the precision of the handset positioner as well as on the interpretation and handling of the person performing the test. In addition, the magnitude of this deviation on the peak spatial-average SAR values depends on the handset design. Since these parameters cannot be separated, the following Type A tests shall be performed.

7.2.2.4.2.1 Positioning uncertainty of a specific handset in a specific device holder

For the device configurations and positions which are evaluated for peak spatial-average SAR values according to standardized protocols, the evaluation shall be repeated at least 4 more times, for a total of $N \geq 5$ tests. The standard deviation in percent of the average value shall be computed, whereby the degrees of freedom is $v_i = N - 1$.

7.2.2.4.2.2 Positioning uncertainty of specific types of handsets in a specific device holder

A Type A uncertainty analysis can be applied for a group of handsets having similar shapes and SAR distributions. The number M should be at least 6, and each of the M tests should be performed according to 7.2.2.4.2.1 (N times). Half of the M tests should be in the cheek position and the other half should be in the tilt position. The corresponding uncertainty shall be estimated by applying the root-mean-square of the M individual standard deviations. The value to be filled in the uncertainty table should be the standard uncertainty with $k = 1$, corresponding to a 68 % confidence level. The degrees of freedom is $v_i = (N \times M) - 1$. If this procedure is applied to determine uncertainty, it may be unnecessary to apply 7.2.2.4.2.1 to individual handsets. It is recommended that the database be updated yearly in order to account for handset design changes.

7.2.3 Contribution of physical parameters

7.2.3.1 Introduction

Details of dielectric parameter test methods are given in Annex J, and uncertainty estimation methods are given in J.7.

NOTE In accordance with usual metrological practices, the measurement uncertainty for each of the dielectric parameters is recommended to be less than or equal to the allowable variations from the target values of the measured dielectric parameters.

7.2.3.2 Liquid density

The electromagnetic parameters of the tissue-equivalent liquids are assumed to have a density of 1 000 kg/m^3. This density shall be used for SAR evaluations.

7.2.3.3 Liquid conductivity

The uncertainty due to the liquid conductivity arises from two different sources. The first source of uncertainty is the allowable variation of ±5 % from the Table 1 target value and the second source of uncertainty arises from the measurement procedures used to assess conductivity. The uncertainty shall be estimated using a rectangular probability (Clause J.7).

7.2.3.4 Liquid permittivity

The uncertainty due to the liquid permittivity arises from two different sources. The first source of uncertainty is the allowable variation of ±5 % from the Table 1 target value and the second source of uncertainty arises from the measurement procedures used to assess permittivity. The uncertainty shall be estimated using a rectangular probability (Clause J.7).

7.2.3.5 Drifts in output power of the device, probe, temperature and humidity

Variations and drifts due to the electronics of the test device and the measurement equipment, as well as temperature and humidity, are accounted for by the first and last step of the measurement process defined in 6.3, and the allowable variation is less than ±5 %. The uncertainty shall be estimated assuming a rectangular probability distribution.

7.2.3.6 Perturbation of the environment

The perturbation of the environment results from various contributing factors:

- reflection of waves in the laboratory,
- influence of the electromagnetic properties of the phantom shell and the wireless device holder,
- background level of electromagnetic fields.

The allowable variation shall be within ±3 % and the uncertainty shall be estimated assuming a rectangular probability distribution.

7.2.4 Contribution of post-processing

7.2.4.1 Introduction

This subclause describes the estimation of the uncertainty resulting from the post-processing of the discrete measured data to determine the 1 g and 10 g peak spatial-average SAR, i.e., the combined uncertainty of interpolation, extrapolation, averaging and maximum finding algorithms. These algorithms may add uncertainty due to general assumptions about field behaviour, and therefore may not perfectly predict the electric field distribution in the tissue-equivalent liquid for a specific handset. The algorithm uncertainty is a function of the resolution chosen for the measurement and the post-processing methods used in the *area* and *zoom scans*.

The actual SAR distribution at the peak location is strongly dependent on the operating frequency and design of the handset, test position, and proximity to the tissue-equivalent liquid. SAR distributions can have a rather flat gradient when a low frequency source is a large distance away, or can have a very steep gradient when a small high frequency source such as a helix antenna is placed next to the tissue. In some cases, the maximum SAR is not at the surface of the phantom due to cancellation of magnetic fields at the surface [36].

The analytical SAR distribution functions presented below are intended to simulate these conditions and were developed for the purpose of this uncertainty estimation. These empirically derived reference functions are used to create artificial or “dummy” SAR data sets for testing the system software post-processing subroutines. Computed reference function values at coarse and fine grid spacings, the same as are used in measurements, are input to the SAR system software. SAR values at grid points corresponding to the *area*- and *zoom-scan* measurement grids are computed according to the three SAR distributions given in 7.2.4.2 and processed by the system interpolation, extrapolation, and integration algorithms as if they were actually measured. The resulting 1 g and 10 g SAR values are compared with reference SAR values listed in 7.2.4.2. Procedures for evaluating the SAR uncertainty of the area and zoom- scan post-processing algorithms are described in 7.2.4.3. The test functions assume a planar tissue-equivalent liquid and phantom interface. The applicability of these functions for curved interfaces is discussed in 7.2.4.4. This uncertainty concept assumes that there are no errors in location of the grid points calculated with the analytical distribution functions, and probe positioning and measurement uncertainties are not included.

7.2.4.2 Evaluation test functions

Three analytical functions, f_1, f_2 and f_3, are used to represent the possible range of SAR distributions expected for handsets tested according to the procedures of this document. A spatially flat distribution, f_1, and a spatially steep distribution, f_3, are used to cover the expected range of field gradients in handset SAR measurements. The function f_2 is used to account for exposure conditions with *H*-field cancellation at the phantom/tissue-equivalent liquid surface. The distribution functions are defined for the phantom surface at $z = 0$, and the half-space tissue-equivalent liquid is defined for all $z > 0$.

$$f_1(x,y,z) = A e^{-\frac{z}{2a}} \cos^2\left(\frac{\pi}{2}\frac{\sqrt{x'^2 + y'^2}}{5a}\right)$$

$$f_2(x,y,z) = A e^{-\frac{z}{a}} \frac{a^2}{a^2 + x'^2}\left(3 - e^{-\frac{2z}{a}}\right)\cos^2\left(\frac{\pi}{2}\frac{y'}{3a}\right)$$

$$f_3(x,y,z) = A \frac{a^2}{\frac{a^2}{4} + x'^2 + y'^2}\left(e^{-\frac{2z}{a}} + \frac{a^2}{2(a+2z)^2}\right)$$

where

$x' = x + d$ mm;

$y' = y + d$ mm;

d = offset parameter;

a = 20 mm;

A = 1 W/kg.

The above parameters a and A do not have any particular physical meaning other than for generation of the appropriate SAR distributions. A value of d = 2,5 mm, for example, provides a lateral shift of the SAR distribution so that the peak location is not aligned with a measurement grid having a 5 mm increment. This offset is used to test the software peak search subroutines and uncertainty. The reference SAR values of the distribution functions f_1, f_2, and f_3 for 1 g and 10 g cubes aligned with the (x, y, z) coordinate axes are given below in Table 2. The reference values are used in the following subclauses for testing other data-processing functions.

Table 2 – Reference SAR values in watts per kilogram used for estimating post-processing uncertainties

Function	Reference SAR value W/kg	
	1 g cube	10 g cube
f_1	0,881	0,759
f_2	1,796	1,375
f_3	3,049	1,385

7.2.4.3 Data-processing algorithm uncertainty evaluations

7.2.4.3.1 Evaluation of the coarse *area scan*

A precondition for peak spatial-average SAR assessment with a given uncertainty is that the location of the maximum exposure can be determined from the *area scan* data with such a precision that the peak spatial-average SAR is entirely enclosed in the *zoom-scan* volume. In other words, the *area-scan* interpolation algorithms should be capable of locating peak SAR locations with an accuracy of $\pm L_z/2$ mm or better, where L_z is the side length of the *zoom-scan* volume. If this precondition is satisfied, which is tested with the procedures of this subclause, then the evaluation of the *area scan* does not contribute to the uncertainty budget.

The reference function values calculated at the usual *area-scan* grid points are input to the system software. The interpolation algorithm treats these data points as if they were measured to complete the *area scan* and determine the peak SAR location (x_{eval}, y_{eval}). This is compared with the actual peak location defined by the analytical functions at (x_{ref}, y_{ref}) = (-2,5, -2,5) mm, when d = 2,5 mm. The subscripts “eval” and “ref” refer to evaluated and reference, respectively. In other words, the following inequalities shall be satisfied:

$$\left|x_{\text{ref}} - x_{\text{eval}}\right| \le L_z/2 \quad \text{mm}$$

$$\left|y_{\text{ref}} - y_{\text{eval}}\right| \le L_z/2 \quad \text{mm}$$

The ability of the two-dimensional *area scan* to accurately locate the SAR peak is dependent on the spatial resolution (Δx, Δy) of the *area-scan* grid, the spatial resolution (Δx_i, Δy_i) of the interpolated values, and the type of interpolation functions [$g_i(x)$, $g_i(y)$] used. It is also dependent on the location of the evaluation grid with respect to the actual peak location (x_{ref}, y_{ref}) and the number of evaluation points used (N_x, N_y).

The following procedure should be used to assess the uncertainty of the interpolation algorithms used in the *area scan* for determining the peak SAR location:

a) Choose the measurement resolution (Δx, Δy), and number of evaluation (corresponding to measurement) points (N_x, N_y). The centre of the *area scan* should be set to (x_0, y_0) = (0, 0).

b) SAR values are computed using the functions f_1, f_2 and f_3 at the *area-scan* evaluation grid points within the ranges:

$$x_0 - \Delta x \times [(N_x - 1)/2] \le x \le x_0 + \Delta x \times [(N_x - 1)/2],$$

$$y_0 - \Delta y \times [(N_y - 1)/2] \le y \le y_0 + \Delta y \times [(N_y - 1)/2],$$

where N_x and N_y are assumed to be odd integers. A value of z = 0 is assumed since the peak location is independent of z for these three functions.

c) The SAR values computed by the three distribution functions are interpolated by the SAR measurement system with a spatial resolution of (Δx_i, Δy_i) according to the interpolation functions [$g_i(x)$, $g_i(y)$] used by the system to determine the peak SAR location (x_{eval}, y_{eval}). If the measurement system does not allow SAR values to be imported to perform the assessment, the same algorithm should be implemented independently by other means to determine the interpolation and peak search uncertainties.

d) The peak SAR location determined by the interpolation algorithms should satisfy the requirements of the inequalities

$$\left|x_{\text{ref}} - x_{\text{eval}}\right| \leq L_{\text{z}}/2 \quad \text{mm}$$

$$\left|y_{\text{ref}} - y_{\text{eval}}\right| \leq L_{\text{z}}/2 \quad \text{mm}\,.$$

Otherwise, the data-processing and measurement systems should use a finer grid resolution and/or a larger number of interpolation points to repeat the assessment starting at step b).

e) The centre of the *area scan* (x_0, y_0) should be shifted in 1 mm steps within the range $0 < x_0 \leq \Delta x/2$ and $0 < y_0 \leq \Delta y/2$ to repeat the assessment starting at step b) for each of the shifted (x_0, y_0) in these ranges.

7.2.4.3.2 Evaluation of the *zoom scan*

The *zoom scan* is evaluated by comparing the highest 1 g or 10 g SAR values with the reference SAR values in 7.2.4.2. From the *area scan* procedure in 7.2.4.3.1, the true peak location (x_{ref}, y_{ref}) will be displaced from the estimated peak location (x_{eval}, y_{eval}) by an amount given by inequalities.

$$\left|x_{\text{ref}} - x_{\text{eval}}\right| \leq L_{\text{z}}/2 \quad \text{mm}$$

$$\left|y_{\text{ref}} - y_{\text{eval}}\right| \leq L_{\text{z}}/2 \quad \text{mm}$$

This displacement is accounted for in the reference functions f_1, f_2, and f_3 in 7.2.4.2 by incorporating the distance d. Since this displacement will vary in practice, the value of d should be varied over the range:

$$|d| \leq (L_{\text{z}} - L_{\text{c}})/2$$

where L_{c} is the cube side length (10 mm for 1 g, 21,5 mm for 10 g). For each distance d, the largest uncertainty produced by any of the three functions is recorded. The root-mean-square of the largest uncertainty values for several distances d is entered as the uncertainty due to extrapolation, interpolation and integration.

NOTE Although the requirement for the *area scan* is that the local peak SAR is located within $|d| \leq L_{\text{z}}/2$, a smaller range of $|d| \leq (L_{\text{z}} - L_{\text{c}})/2$ is used here to ensure that the 1 g or 10 g cube can be computed on the first attempt. For values of $(L_{\text{z}} - L_{\text{c}})/2 < |d| \leq L_{\text{z}}/2$, the measurement software should alert that the 1 g or 10 g cube is not captured and the measurement should be re-attempted. This will not affect the uncertainty, so it is not necessary to consider this case here.

a) Choose a displacement d for the evaluation of the functions f_1, f_2 and f_3. d should vary from $-(L_{\text{z}} - L_{\text{c}})/2$ to $+(L_{\text{z}} - L_{\text{c}})/2$ in small increments (e.g., 1 mm steps). The displacement should also vary separately in the x and y directions.

b) SAR values are computed according to the functions f_1, f_2 and f_3, at the evaluation grid points that correspond to measured *zoom-scan* volume points. The *zoom-scan* volume should be centred at

$$(x, y, z) = (0, 0, L_{\text{h}}/2 + d_{\text{be}})$$

where

L_h is the height of the *zoom-scan* volume, and

d_{be} is the distance of the closest measurement point from the inner surface.

c) The computed SAR values are extrapolated to the phantom surface at $z = 0$ by the system software to obtain the additional points in the *zoom-scan* volume that cannot be measured due to probe constraints. Both the computed and extrapolated data points are then interpolated to a finer resolution by the system software, which subsequently applies the integration algorithms as well as the search algorithm for finding the peak spatial-average SAR within the *zoom-scan* volume to determine the highest 1 g or 10 g SAR. Other procedures are possible. If the system does not allow SAR values to be imported to perform the assessment, the same algorithm shall be implemented independently by other means to test the extrapolation, interpolation and integration algorithms.

d) The 1 g and 10 g SAR values determined by the system or data processing software ($\mathrm{SAR}_{\mathrm{eval}}$) are compared to the reference SAR values given in 7.2.4.2. The SAR uncertainty for each distribution function is calculated using equation

$$\mathrm{SAR}_{\mathrm{uncertainty}}[\%] = 100 \times \left| \frac{\mathrm{SAR}_{\mathrm{eval}} - \mathrm{SAR}_{\mathrm{ref}}}{\mathrm{SAR}_{\mathrm{ref}}} \right|$$

e) The highest SAR uncertainty estimated by either of the three distribution functions is recorded.

f) Repeat steps b) to d) for other displacement values *d*.

g) Compute the root-mean-squared value of the uncertainties calculated in step d) for each displacement *d* above. This value should be entered as the uncertainty due to extrapolation, interpolation and integration in the corresponding row and column of Table 3.

h) Record the following parameters used to estimate the *zoom-scan* uncertainty:

- the dimension of the grid used to sample the reference functions both in terms of number of points and sample steps in the three dimensions;
- the number of interpolation points included between two test points, or the interpolation resolution in the three directions, for the reference functions.
- the dimension d_{be} of the extrapolation region, i.e., the distance between the probe sensor location at the first measurement point and the phantom surface (measurement point is behind the probe tip).
- the interpolation, extrapolation and averaging algorithms used.

The computational conditions (such as the number of grid points, the grid increments, and the number of interpolation points in the three directions) shall be the same for all the functions.

7.2.4.4 Evaluation of curved surfaces

The procedures in 7.2.4.3 assume that the tissue-equivalent liquid and phantom boundary is planar. However, the uncertainty estimated with these functions for flat tissue-equivalent liquid and phantom boundaries is also valid for smooth curved surfaces. The fact that the function is based on a flat surface does not provide any restrictions with respect to applicability for the test provided the procedure is based on equivalent distances of the grid from surfaces. This produces the averaging volumes as illustrated in Figure 10. However, the uncertainty estimated with these functions for flat tissue-equivalent liquid and phantom boundaries is also valid for smooth curved surfaces. Figure 10 illustrates an acceptable method for shaping the cube during SAR post-processing. The front face of the volume facing the phantom/liquid interface conforms to the curved boundary, to ensure that all SAR peaks are captured. The back face should be equally distorted to maintain the correct averaging mass. The flatness and orientation of the four side faces are unchanged.

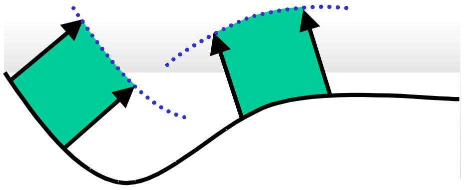

Figure 10 – Orientation and surface of the averaging volume relative to the phantom surface

7.3 Uncertainty estimation

7.3.1 Combined and expanded uncertainties

The contributions of each component of uncertainty shall be recorded with description, probability distribution, sensitivity coefficient and uncertainty value. A recommended tabular form is shown in Table 3. The combined standard uncertainty u_{c} shall be estimated according to the following formula:

$$u_{\mathrm{c}} = \sqrt{\sum_{i=1}^{m} c_i^2 \cdot u_i^2}$$

where c_i is the sensitivity coefficient, and u_i is the standard uncertainty. The expanded uncertainty U shall be estimated using a confidence interval of 95 %.

7.3.2 Maximum expanded uncertainty

The expanded uncertainty with a confidence interval of 95 % shall not exceed 30 % for peak spatial-average SAR values in the range from 0,4 to 10 W/kg. If the uncertainty is greater than 30 %, reported data may need to take into account the percentage difference between the actual uncertainty and the 30 % target value.

Table 3 – Measurement uncertainty evaluation template for handset SAR test

A	*b*	*c*	*d*	*e* = *f*(*d*,*k*)	*f*	*g*	*h* = *c* x *f* / *e*	*i* = *c* x *g* / *e*	*k*
Source of uncertainty	**Descrip-tion**	**Tolerance/ uncertainty ± %**	**Probability distribution**	**Div.**	**c_i (1 g)**	**c_i (10 g)**	**Standard uncer-tainty ± %, (1 g)**	**Standard uncer-tainty ± %, (10 g)**	**ν_i or ν_{eff}**
Measurement system									
Probe calibration	7.2.1		N	1	1	1			∞
Isotropy	7.2.1.2		R	√3	1	1			∞
Boundary effect	7.2.1.5		R	√3	1	1			∞
Linearity	7.2.1.3		R	√3	1	1			∞
Detection limits	7.2.1.4		R	√3	1	1			∞
Readout electronics	7.2.1.6		N	1	1	1			∞
Response time	7.2.1.7		R	√3	1	1			∞
Integration time	7.2.1.8		R	√3	1	1			∞
RF ambient conditions – noise	7.2.3.6		R	√3	1	1			∞
RF ambient conditions – reflections	7.2.3.6		R	√3	1	1			∞
Probe positioner mech. restrictions	7.2.2.1		R	√3	1	1			∞
Probe positioning with respect to phantom shell	7.2.2.3		R	√3	1	1			∞
Post-processing	7.2.4		R	√3	1	1			∞
Test sample related									
Test sample positioning	7.2.2.4		N	1	1	1			*M*-1
Device holder Uncertainty	7.2.2.4.2		N	1	1	1			*M*-1
Drift of output power	7.2.3.5		R	√3	1	1			∞
Phantom and set-up									
Phantom uncertainty (shape and thickness tolerances)	7.2.2.2		R	√3	1	1			∞
Liquid conductivity (target)	7.2.3.3		R	√3	0,64	0,43			∞
Liquid conductivity (meas.)	7.2.3.3		N	1	0,64	0,43			*M*
Liquid permittivity (target)	7.2.3.4		R	√3	0,6	0,49			∞
Liquid permittivity (meas.)	7.2.3.4		N	1	0,6	0,49			*M*
Combined standard uncertainty			RSS						
Expanded uncertainty (95 % confidence interval)									

Table 3 *(continued)*

NOTE 1 Column headings *a-k* are given for reference.

NOTE 2 Abbreviations used in this table:

RSS – root sum square

N, R, U – normal, rectangular, U-shaped probability distributions

Div. – divisor used to get standard uncertainty

NOTE 3 The uncertainty components indicated in this table are based on the test procedures and protocols developed for this document. When test protocols and procedures vary, different uncertainty components may apply, e.g., parameters defined for testing other phantom configurations and device positions.

NOTE 4 The divisor is a function of the probability distribution and degrees of freedom (ν_i and ν_{eff}).

NOTE 5 c_i is the sensitivity coefficient that should be applied to convert the variability of the uncertainty component into a variability of SAR.

NOTE 6 See 7.1.3 for discussions on degrees of freedom (ν_i) for standard uncertainty and effective degrees of freedom (ν_{eff}) for the expanded uncertainty.

NOTE 7 *M* in the ν_i column is number of tests.

NOTE 8 Interim dielectric constant tolerance of 10 % may be used for glycol-based liquids at frequencies above 2 GHz.

NOTE 9 Some of the uncertainty influence quantities may be estimated from performance specifications provided by the equipment manufacturers; the uncertainty of certain other components that vary from test to test may need to be estimated for each measurement.

NOTE 10 All influence quantities in this template are applicable for *system validation* testing except the three items in the *Test Sample Related* group are replaced by a *Dipole* group containing two influence quantities described as: Dipole Axis to Liquid Distance, Input Power and SAR Drift.

8 Measurement report

8.1 General

The results shall be recorded, usually in a test report, and shall include all the information necessary for the interpretation of the test or calibration results and all information required by the method used.

Further guidelines on the test report can be found in 5.10 of ISO/IEC 17025.

8.2 Items to be recorded in the test report

All of the information needed for performing repeatable tests, calculations, or measurements giving results within the required calibration and uncertainty limits shall be recorded. The test report should include:

a) General introduction
    1) Referring to DUT
    2) Requirements
    3) Standards used
b) Measurement system
    1) Measurement system
    2) Positioner
    3) Description of interpolation/extrapolation scheme
c) Uncertainty estimation – report of Table 3 in 7.3

d) Device and test details
    1) Description of the device / Serial number, e.g., IMEI (International Mobile Equipment Identity)
    2) Testing condition (temperature, etc.)
    3) Liquids used and characteristics
    4) Results of *system validation* check
    5) Results of tests performed (peak spatial-average SAR value for each test, and graphical representation of the coarse scans with respect to the device for the maximum SAR value of each mode).
e) Report Summary
    1) SAR values over the testing positions, bands, modes and antenna configurations
    2) If applicable, reference to basic restriction recommendation and a statement of compliance, or otherwise.

Annex A
(normative)

Phantom specifications

A.1 Rationale for the phantom shape

Phantom body-parts are essential components of electromagnetic dosimetry. While it is desirable that they emulate the anatomical details of the body part they represent, it is not always necessary or practical for them to do so. It is therefore important to define and standardise the relevant features, dimensions and material properties that affect SAR measurement.

The statistical breakdown of anatomical shapes and sizes can be obtained from anthropometric studies of human population to guide the specification of a realistic phantom shape. A 1988 anthropometric study of U.S. army personnel provides data based on a sample of mixed age, race, and ethnic identity [18]. The shape of the head is defined by a number of lines and curves as illustrated in Figure A.1.

Dosimetric studies suggest that larger heads (adult, male user) couple more energy and constitute a worst case exposure scenario compared to smaller heads (women and children) [34], [35], [58]. A 90th-percentile large (adult male) head dimension shall be used to ensure that well over 90 % of all users have smaller heads and would therefore sustain a lower exposure.

The back ear protrusion has a direct effect on determining the closeness of the mobile device and antenna to the head and is an important parameter for determining SAR. The ear protrusion has to be adjusted to simulate the pressure of the device on the ear. The shape of the ear is a factor in positioning the mobile device and shall be designed to enable correct and reproducible positions.

With respect to modelling the hand, there are practical difficulties in specifying a unique hand holding position that is applicable to all mobile devices. Moreover, dosimetric studies suggest that not modelling the hand constitutes a conservative case scenario for SAR in the head [31]. For these reasons, in this standard the mobile device is not held in a hand model during SAR evaluations.

A.2 SAM phantom specifications

The dimensions have been derived from the Gordon report [18], and are listed in Table A.1 and shown in Figure A.1. Table A.1 shall take precedence over Figure A.1. Specific guidelines have been added to consider the particular condition of using a mobile device near the ear and cheek, as reported in Table A.2. Particularly, at the ear reference point (ERP), a thickness of 6 mm including the 2 mm shell is selected to model the external ear (pinna). This thin ear spacer also simulates users with small ears, and gives a conservative SAR representation. A system of reference points and reference lines shall be used to correlate the handset positioning with the phantom (Figure A.2). The point “M” is the mouth reference point, “LE” is the left ear reference point (ERP), and “RE” is the right ERP. The ERPs are 15 mm posterior to the entrance to ear canal (EEC) along the B-M Line (back-mouth) (Figure A.2).

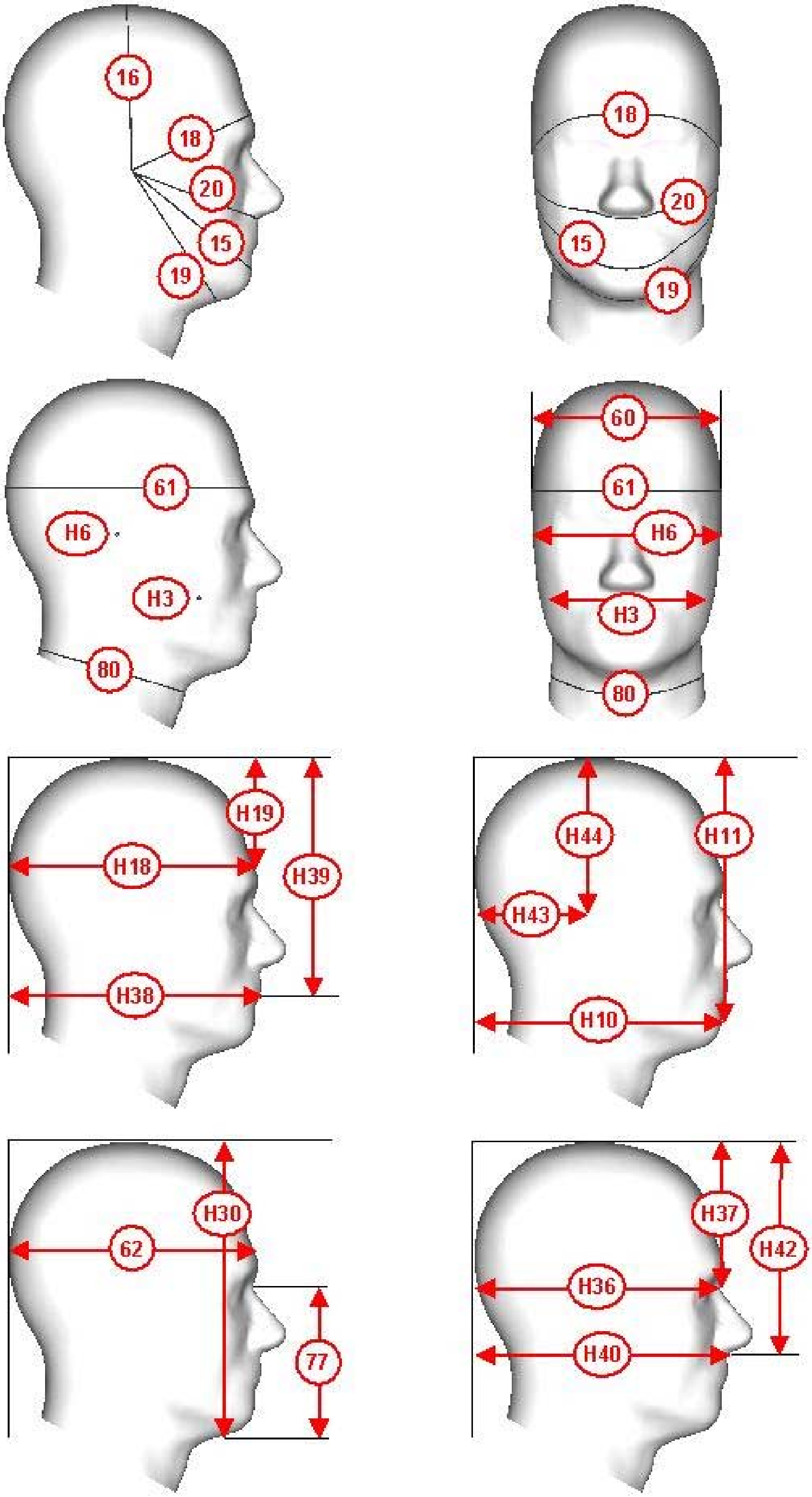

Key

Hx, xX Reference distances as specified in Table A.1

Figure A.1 – Illustration of dimensions in Table A.1

Table A.1 – Head dimensions relevant to phantom shape: SAM dimensions compared to 90th-percentile large male head from Gordon report [18]

Ref.	Anatomy	Gordon report mm			SAM mm	Deviation %
		Mean value	Standard deviation	90th percentile		
H3	Bigonial breadth	118,9	7,9	129,2	130,0	0,6
H6	Bitragion breadth	144,8	6	152,3	152,7	0,2
H10	Chin-Back of head	194,2	10,3	207,3	206,5	-0,4
H11	Chin-Top of head	216,8	8,9	228,3	220,4	-3,5
H18	Glabella-Back of head	199,7	7,2	208,5	209,2	0,3
H19	Glabella-Top of head	96,2	7,3	105,6	104,4	-1,1
H30	Menton-Top of head	232,0	8,8	243,3	246,7	1,4
H36	Sellion-Back of head	197	7,1	205,9	205,3	-0,3
H37	Sellion-Top of head	112	6,9	120,9	121,7	0,7
H38	Stomion-Back of head	199,4	9,6	211,9	211,4	-0,2
H39	Stomion-Top of head	186,3	7,8	196,3	196,3	0,0
H40	Subnasale-Back of head	203,5	8,3	213,6	213,0	-0,3
H42	Subnasale-Top of head	161,9	7,7	171,8	177,6	3,4
H43	Tragion-Back of head	98,9	8,5	106,4	106,4	0,0
H44	Tragion-Top of head	131	5,7	138,2	138,2	0,0
15	Bitragion chin arc	325,8	13,4	343,1	329,3	-4,0
16	Bitragion coronal arc	353,3	12,9	369,7	367,3	-0,6
18	Bitragion frontal arc	304,3	10,6	318,2	314,1	-1,3
19	Bitragion submandibular arc	304,2	14,5	323,2	333,5	3,2
20	Bitragion subnasal arc	292	11,1	306,3	305,3	-0,3
60	Head breadth	151,7	5,4	158,6	158,4	-0,1
61	Head circumference	567,7	15,4	587,3	594,8	1,3
62	Head length	197,1	7,1	206	206,0	0,0
77	Menton-Sellion length	121,9	6,5	130,4	125,0	-4,1
80	Neck circumference	379,6	19,7	405,3	395,4	-2,5

Table A.2 – Specific guidelines for the design of SAM phantom and CAD file

Ref.	SAM guidelines
SG1.	The reference plane is defined by left and right tragion as well as stomion (mouth)
SG2.	The ear reference point (ERP) is in the reference plane at a distance of 15 mm from tragion
SG3.	The thickness of the shell at the position of ERP is 6 mm
SG4.	N-F line on outer surface is straight 60 mm long and included in plane perpendicular to reference plane
SG5.	N-F line on outer surface is tilted in plane perpendicular to the reference plane so that the contact point in the cheek position between a flat device and the outer surface is on the reference line
SG6.	B-M line on outer surface is straight from ERP to upper part of the ear, and shell thickness along this line portion is less than 6 mm
SG7.	Outer surface of the ear is flat and defined by NN-F line and B-MMB' line overall thickness of the shell is 2 mm except ear region
SG8.	There must be no S-shape in cheek region of the cut planes parallel to the reference plane from H-30 mm to H+30 mm
SG9.	Thickness of the shell is measured as distance normal to the inner surface

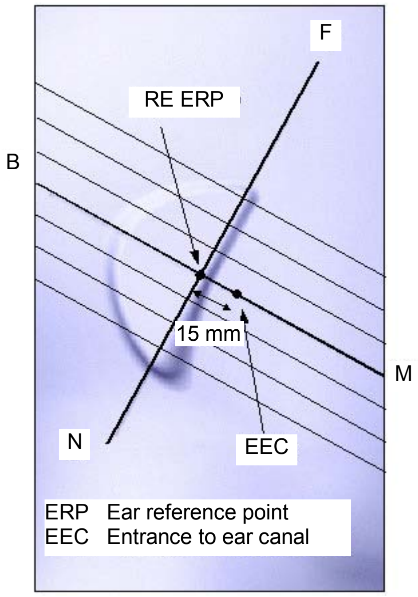

Key

B	Direction of B-M line back endpoint
F	Direction of N-F line front endpoint
N	Direction of N-F line neck endpoint
M	Mouth reference point
RE	Right ear reference point (ERP)

Figure A.2 – Close up side view of phantom showing the ear region

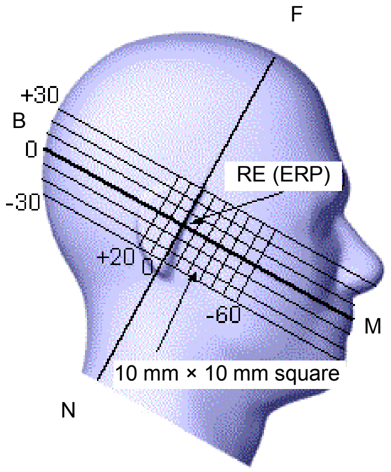

Key

Dimensions in millimetres

B	Line B-M back endpoint (information only – mark on phantom not required)
F	Line B-M front endpoint (information only – mark on phantom not required)
N	Line N-F neck endpoint (information only – mark on phantom not required)
M	Line N-F front endpoint (information only – mark on phantom not required)
RE	Right ear reference point (ERP)

Figure A.3 – Side view of the phantom showing relevant markings

NOTE Full-head model is for illustration purposes only–procedures in this standard are derived primarily for the phantom set-up of Figure 2.

The plane passing through the two ear reference points and M is defined as the reference plane. The line N-F (neck-front), also called the reference pivoting line, is along the front truncated edge of the ear. Both N-F and B-M lines should be marked on the external phantom shell to facilitate handset positioning. Posterior to the N-F line, the thickness of the phantom shell with the shape of an ear is a flat surface 6 mm thick at the ERPs. Anterior to the N-F line, the ear is truncated as illustrated in Figure A.2. The ear truncation is introduced to preclude the ear lobe from interfering with handset tilt, which could lead to unstable positioning at the cheek.

The projection of the reference line B-M and reference line N-F shall be drawn on the phantom. Additional lines may be chosen for convenience, but the additional lines are optional. The optional markings in Figure A.3 may be etched into the external surface of the phantom without affecting the specifications.

A.3 Tissue-equivalent liquids

To derive appropriate parameters for homogeneous liquids, a simple analytical model of an infinite half-space layered tissue model exposed to a plane-wave was utilized to investigate the impact of impedance-matching, standing-waves, etc., on the peak spatial-average SAR [8]. The tissue layers were varied in composition and thickness to represent the anatomical variation of the exposed head region, covering the user group including adults and children (between the 10th and 90th percentile). Based on the worst-case tissue layer compositions with respect to absorption at each frequency, head tissue-equivalent liquid dielectric parameters for homogeneous modelling were derived resulting in the same (or slightly higher) spatial peak absorption. The Cole-Cole analysis dielectric property data was used, which can be obtained from [17]. The validity of this approach for near-field exposures was demonstrated by replacing the plane-wave by half-wave dipole and quarter-wave monopole sources in the closest proximity to the layered structures, as well as by comparison with results from magnetic-resonance-imaging (MRI)-based non-homogeneous human head models of adults and children from the literature.

Table 1 of 5.2.4 shows the dielectric constant and conductivity of the resulting head tissue-equivalent liquids also as published in [8]. For dielectric properties of head tissue-equivalent liquid at other frequencies within the frequency range, linear interpolations should be used. Suggested formulas for the liquids are listed in Annex I.

Annex B
(normative)

Calibration (linearity, isotropy, sensitivity) of the measurement instrumentation and uncertainty estimation

B.1 Introduction

The measurement instrumentation is composed of the probe, amplifiers and the measurement device. Currently available probes are based on Schottky diode detectors. The measured signal, the output of the probe, is a voltage proportional to E or E^2 depending on the level of RF exposure.

Most isotropic probes consist of three small dipole sensors with orthogonal directivity patterns and detector diodes in the sensor gap. The total electric field can be evaluated as the root sum square of the three E-field components. In the square-law region of the diode response, the sensor output voltage is proportional to the mean square of the corresponding field component. Beyond that range the output voltage is compressed and therefore requires linearization of the dynamic range. Manufacturing tolerances between the sensors and diodes will produce different sensitivities for each sensor.

B.2 Assessment of the sensitivity of the dipole sensors

The sensitivity factors can be determined by applying either “one-step” or “two-step” calibration procedures.

B.2.1 Two-step calibration procedures

The total field shall be evaluated according to:

$$|E|^2 = \sum_{i=1}^{3} |E_i|^2 = \sum_{i=1}^{3} \frac{f_i(V_i)}{\eta_i \gamma_i}$$

where

$f_i\ (V_i)$ is the linearization function of the rectified sensor signal V_i;

η_i are the absolute sensitivities [μ V/(V/m)^2] of the dipole sensors in free space;

γ_i are the ratios of the sensitivities of the probe sensors in media to their sensitivities in free space.

The separation of the probe sensitivity into two factors (η_i and γ_i) allows use of some standardised probe-in-air calibration procedures and provides additional validation of the probe performance and calibration set-up. Calibration is only valid sufficiently far away from any media boundaries. At very close distances, the sensitivity may change. This effect is referred to as a boundary effect, which like isotropy requires separate evaluation.

B.2.1.1 Sensitivity in air (1st step)

The most accurate setups used for the generation of well-defined standard fields and that simulate free-space conditions for use in probe calibration are waveguides. The reasons are as follows:

- waveguide set-ups require moderate power and less space than far-field calibration set-ups,
- generation of the most accurate fields traceable to power readings is possible,
- the uncertainty produced by the field disturbance due to the probe insertion is negligible for small near-field probes when the waveguide dimensions are considerably larger than probe dimensions,
- the set-ups allow easy access for orienting the probe axis normal or parallel to the field polarisation inside the set-up,
- in addition, cross validation of the general field strengths is possible by using a set of waveguides with overlapping frequency ranges.

At lower frequencies (below about 750 MHz), TEM cells can be employed instead. However, the field inside a TEM cell is less well-defined, i.e., there is rather large deviation from the predicted homogeneous field distribution [44]. For example, in some commercial TEM cells fields vary by ±6 % when moving along the central axis from the septum to the outer wall. However, comparisons between the probe response in a TEM cell and within waveguides allows transfer calibration of a specific measurement location inside the TEM cell.

The probe is generally inserted through small holes in the walls of each set-up and positioned at the centre where the field is mostly homogeneous over the probe dimensions. Each sensor is evaluated with respect to the field component parallel to the sensor.

As long as the resistive line does not load the dipole-diode sensor and the probe is small compared to the wavelength, the sensitivity will be independent of the frequency. This gives an additional validation of the calibration set-ups, and checks for eventual possible field perturbations due to the probe. Effects due to probe insertion are typically negligible, if high-quality waveguide couplers and matched sources are used. An additional uncertainty source in the waveguide set-ups is due to reflections from the terminating load, which can result in a standing wave pattern within the set-up. Reflections can be kept below 1 % if high-quality waveguide loads are used. Furthermore, the uncertainty can be compensated by performing supplementary measurements with a $\lambda/4$-shifted load and averaging of two readings.

B.2.1.2 Sensitivity in media (2nd step)

The sensitivity in liquid is determined by generating locally-known field values inside the media. Two methods which can be used are:

- transfer calibration with temperature probe;
- calibration with analytical fields.

B.2.1.2.1 Transfer calibration with temperature probes

In lossy liquids SAR is related both to the electric field (E) and the temperature gradient (dT/dt) in the liquid. Hence, based on the relation:

$$\mathrm{SAR} = \sigma \frac{E^2}{\rho} = c_\mathrm{h} \left.\frac{\mathrm{d}T}{\mathrm{d}t}\right|_{t=0}$$

The electric field in lossy liquid can be measured indirectly by measuring the temperature gradient in the liquid. Non-disturbing temperature probes (optical probes or thermistor probes with resistive lines) with high spatial resolution (<1 mm to 2 mm) and fast response time (< 1 s) are available and can be easily calibrated with high precision [32]. The set-up and the exciting source have no influence on the calibration; only the relative positioning uncertainties of the standard temperature probe and the E-field probe to be calibrated must be considered. However, several problems limit the available accuracy of probe calibrations with temperature probes.

- The temperature gradient is not directly measurable but must be evaluated from temperature measurements at different time steps. Special precaution is necessary to avoid measurement uncertainties caused by temperature gradients due to energy equalising effects or convection currents in the liquid. Such effects cannot be completely avoided, because the measured field itself perturbs the thermal equilibrium in the liquid. With a careful set-up these uncertainties can be kept small.
- The measured volume around the temperature probe is not well defined. It is difficult to calculate the energy transfer from a surrounding gradient temperature field into the probe. These effects must be considered, since temperature probes are calibrated in liquid with homogeneous temperatures.
- The calibration depends on the assessment of the specific density, the heat capacity and the conductivity of the medium. While the specific density and heat capacity can be measured accurately with standardised procedures (~ ±2 % for c_h; much better for ρ), there is no standard for the measurement of the thermal conductivity. Depending on the method and liquid, the uncertainty can well exceed ±5 %.
- Temperature rise measurements are not very sensitive and therefore are often performed at a higher power level than the E-field measurements. The non-linearities in the system (e.g., power measurements, different field components, etc.) must be considered.

Considering these problems, the possible accuracy of the calibration of E-field probes with temperature gradient measurements in a carefully designed set-up is about ±10 % (combined standard uncertainty) [38]. A set-up that is a combination of waveguide techniques and thermal measurements was presented in [27]. The estimated combined standard uncertainty of this set-up is ±5 % when the same liquid is used for the calibration and for actual measurements, and ±7 % to ±9 % when not, which is in good agreement with the estimates given in [38]. When performing an uncertainty analysis of the transfer calibration using a temperature probe, at least the parameters included in Table B.1 should be considered.

Table B.1 – Uncertainty analysis for transfer calibration using temperature probes

Source of uncertainty	Uncertainty value ± %	Probability distribution	Divisor	c_i	Standard uncertainty u_i ± %	v_i or v_{eff}
Positioning of *E*-field probe		N	1	1		∞
Positioning of temp. probe		N	1	1		∞
E-field probe linearity		R	√3	1		∞
Temperature probe drift and noise		R	√3	1		∞
Temperature probe linearity		R	√3	1		∞
Liquid conductivity		R	√3	1		∞
Specific heat of liquid		R	√3	1		∞
Liquid density		R	√3	1		∞
Temperature probe accuracy		R	√3	1		∞
Combined standard uncertainty		RSS				

NOTE 1 c_i is the sensitivity coefficient

NOTE 2 v_i , v_{eff} are the degrees of freedom in the standard uncertainty $u(x_i)$, for the input estimate (x_i); and the effective degrees of freedom in the combined standard uncertainty $u_c(x_i)$, used to obtain $t_p(v_{\text{eff}})$, respectively.

B.2.1.2.2 Calibration with analytical fields (waveguides)

In this method a test set-up is used in which the field can be calculated analytically from measurements of other physical magnitudes (e.g., input power). This corresponds to the standard field method for probe calibration in air; however, there is no standard defined for fields in lossy liquids.

When using calculated fields in lossy liquids for probe calibration, several points must be considered in the estimation of the uncertainty:

- the set-up must enable accurate determination of the incident power;
- the accuracy of the calculated field strength will depend on the assessment of the dielectric parameters of the liquid;
- due to the small wavelength in liquids with high permittivity, even small set-ups with small physical dimensions may be above the resonant mode cut-off frequencies. The field distribution in the set-up must be carefully checked for conformity with the theoretical field distribution.

Rectangular waveguides are self-contained systems in which the cross-sectional field distributions are not dependent upon reflections. Waveguides can be utilised to generate an analytically known field inside tissue-equivalent liquids, e.g., the set-up presented in [52]. In this set-up (see Figure B.1), the upper part of a vertically-oriented open-ended waveguide is filled with liquid. A dielectric slab at a distance > λ from the feeding coupler provides an impedance match (>10 dB return loss) between air and liquid. The symmetry of the construction and high losses in the liquid ensure that the field distribution inside the tissue-equivalent liquid follows the TE_{10} waveguide mode pattern, although higher-order modes theoretically may exist. In [51] the absence of higher modes was carefully validated by a complete volume scan in the liquid, which showed a deviation from the theoretical TE_{10} mode pattern of only < ±1 % to ±2 %.

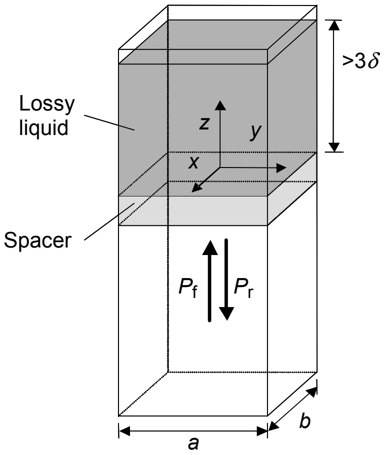

Key

x,y,z	Axes of cartesian coordinate system
3δ	Liquid depth (>3 skin depths)
a	Waveguide cross-section width
b	Waveguide cross-section height
P_f	Incident power
P_r	Reflected power

Figure B.1 – Experimental set-up for assessment of the sensitivity (conversion factor) using a vertically-oriented rectangular waveguide

Inside the liquid, the field propagates almost like a TEM wave, because of the low cut-off frequency. The liquid depth (> 3 skin depths) was chosen so that the reflections at the upper surface of the liquid are negligible. The power absorbed in the liquid is evaluated by measuring forward and reflected power inside the waveguide:

$$\mathrm{SAR}(z) = \frac{4(P_f - P_r)}{\rho a b \delta} \mathrm{e}^{-2z/\delta}$$

where

ab	is the cross-sectional area of the waveguide;
P_f	is the forward power into the waveguide;
P_r	is the reflected power from the waveguide spacer and liquid;
z	is longitudinal coordinate of dipole centres at probe location;
ρ	is the liquid density;
δ	is the skin depth inside the lossy liquid.

NOTE The density ρ is defined to be 1 000 kg/m^3 in for the purposes of this standard.

This technique provides excellent accuracy, with a combined standard uncertainty of <±3,6 % depending on the frequency and media. The calibration itself is reduced to power measurements traceable to a standard calibration procedure. The practical limitation given by the waveguide size to the frequency range between 800 MHz and 2 500 MHz is not severe in the context of compliance testing, because most of the operational frequencies for mobile communications systems are covered within this range. For frequencies below 800 MHz, transfer calibration with temperature probes remains the most practical way to achieve calibration with the lowest uncertainties. When performing an uncertainty analysis of the calibration with analytical fields, at least the parameters included in Table B.2 should be considered.

Table B.2 – Uncertainty template for calibration using analytical field distribution inside waveguide

Source of uncertainty	**Uncertainty value** **± %**	**Probability distribution**	**Divisor**	c_i	**Standard uncertainty** u_i **± %**	v_i **or** v_{eff}
Incident or forward power		R	√3	1		∞
Reflected power		R	√3	1		∞
Liquid conductivity		R	√3	1		∞
Liquid permittivity		R	√3	1		∞
Field homogeneity		R	√3	1		∞
Field probe positioning		R	√3	1		∞
Field probe linearity		R	√3	1		∞
Combined standard uncertainty		RSS				

B.2.2 One-step procedure

The procedure of B.2.1 can be combined into a one-step procedure using reference antennas, as follows.

The total field shall be evaluated according to:

$$|E|^2 = \sum_{i=1}^{3} |E_i|^2 = \sum_{i=1}^{3} \frac{V_i}{K_i}$$

where K_i is the absolute sensitivity of the dipole sensors in the liquid.

Reference antennas are small antennas designed for operating within the appropriate tissue-equivalent liquid. Examples of antennas developed at 900 MHz and 1 800 MHz have been described in [48], [49]. At least 2 identical antennas are necessary to evaluate the gain of the main lobe for use in probe calibration.

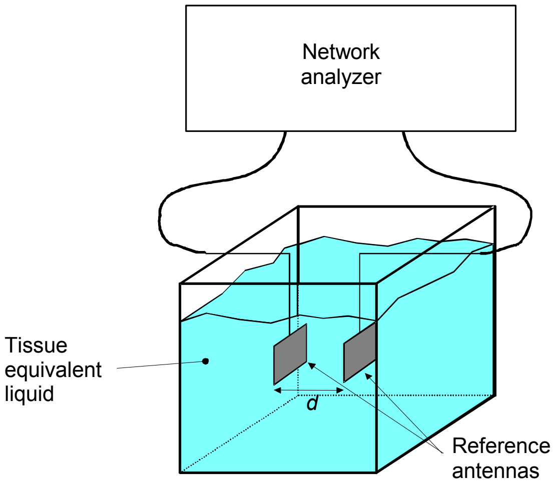

Figure B.2 – Description of the antenna gain evaluation set-up

a) The reference antenna gain evaluation is performed according to the following protocol:

   1) position the antennas in the liquid such that their main-beam axes are aligned and at a well-defined distance d, where $d \geq 2D^2/\lambda_{\text{liquid}}$, D is the largest dimension of the reference antenna, and λ_{liquid} is the wavelength in the liquid. The antennas shall be at least 10 cm from any walls of the liquid container;
   2) measure the reflection coefficients ρ_1 and ρ_2 at the input ports of each antenna;
   3) measure the transmission coefficient S_{21} between the two antennas at the same ports;
   4) the gain is

$$G = \left|S_{21}(d)\right| \times e^{\alpha d}\left(\frac{4\pi d}{\lambda_{\text{liquid}}}\right) \times \frac{1}{\sqrt{\left(1-\left|\rho_1\right|^2\right)\left(1-\left|\rho_2\right|^2\right)}}$$

where the attenuation coefficient is

$$\alpha = \frac{2\pi f}{c} \times \left(\varepsilon_{\text{r}}^{'2} + \varepsilon_{\text{r}}^{''2}\right)^{1/4} \times \sin\left[\frac{1}{2}\arctan\left(\frac{\varepsilon_{\text{r}}^{''}}{\varepsilon_{\text{r}}^{'}}\right)\right]$$

When performing an uncertainty analysis of the reference antenna gain, at least the parameters included in Table B.3 should be considered.

Table B.3 – Uncertainty template for evaluation of reference antenna gain

Source of uncertainty	Uncertainty value ± %	Probability distribution	Divisor	c_i	Standard uncertainty u_i ± %	v_i or v_{eff}
Incident power		R	√3	1		∞
Reflection coefficients		R	√3	1		∞
Distance		R	√3	1		∞
Liquid conductivity		R	√3	1		∞
Liquid permittivity		R	√3	1		∞
Combined standard uncertainty		RSS				

b) The following protocol shall be used for evaluating the sensitivity coefficients of the probe:

1) position one antenna in the tissue-equivalent liquid. The antenna shall be at a minimum distance of 10 cm from the walls of the liquid container;
2) connect a power source to the input port of the reference antenna. The theoretical electric field E_{th} at a distance d from the antenna is:

$$E_{\mathrm{th}} = \left[\left(\frac{P_{\mathrm{in}} \left(1 - |\rho|^2 \right) G e^{-2\alpha d}}{4\pi d^2} \right) \times \left(\frac{120\pi}{\mathrm{Re}\sqrt{\varepsilon_{\mathrm{r}}}} \right) \right]^{1/2}$$

where

d is the distance from the antenna where $d \geq 2D^2 / \lambda_{\mathrm{liquid}}$;,

G is the antenna gain;

D is the largest dimension of the reference antenna;

P_{in} is the input power;

ρ is the reflection coefficient of the antenna

$\lambda_{\mathrm{liquid}}$ is the wavelength in the liquid.

It is recommended to connect a bi-directional coupler to control the input power. Tune the input power so that E_{th} ~ 30 V/m;

3) position the probe in the liquid so that the centre of the detectors is at a distance d from the antenna;
4) orient the probe in order to align the direction of the dipole with the polarisation of the reference antenna;
5) measure the voltage signal at the port of the probe related to the exposed dipole $V_{1,\mathrm{meas}}$;
6) the sensitivity coefficient K_1 for this dipole is $K_1 = \dfrac{V_{1,\mathrm{meas}}}{E_{\mathrm{th}}^2}$;
7) repeat steps 4) to 6) for the other two dipoles to evaluate K_2 and K_3.

Using the sensitivity coefficients of the probe, SAR is determined by the equation:

$$\mathrm{SAR} = \frac{\sigma}{\rho}\left(\frac{V_1}{K_1} + \frac{V_2}{K_2} + \frac{V_3}{K_3}\right)$$

where ρ is the density (1 000 kg/m^3).

When performing an uncertainty analysis of the calibration with reference antennas, at least the parameters included in Table B.4 should be considered.

Table B.4 – Uncertainty template for calibration using reference antenna

Source of Uncertainty	**Uncertainty value ± %**	**Probability distribution**	**Divisor**	c_i	**Standard uncertainty** u_i **± %**	v_i **or** v_{eff}
Incident power		R	√3	1		∞
Reflection coefficients		R	√3	1		∞
Antenna gain		N	1 or k	1		∞
Liquid conductivity		R	√3	1		∞
Liquid permittivity		R	√3	1		∞
Probe positioning		R	√3	1		∞
Combined standard uncertainty		RSS				

B.3 Isotropy

B.3.1 Axial isotropy

The probe shall be exposed to a reference wave incident normally with respect to the major axis of the probe. The axial isotropy is determined by rotating the probe along its major axis from 0° to 360° with a step size less than or equal to 15°.

B.3.2 Spherical and hemispherical isotropy

The probe shall be exposed to a reference wave with varying angles of incidences. The hemispherical isotropy shall be determined by rotating either the probe or the polarisation of the reference wave. The angles of incidence shall vary from 90° (axial) to 0° (normal) with a step size less than or equal to 30°. For each incidence angle, the probe shall be rotated through a range of 360° and a step size less than or equal to 15°.

The following three methods can be used for hemispherical isotropy, each producing similar results:

- flat phantom with dipole at side,
- flat phantom with dipole beneath,
- spherical phantom with dipole.

B.3.3 Isotropy with flat phantom and dipole at side

The set-up consists of a thin plastic box filled with tissue-equivalent liquid exposed to a half-wave resonant dipole operating at the test frequency. The following protocol shall be used for evaluating the spherical isotropy of the probe:

a) mount the dipole antenna on a turntable and position it parallel to the flat phantom (see Figure B.3). The antenna shall be positioned at a maximum distance of $e = \lambda/10$ from the adjacent wall of the liquid container;

b) insert the probe vertically in the liquid so that the centre of the three probe sensors is positioned in the extension of the dipole axis;

c) the horizontal placement of the probe shall be, whenever possible, at the maximum of the standing wave near the back side of the box, at a distance *d* from the phantom/liquid interface, where the *E*-field is partially homogeneous and the *H*-field is at a minimum. The measurement can also be performed in a gradient field. (The maximum of the *E*-field can be assessed by performing a line scan in the *x*-direction),

d) the dipole shall be rotated around its axis from at least 0° to 90° with incremental steps of less than or equal to 30°,

e) at each step the probe is rotated about its axis from 0° to 360° by the probe positioner and measurement data is recorded in steps of less than or equal to 15°,

f) the deviation from spherical isotropy is then expressed as the maximal SAR deviation from the average values among all measured probe positions (± xx dB).

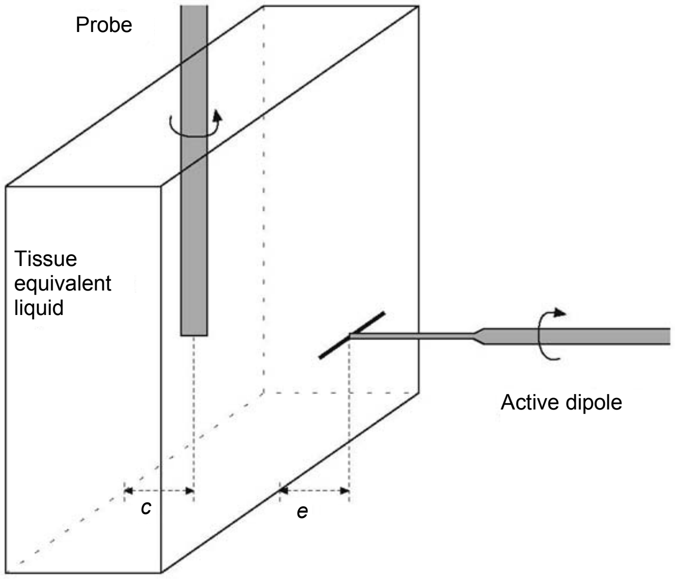

Key

c	Distance from probe to backwall
e	Maximum distance from the adjacent wall of the liquid container

NOTE The assessment is preferably performed in the location *c* of minor field gradients resulting from the standing wave. The dimension *e* is the distance between the dipole axis feedpoint and the liquid surface.

Figure B.3 – Set-up to assess spherical isotropy deviation in tissue-equivalent liquid

B.3.4 Isotropy with flat phantom and dipole beneath

An alternative set-up for isotropy evaluation is shown in Figure B.4. A half-wave dipole mounted on a holder is positioned with arms parallel to and below a flat phantom filled containing tissue-equivalent liquid. A probe is positioned at a point directly above the dipole feed-point. A probe is inserted and positioned at the same measurement location above the dipole feed-point. All probe rotations are performed and controlled by a high-accuracy positioner. The rotation of the probe about its axis (ϕ rotation from 0° to 360°), along with dipole rotation (θ rotation from 0° to 180°) and change of probe inclination angle ϑ (from 0° to 75°), produces a 3-D evaluation of a significant portion of the hemispherical receiving pattern.

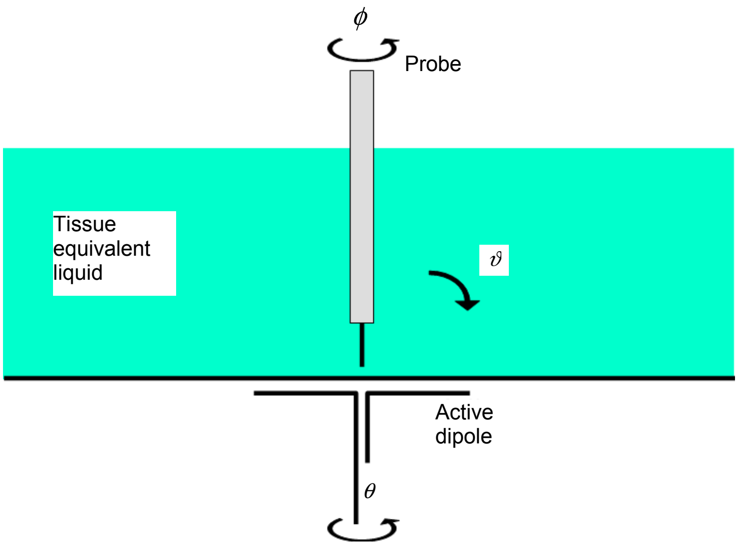

Key

ϑ	Probe axis tilt angle
θ	Rotation angle of the dipole axis
ϕ	Probe axis rotation angle of the probe

Figure B.4 – Alternative set-up to assess spherical isotropy deviation in tissue-equivalent liquid

B.3.5 Isotropy with dipole and spherical phantom

The isotropy of the probe receive pattern over an entire hemisphere can be assessed using a set-up comprised of a mixture-filled spherical flask and an external dipole [11]. The hemispherical receiving pattern of the probe can be obtained by positioning the probe sensors in the geometrical centre of the flask and completely rotating the probe about its axis under several different excitation conditions (impinging wave incidence angle and polarization) provided by the external dipole antenna. In this set-up, the probe positioner is not required to tilt and simultaneously rotate the probe.

The measurement set-up, shown in Figure B.5, consists of a balloon flask that is filled with tissue-equivalent mixture. The probe is vertically positioned with its sensors at the volumetric centre of the sphere. The excitation is provided by an external half-wave dipole tuned to the desired operating frequency. The dipole is held parallel to the tangent plane at the closest point on the sphere.

NOTE Smaller flasks may be preferred because increased mixture conductivity or operating frequency implies a higher path-loss for the wave transmitted to the probe. Larger flasks feature a locally flatter surface (longer curvature radius), which produces a locally flatter wave front impinging on the probe tip and relaxes the tolerance on the position of the dipole.

Figure B.6 shows the conventions used to describe the antenna position and polarization. A 3-D measurement of the probe receive pattern over a hemisphere is accomplished by rotating the probe by 360° around its axis (ϕ) while positioning the external dipole at angles $0° \leq \xi \leq 360°$. Every desired polarization of the impinging wave is achieved by rotating the dipole around its axis $0° \leq \theta \leq 180°$. Multiple θ-positions are not needed when $\xi = 0°$. While a large number of measurement points is possible with this set-up, usually steps of 30° in ξ and 15° in θ are sufficient for characterization.

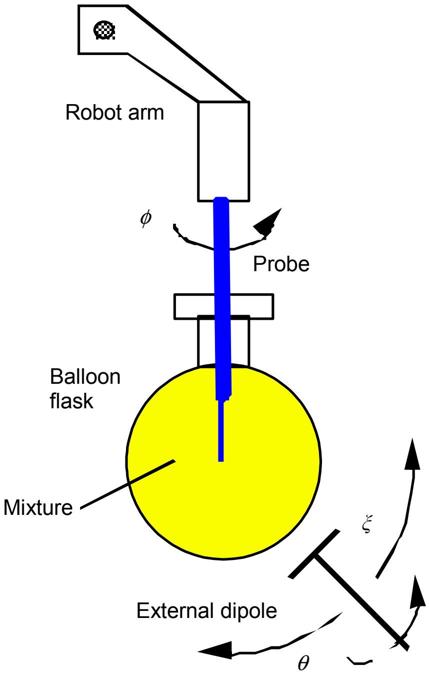

Key

ξ	Elevation angle to dipole axis
θ	Dipole element rotation angle
ϕ	Probe axis rotation angle

Figure B.5 – Experimental set-up for the hemispherical isotropy assessment [11]

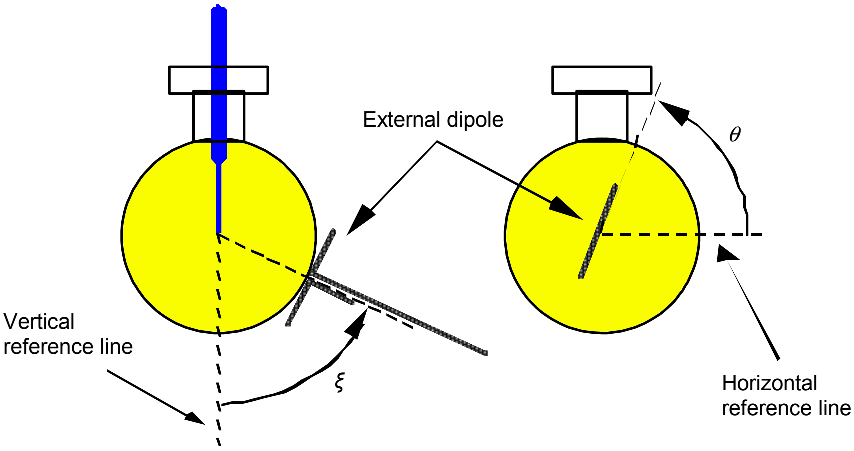

Key

ξ	Elevation angle to dipole axis
θ	Dipole element rotation angle

Figure B.6 – Conventions for dipole position (ξ) and polarization (θ) [11]

Preliminary measurements should ensure that the sensor diodes operate in the square-law region for the given power emitted by the dipole. The measurements consist of complete 360° rotations of the probe for each dipole position and polarization (ξ,θ). The power radiated during each rotation should be monitored and recorded for every ϕ-position of the probe, and the SAR samples should be normalized to a nominal value. Although it cannot be a priori excluded, there is no particular reason why any positions and polarizations of the external dipole other than what is considered here should produce significantly worse isotropic performance. However, the matrix of tests can be expanded to include any particular case of interest, e.g., polarization conditions that match the sensor orientation in some probes.

As with the flat-phantom isotropy test, a rectangular uncertainty distribution is assumed. However, proper experimental practices can substantially reduce this uncertainty, such as for the case where probe calibration is performed under a specific polarization and direction of the impinging wave, and then essentially the same conditions are maintained during SAR measurements.

B.3.6 Isotropy with reference antennas

The following protocol shall be used for evaluating the isotropy of the probe using the reference antenna set-up:

a) position one antenna in the tissue-equivalent liquid. The antenna shall be at a minimum distance of 10 cm from the walls of the liquid container;

b) position the probe in the liquid so that the centre of the detectors is at a distance d from the antenna, where $d \geq 2D^2 / \lambda_{\text{liquid}}$, D is the largest dimension of the reference antenna, and λ_{liquid} is the wavelength in the liquid. It is recommended that the SAR value is set to between 0,5 and 1 W/kg at this position;

c) orient the probe axis so that its main axis is orthogonal to the direction of the exposure from the antenna (see Figure B.7);

d) rotate the probe along its main axis from 0° to 360° with a step size less than or equal to 15°. Record the SAR values. The axial isotropy is defined by the SAR deviation from the r.m.s. value;

e) vary the incidence of the reference field by rotating the reference antenna or the probe axis (see Figure B.8) from 0° to 90° with a step size of 15° or 30°;

f) for each incidence angle, rotate the probe along its main axis from 0° to 360° with a step size less than or equal to 15°. Record the SAR values;

g) the hemispherical isotropy is defined by the SAR deviation from the r.m.s. value among non- normal incidence exposure of the probe.

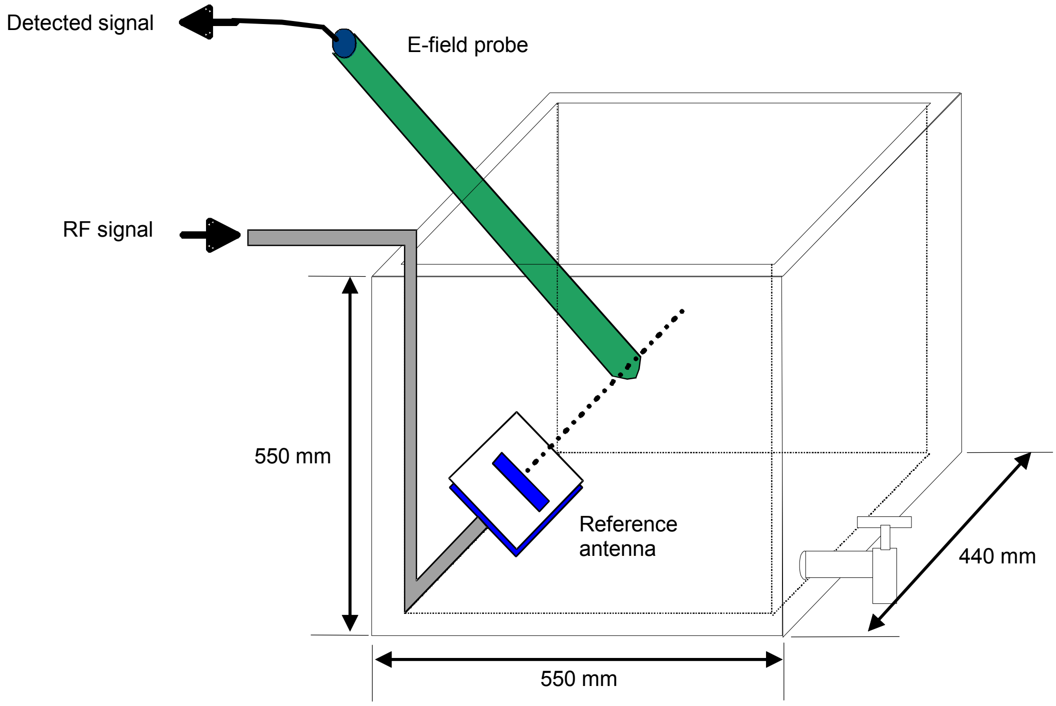

Figure B.7 – Measurement of axial isotropy with a reference antenna

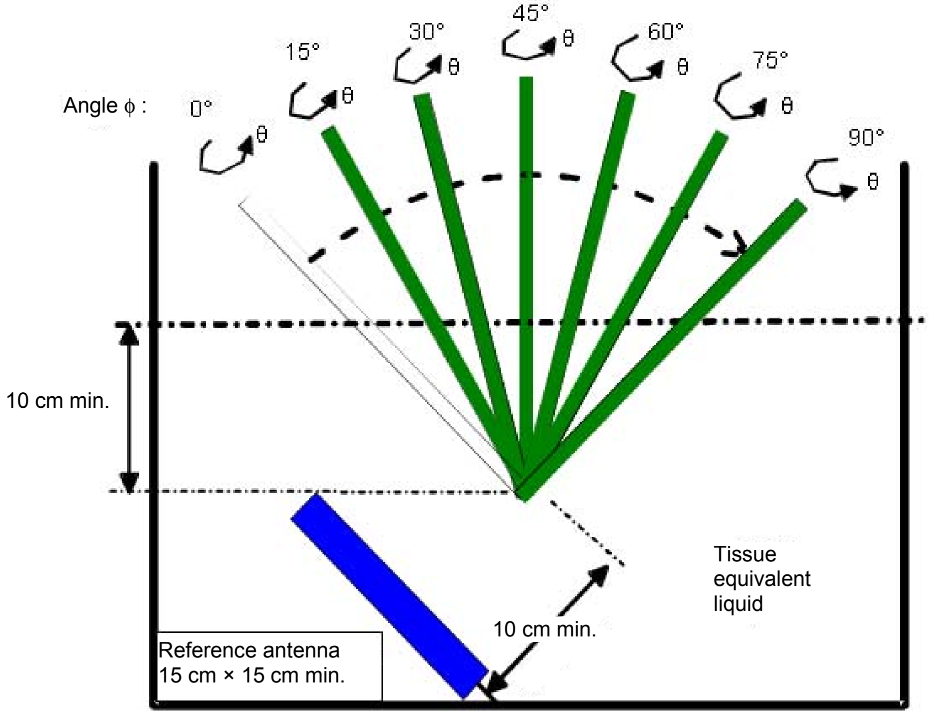

Key

θ	Probe axis rotation angle
Φ	Probe axis tilt angle

Figure B.8 – Measurement of hemispherical isotropy with reference antenna

B.4 Linearity

Since the non-linear response of the probe depends only on the characteristics of the diode, the evaluation of the linearising functions may be done either in free space or in the tissue-equivalent liquid. This is performed by a power sweep covering the requested detection range. Small TEM cells, waveguides or reference antennas can be used, since high field strengths can be produced with medium power amplifiers.

The linearity error is defined by the maximum deviation over the measurement range of the measured quantity from the closest linear reference curve defined over the interval 0,01 W/kg – 100 W/kg. The evaluation can be performed by using one of the set-ups described in Clause B.2 or Figure D.1. The power shall be increased in steps not larger than 1 dB over the interval of 0,01 W/kg to 100 W/kg.

B.5 Lower detection limit

The lower detection limit is related to the noise level, offset and asymmetry of the measurement system. Saturation and other non-linearity effects define the upper detection limit. The lower and upper limit can be assessed with various set-ups, e.g., the test set-up of clause B.2, Figure D.1, etc. Lower detection limit is defined as the level from which the response deviates from linearity by more than 0,5 dB (see also clause B.4). In actual operational conditions of the measurement system, the lower detection limit may be impaired by the background electromagnetic environment.

B.6 Boundary effects

In the closest vicinity of the inner surface of the phantom shell, the sensitivity deviates from what is determined in normal calibration conditions. This deviation shall be evaluated by using a field distribution inside a flat phantom that approximately corresponds to that of a plane wave exposure. To determine this effect, a set-up similar to the one described in Figure D.1 can be used, whereby the boundary effect is defined as the deviation between the SAR measured data and the expected exponential decay in the liquid when the probe is oriented normal to the interface. This effect can be largely compensated as described in [51], [53]. The uncertainty of the procedure shall be evaluated according to 7.2.1.5.

B.7 Response time

The probe shall be exposed to a reference wave. The response time is the time required by the measurement equipment to reach 90 % of its final value after a step variation or switch on/off of the power source. The step shall be defined to provide at least 0,4 W/kg local SAR.

Annex C
(normative)

Post-processing techniques and uncertainty estimation

C.1 Extrapolation and interpolation schemes

C.1.1 Introduction

The local SAR inside the phantom is measured using small dipole sensing elements enclosed in a probe cover/case. Probe calibration and hence *E*-field measurement are usually done with respect to the geometric centre of the internal dipole set. It is necessary to account for the fact that dipoles are a few millimetres from the physical tip of the probe when defining the measurement positions. In order to minimise measurement uncertainties the probe tip shall not be in contact with the phantom surface, although the highest local SAR will usually occur at the surface of the phantom. These highest local SAR values are essential to determine the peak spatial-average SAR, and must be obtained by extrapolation from measurements done at several distances from the shell. The accurate assessment of the peak spatial-average SAR requires a very fine resolution in the three-dimensional scanned data array. Because the measurements shall be performed over a limited time period, e.g., due to battery life duration, the measured data shall be interpolated to provide an array with sufficient resolution. The uncertainty resulting from the interpolation, extrapolation, integration, and averaging procedures is derived assuming no uncertainties in location of the measurement points.

C.1.2 Interpolation schemes

Interpolation can be performed using various mathematical techniques such as statistics [13], basis function curvefits [33], Fourier analysis [12] and wavelet [14] or polynomial or spline curvefits [63]. Various numerical analysis textbooks, e.g., [55], describe how to implement some of these methods.

C.1.3 Extrapolation schemes

Extrapolation can be performed using splines, biharmonic splines, wavelets, polynomials, or rational functions. Various computational mathematics books describe how to implement some of these methods. Because the accuracy of the extrapolation depends on the distance and on the field distribution being extrapolated, the uncertainty associated with the extrapolation shall be estimated carefully.

C.2 Averaging scheme and maximum finding

C.2.1 Introduction

The cubical volumes evaluated to average the local SAR measurements after extrapolation and interpolation shall be close to the phantom surface in order to include the highest values of local SAR. In post-processing, the averaging cube should therefore be rotated and shifted to be co-incident with the surface.

C.2.2 Choice of the cube

C.2.2.1 Method of the three points

A cube face may be fitted to the phantom surface by orienting it such that three of its vertices are co-incident with the surface. The positions of the remaining five vertices of the cube can then be identified. The space between the cube and the phantom surface shall be included in the averaging volume because it is likely to be a region of high localised SAR. This may be accomplished by distorting the surface of the cube to conform to the concave inner surface of the phantom, then distorting the opposite surface of the cube in the same way to maintain a 1 g or 10 g averaging mass. The 3 locating points should be scanned over the phantom surface in order to evaluate the maximum SAR occurring over any 1 g or 10 g cube. Figure C.1 illustrates the method of three points.

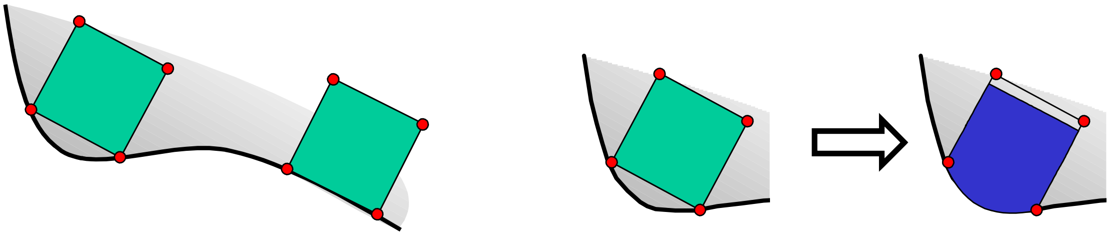

Figure C.1 – Methods of three points

C.2.2.2 Method of the tangential face

Another method is to choose a point on the phantom surface and define this to be co-incident with the centre of one cube face. Two tangential vectors are then evaluated and these can be used to arrange the surface of the cube at a tangent to the phantom surface. The remaining faces of the cube are then located before the cube is rotated about a vector normal to the phantom surface in order to evaluate the peak spatial-average SAR. As with the previous method, the surface of the cube in contact with the phantom shell shall be made conformal in order to fully include the region of highest localised SAR. The opposite face of the cube is then either extended or contracted in order to maintain a 1 g or 10 g averaging mass. The cube should be scanned and rotated at points along the surface of the phantom in order to find the maximum SAR over any 1 g or 10 g cube. Figure C.2 illustrates the method of the tangential face.

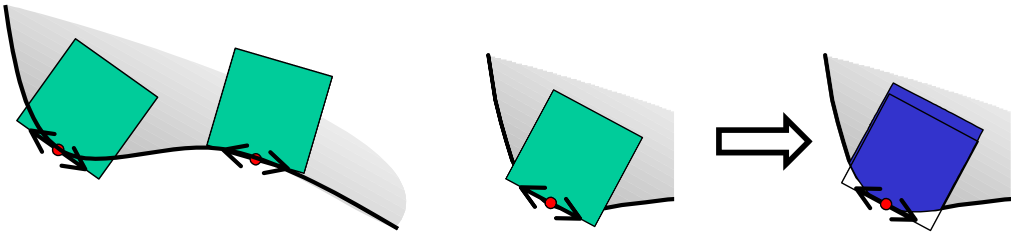

Figure C.2 – Method of the tangential face

C.2.2.3 Method of averaging

The main objective is to obtain an averaging mass of 1 g or 10 g. To achieve this, SAR points may be added layer by layer to make the cube grow until its mass exceeds 1 g or 10 g. Then, the corresponding absorbed power may be deduced by linear interpolation. Figure C.3 illustrates the method of averaging.

NOTE Usually, the averaging cube is described in a staircased form due to the grid on which the measurement points have been interpolated. Though an interpolation could be done especially for the cube, such a method is time-consuming because the interpolation is different for each averaging cube.

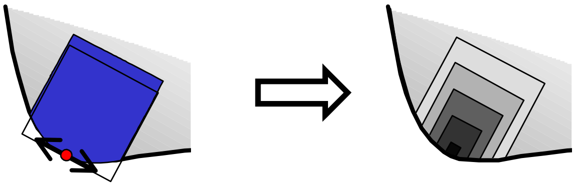

Figure C.3 – Method of averaging

C.2.3 Extrude method of averaging

The method of averaging is intrinsically simple since the cube essentially conforms to the measurement grid, or at least conforms to the extrapolated and interpolated data grid. The peak spatial-average SAR is found by moving the averaging cube over a selected region, e.g., a region with a local SAR above some criterion. Figure C.4 illustrates the extrude method of averaging. The scanning of the volume may be done parallel to the surface of the phantom. This ensures that the extruded volume is close to a cubical shape, and conformal to the surface.

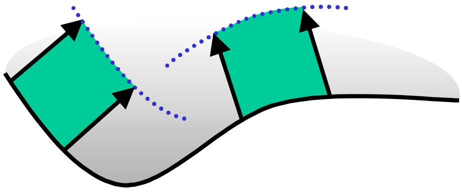

Figure C.4 – Extrude method of averaging

C.2.4 Averaging scheme and maximum finding uncertainty estimation

The peak local SAR will occur at the inner surface of the phantom, so the peak spatial-average SAR should occur in a cubical tissue volume at the surface of the phantom. It therefore follows that high-resolution measurement scans should be centred on the peak localised SAR determined from a scan of the interior surface of the phantom. This scanned surface should extend in all directions at least 1,5 times the linear dimension of the tissue cube used for mass averaging. Computer controlled algorithms should be used to determine the highest SAR according to the local SAR gradients in the mass averaging cube. The uncertainty contribution of the averaging scheme and maximum finding is included in the evaluation methods of 7.2.4 because that not only serves as a benchmark for the interpolation and extrapolation but also for the averaging and maximum finding schemes.

C.3 Example implementation of parameters for scanning and data evaluation

C.3.1 Introduction

The following describes example parameters for implementing SAR scanning and data evaluation procedures. This is only intended to illustrate one particular implementation; other implementations are possible.

C.3.2 *Area scan* to search for maximum

For handsets operating above 300 MHz evaluated with the homogeneous head model, the SAR distribution is measured on a two-dimensional coarse grid at a fixed separation distance of less than 8 mm from the surface of the phantom shell. The scan region should cover all areas that are exposed and encompassed by the projection of the handset. In order to maintain a fixed distance of less than 8 mm from the surface to within ±1 mm, as required by the measurement protocol, the exact shape and dimensions of the phantom inner surface shall be known, pre-calibrated, or preferably detected during the SAR measurement with a mechanical or optical surface-detection mechanism that meets the probe positioning requirements. This evaluation technique determines the maximum spacing between the grid points, i.e., it has been found that a 20 mm × 20 mm grid is usually sufficient to achieve the required precision if two staggered one-dimensional cubic splines [55] are used to locate the maximum SAR location [57].

C.3.3 Zoom scan

The maximum local SAR is evaluated on an interpolated grid at 1 mm to 2 mm resolution during the *zoom scan*. A *zoom-scan* volume of 32 mm x 32 mm x 30 mm, consisting of 5 x 5 x 7 points with the centre at the peak SAR location determined during the *area scan*, can be chosen. Although a scan resolution of 8 mm is sufficient for directions parallel to the surface, 5 mm is needed in the direction normal to the surface of the phantom to achieve the required extrapolation accuracy.

C.3.4 Extrapolation

Because the actual measurement location of the field probe corresponds to the geometrical centre of the dipole sensors, which is displaced from the tip of the probe, the SAR values required for computing the 1 g or 10 g SAR between the surface of the phantom and the closest measurable points shall be determined by extrapolation. While a basic exponential fit may not be suitable for extrapolating many of the typical SAR distributions that occur in handset evaluations, a fourth-order least-square polynomial fit of the measured data usually provides satisfactory results. The triangular points shown in Figure C.5 represent the SAR values extrapolated at 1 mm steps for points next to the phantom surface that cannot be measured.

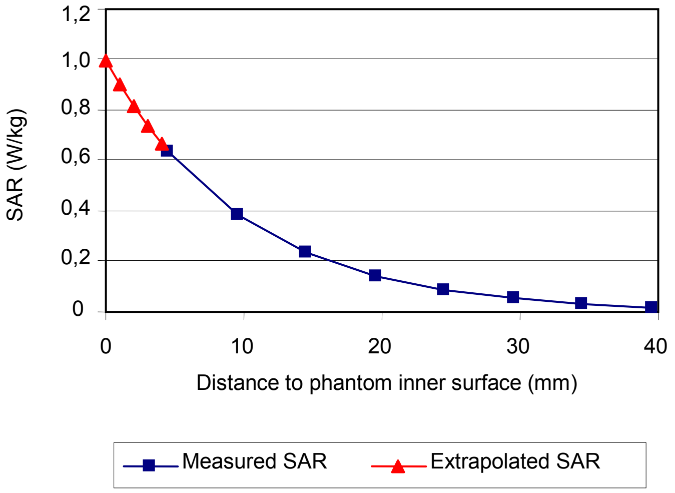

NOTE The triangles represent the extrapolated values at 1 mm intervals.

Figure C.5 – Extrapolation of SAR data to the inner surface of the phantom based on a least-square polynomial fit of the measured data (squares)

C.3.5 Interpolation

The measured and extrapolated SAR values within the *zoom-scan* volume are interpolated to a 1 mm grid for use to determine the 1 g or 10 g peak spatial-average SAR for example, by using three staggered one-dimensional cubic splines [55].

C.3.6 Integration

One way to integrate the SAR over a 1 g or 10 g cube is by the basic trapezoidal algorithm. The maximum peak spatial-average SAR may be evaluated by numerical integration of all possible 1 g or 10 g cubes within the *zoom-scan* volume or by applying more complex search algorithms. If a surface of the 1 g or 10 g cube is touching the boundary of a *zoom-scan* volume, the entire *zoom scan* test should be repeated with the new centre located at the maximum SAR location indicated by the preceding 1 g or 10 g spatial peak measurement.

Annex D
(normative)

SAR measurement system validation

D.1 Introduction

This clause provides procedures for the following two levels of SAR measurement *system validation*.

a) *system check*

b) *system validation*

The objectives and applications of these different levels of validation procedures are as follows:

The *system check* provides a fast and reliable test method that can be performed daily or before every SAR measurement. The objective here is to ascertain that the set-up components are still within laboratory calibration limits, including drift effects. This test requires a flat phantom and a standard source, e.g., a half-wave dipole.

System validation provides a means of system-level validation. The test set-up consists of a flat phantom and a reference dipole (see Annex G). Therefore, *system validation* does not include uncertainty due to the use of anthropomorphic phantoms, nor does it include the uncertainty due to device positioning variability. This test is performed annually (e.g., after probe calibration), before measurements related to interlaboratory comparison (Annex E), and every time modifications have been made to the system, such as a new software version, different readout electronics, or different types of probes.

NOTE Interlaboratory comparisons provide laboratory qualification using a reference handset (Clause E.3) and a standard anthropomorphic phantom. This qualification method includes the data scatter due to the human-like phantom and due to device positioning effects. This test is used to compare the accuracy and precision performance of various laboratories.

D.2 System check

D.2.1 Purpose

The purpose of the *system check* is to verify that the system operates within its specifications. The *system check* is a check of repeatability to make sure that the system works correctly at the time of the compliance test. It is not a validation of the system with respect to external standards. The *system check* detects possible short-term drift and uncertainties in the system, such as:

a) changes in the liquid parameters (e.g., due to water evaporation or temperature change)

b) component failures

c) component drift

d) operator uncertainties in the set-up or software parameters

e) adverse conditions in the system, e.g., RF interference

The *system check* is a complete 1 g or 10 g averaged SAR measurement in a simplified set-up with a standard source (see D.2.3). The instrumentation and procedures in the *system check* are the same as those used for the compliance tests. The *system check* shall be performed using the same liquid as in the compliance test and at a chosen fixed frequency that is within ±10 % of the compliance test mid-band frequency. The *system check* is performed prior to compliance tests and the result shall always be within ±10 % of the target value corresponding to the test frequency and the source used. The target values are 1 g or 10 g averaged SARs measured by any system on which *system validation* has been performed using the *system check* set-up in Figure D.1. These target values should be determined using a controlled standard source.

D.2.2 Phantom set-up

A flat phantom shall be used with the recommended tissue-equivalent liquid for the *system check* and *system validation* purposes (see Clause 7). The minimum transverse dimensions (width and length) shall be such that the SAR measurements are not affected by more than 1 %. The minimal dimensions of the bottom surface of the flat phantom are given by an ellipse having major axis a, minor axis b. and shell of thickness d, where criteria are:

$a \geq 0{,}6\ \lambda$; $b \geq 0{,}4\ \lambda$; 6,0 mm $\leq d \leq$ 6,3 mm for $f <$ 800 MHz,

$a \geq$ 225 mm; $b \geq$ 150 mm; d = 2 mm for $f \geq$ 800 MHz,

where the wavelength λ is for free-space, and the thickness d shall be uniform within a tolerance of ±0,2 mm. For dipole sources the feedpoint shall be placed at the centre of the ellipse, and the dipole arms shall be aligned with the major axis (see Annex G for dipole specifications) [5]. The relative permittivity of the phantom shell plastic material shall be less than 5 and the loss tangent less than 0,05. The material shall be resistant to damage or reaction with tissue-equivalent liquid chemicals. When filled with liquid to the 15 cm minimum depth, the sagging of the portion of the inner surface that is directly above the source (e.g., a dipole) at the liquid interface, shall be less than 1 % of the free-space wavelength in the frequency range of 800 MHz to 3 000 MHz, and less than 0,5 % of the free-space wavelength at frequencies below 800 MHz.

D.2.3 Standard source

The phantom shall be irradiated using a standard source for the required frequency (e.g., a half-wave dipole or patch antenna). The reference dipoles used for *system validation* (see Annex G) can also but are not required to be used for the *system check*, but are not required to be used. A standard source shall be selected which has good positioning repeatability, mechanical stability, and impedance matching. In the following positioning instructions, a half-wave dipole is assumed as an example of a standard source.

A half-wave dipole shall be positioned below the bottom of the phantom and centred with its axis parallel to the longest dimension of the phantom. The distance between the liquid-filled phantom inner surface and the dipole centre, *s*, (see Figure D.1 and Table H.1) shall be specified for each test frequency. A low loss (loss tangent <0,5) and low dielectric constant (relative permittivity <5) spacer shall be used to establish the correct distance between the top surface of the dipole and the bottom surface of the phantom. The dipole shall have a return loss less than –20 dB at the resonant frequency (as measured in the set-up) to reduce the uncertainty in the power measurement. The acceptable tolerance of the distance *s* shall be within ±0,2 mm.

D.2.4 Standard source input power measurement

The uncertainty of the power to the source shall be as low as possible. This requires the use of a test set-up with directional couplers and power meters during the *system check*. The recommended set-up is shown in Figure D.1 (which uses a half-wave dipole as an example of a standard source).

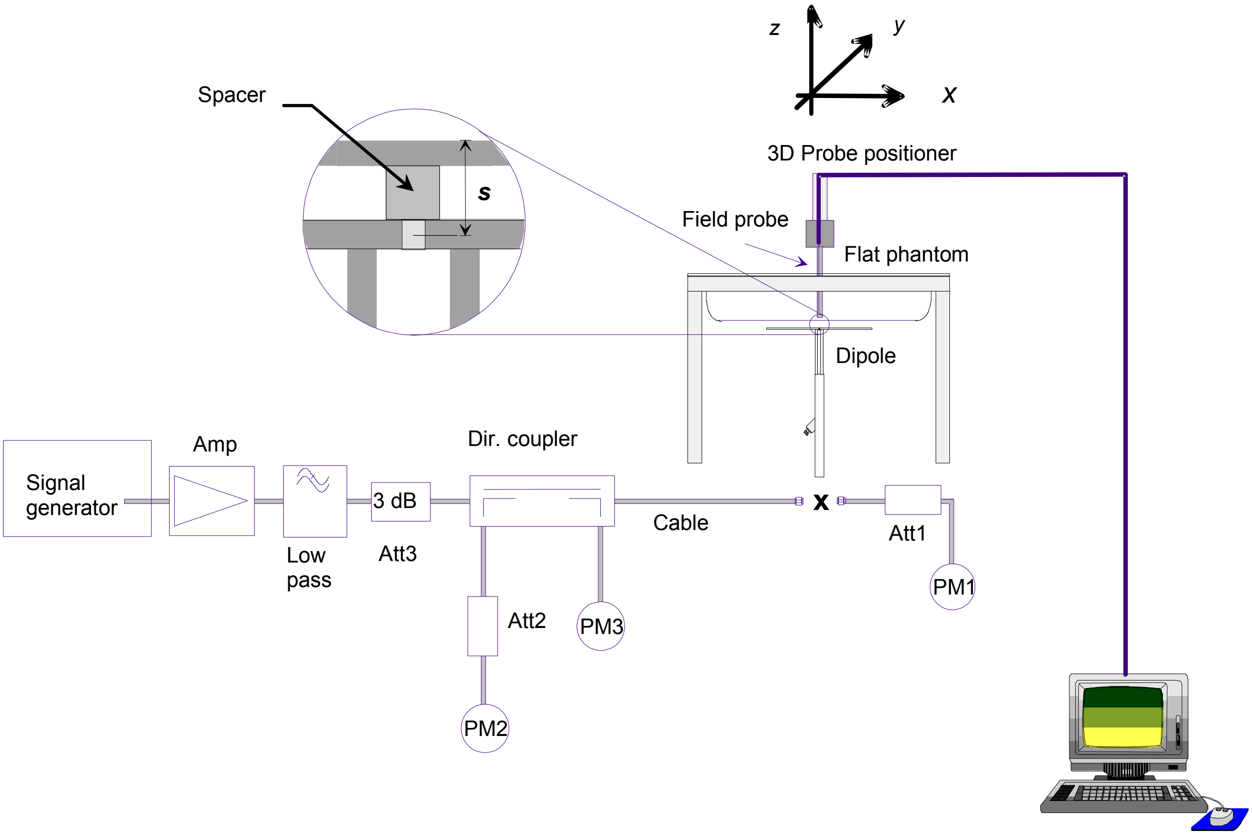

Figure D.1 – Set-up for the *system check*

First the power meter PM1 (including attenuator Att1) is connected to the cable to measure the forward power at the location of the dipole connector (X). The signal generator is adjusted for the desired forward power at the dipole connector (taking into account the attenuation of Att1) as read by power meter PM1. After connecting the cable to the dipole, the signal generator is readjusted for the same reading at power meter PM2. If the signal generator does not allow adjustment in 0,01 dB steps, the remaining difference at PM2 must be taken into consideration. The matching of the dipole should be checked using a network analyser (e.g., during annual performance characterization intervals) to ensure that the reflected power is at least 20 dB below the forward power.

The component and instrumentation requirements are as follows:

a) The signal generator and amplifier shall be stable (after warm-up). The forward power to the dipole shall be high enough to produce a SAR value exceeding the lower detection limit of the probe system (see Clause B.5). If the signal generator can deliver 15 dBm or more, an amplifier is generally not necessary. Some high power amplifiers shall not be operated at a level far below their maximum output power, e.g., a 100 W power amplifier operated at 250 mW output power can be quite noisy. An attenuator between the signal generator and amplifier is recommended to protect the amplifier input.

b) The low pass filter inserted after the amplifier reduces the effect of harmonics and noise from the amplifier. For most amplifiers in normal operation the filter is not necessary.

c) The attenuator after the amplifier improves the source matching and the accuracy of the power sensor (consult the power meter manual).

d) The directional coupler (recommended –20 dB coupling coefficient) is used to monitor the forward power and adjust the signal generator output for constant forward power. A medium-quality coupler is sufficient because the loads (dipole and power head) are both well matched.

e) The power meters PM2 and PM3 shall have low drift and a resolution of 0,01 dBm, but otherwise the accuracy has negligible impact on the power setting (absolute calibration is not required).

f) The power meter PM1 and attenuator Att1 must be high-quality components. These shall be calibrated, preferably together. The attenuator (–10 dB) improves the accuracy of the power reading (some high-power heads come with a built-in calibrated attenuator). The exact loss factor of the attenuator at the test frequency must be known; many attenuators vary up to 0,2 dB from the specified value.

g) Use the same power level for PM1 test as used for the actual measurement to avoid linearity and range switching uncertainties in the power meters PM2 and PM3. If the power level is changed, the power level setting procedure shall be repeated.

h) The dipole shall be connected directly to the cable at location "X". If the power meter has a different connector type, use high-quality adapters.

D.2.5 *System check* procedure

The *system check* is a complete 1 g and/or 10 g averaged SAR measurement. The measured 1 g and/or 10 g averaged SAR value is normalized to the target input power of the standard source and compared with the previously recorded target 1 g and/or 10 g value corresponding to the measurement frequency and the standard source. The acceptable tolerance must be determined for each *system check* and shall be within ±10 % of previously recorded *system check* target values.

D.3 System validation

D.3.1 Purpose

The *system validation* procedure tests the system against reference SAR values, and the performance of probe, readout electronics and software. It is a validation of the system with respect to external standards. This set-up utilizes a flat phantom and a reference dipole. Thus, this validation process does not include data scatter due to the use of anthropomorphic phantoms, or uncertainty due to device positioning variability.

System validation is performed annually, when a new system is put into operation, or whenever modifications have been made to the system, such as a new software version, different readout electronics, or different types of probes. *System validation* shall be done with a calibrated probe.

The objective of this clause is to provide a methodology for SAR measurement *system validation*. Since SAR measurement equipment, calibration techniques, phantoms, and head tissue-equivalent liquids can vary widely between various laboratories, a validation methodology is needed to ascertain that uniform results are obtained within reasonable measurement uncertainties. Numerically calculated reference SAR values for use in *system validation* are listed in Table D.1.

NOTE The *system validation* procedure is neither an alternative to probe calibration nor to the uncertainty estimation of Clause 7. The probe and the readout electronics are calibrated regularly according to the procedures given in Annex B. Probe hemispherical isotropy is not considered in the protocol for *system validation*.

D.3.2 Phantom set-up

The flat phantom set-up described for the *system check* (see Figure D.1) is also used for the *system validation* tests. The *system validation* shall be performed using head tissue-equivalent liquids having dielectric properties as defined in Table 1.

D.3.3 Reference dipole source

The phantom shall be irradiated using a reference dipole specified in Annex G for the required frequency. The reference dipole shall be positioned below the bottom of the phantom and centred with its axis parallel to the longest side of the phantom. A low loss and low dielectric constant spacer can be used to establish the correct distance between the top surface of the reference dipole and the bottom surface of the phantom. The distance between the liquid-filled phantom bottom surface and the reference dipole centre (designated *s*) is specified within 0,2 mm for each test frequency. The reference dipole shall have a return loss better than –20 dB (measured in the set-up) at the resonant frequency to reduce the uncertainty in the power measurement.

For the reference dipoles described in Annex G, the spacing distance *s* is given by:

a) s = 15 mm ± 0,2 mm for 300 MHz $\leq f \leq$ 1 000 MHz

b) s = 10 mm ± 0,2 mm for 1 000 MHz $< f \leq$ 3 000 MHz

The reference dipole arms shall be parallel to the flat surface of the phantom within a tolerance of ±2° or less (see Figure D.1).

D.3.4 Reference dipole input power measurement

The input power measurement set-up described for the *system check* (see D.2.4) is also used for *system validation* tests.

D.3.5 *System validation* procedure

System validation is used for verifying the accuracy of the complete measurement system and performance of the software. Device positioning and head phantom shape uncertainties are not considered. The *system validation* procedure consists of 6 steps, a) to f). Step a) is the most important part of the *system validation* procedure and shall be done every time. Steps b) to f) (recommended) offer a means for quick and simple validations of the performance of probe, readout electronics, and software. These additional tests shall be done any time system components have been modified (e.g., new software release, new readout electronics, new probe type) but need only to be performed for the same system version by each laboratory (e.g., by the calibration laboratory or by the SAR measurement system end-user laboratory). The *system validation* procedure is as follows:

a) **SAR evaluation:** A complete 1 g and/or 10 g averaged SAR measurement is performed. The reference dipole input power is adjusted to produce a 1 g and/or 10 g averaged SAR value falling in the range of 0,4 W/kg to 10 W/kg. The 1 g and/or 10 g averaged SAR is measured at frequencies in Table D.1 within the range to be used in compliance tests. The results are normalized to 1 W forward input power and compared with the reference SAR value for the reference dipole and flat phantom shown in columns 2 and 3 of Table D.1. The differences from the reference values given in Table D.1 should be less than the tolerance specified for the SAR measurement system by the manufacturer or designer, i.e., within the expanded uncertainty for the *system validation* using the procedures of Table 3 (see Table 3 Note 10).

b) **Extrapolation routine:** Local SAR values are measured along a vertical axis directly above the reference dipole feed point using the same point spacing as used for the evaluation of the peak spatial-average SAR. This measurement is repeated along another vertical axis with a 2 cm horizontal offset (*y* direction – see Figure D.1) from the reference dipole feed point. SAR values at the phantom surface are extrapolated and compared with the numerical values given in columns 4 and 5 of Table D.1. The difference from the reference values given in Table D.1 should be less than the tolerance specified for the SAR measurement system by the manufacturer or designer, i.e., within the expanded uncertainty for the *system validation* using the procedures of Table 3 (see Table 3 Note 10).

c) **Probe linearity:** The measurements in step a) are repeated using different reference dipole input power levels. The power levels selected for each frequency are selected to produce 1 g and/or 10 g averaged SAR values of approximately 10 W/kg or 8 W/kg, 2 W/kg or 1,6 W/kg, and 0,4 W/kg. The measured SAR values are normalized to 1 W forward input power and compared with the 1 W normalized values from step a). The difference between these values should be less than the tolerance specified for the SAR measurement system by the manufacturer or designer, i.e., within the expanded uncertainty for the linearity component using the procedures of Table 3 and 7.2.1.3.

d) **Modulation response:** The measurements in step a) are repeated with pulse-modulated signals having a duty factor of 0,1 and pulse repetition rate of 10 Hz. The power is adjusted to produce a 1 g and/or 10 g averaged SAR of approximately 8 W/kg with a CW signal or a peak power of approximately 80 W/kg. The measured SAR values are normalized to 1 W forward input power and duty factor of 1, and compared with the 1 W normalized values from step a). The difference between these values should be less than the tolerance specified for the SAR measurement system by the manufacturer or designer, i.e., within the expanded uncertainty for *system validation* using the procedures of Table 3 (see Table 3 Note 10).

e) **System offset:** The measurements in a) are repeated with a reference dipole input forward power that produces a 1 g and/or 10 g averaged SAR of approximately 0,05 W/kg. The measured SAR values are normalized to 1 W forward input power and compared with the 1 W normalized values from step a). The difference between these values should be less than the tolerance specified for the SAR measurement system by the manufacturer or designer, i.e., within the expanded uncertainty for *system validation* using the procedures of Table 3 (see Table 3 Note 10).

f) **Probe axial isotropy:** The probe is placed directly above the reference dipole centre at a measurement distance of 5 mm from the phantom inner surface. The probe (or reference dipole) is rotated around its axis at least 180° in steps no larger than 15°. The maximum and minimum SAR readings are recorded. The difference between these values should be less than the tolerance specified for the SAR measurement system by the manufacturer or designer, i.e., within the expanded uncertainty for the isotropy component using the procedures of Table 3 and 7.2.1.2.

D.3.6 Reference SAR values

In the *system validation* test, the reference dipole constructed for the frequency f_i (described in Annex G) shall produce the numerical reference peak spatial-average SAR values shown in columns 2 and 3 of Table D.1, within the uncertainty for *system validation* (see Table 3 Note 10). Columns 4 and 5 of Table D.1 are used to validate the system extrapolation routines, as described in D.3.5. The reference SAR values have been calculated using the finite-difference time-domain numerical-computation method with the parameters of the flat phantom of Table H.1. The values for frequencies between 800 MHz and 3 000 MHz have been experimentally verified, using 4th-order polynomial extrapolation. The reference SAR values for frequencies of 300 MHz and 450 MHz will be experimentally verified in the next revision of the standard. The parameters for the lossless phantom model used in the simulations (dimensions, shell thickness and permittivity), and the distance *s* between the reference dipole and liquid are given in Table H.1. The dielectric properties used for the liquid are defined in Table 1, and the dimensions of the reference dipoles are shown in Table G.1.

Table D.1 – Numerical reference SAR values for reference dipole and flat phantom

Frequency MHz	**1 g SAR** W/kg	**10 g SAR** W/kg	**Local SAR at surface (above feedpoint)** W/kg	**Local SAR at surface (y = 2 cm offset from feedpoint)** W/kg
1	**2**	**3**	**4**	**5**
300	3,0	2,0	4,4	2,1
450	4,9	3,3	7,2	3,2
835	9,5	6,2	14,1	4,9
900	10,8	6,9	16,4	5,4
1 450	29,0	16,0	50,2	6,5
1 800	38,1	19,8	69,5	6,8
1 900	39,7	20,5	72,1	6,6
1 950	40,5	20,9	72,7	6,6
2 000	41,1	21,1	74,6	6,5
2 450	52,4	24,0	104,2	7,7
3 000	63,8	25,7	140,2	9,5
All values are normalized to a forward power of 1 W.				
NOTE The phantom dimensions given in D.2.2 must be used.				

Annex E
(informative)

Interlaboratory comparisons

E.1 Purpose

The purpose of the interlaboratory comparison is to validate various SAR measurement systems by comparing results from several different laboratories. The general concept is to use reference handsets and the SAM anthropomorphic phantom filled with a head tissue-equivalent liquid having dielectric parameters as specified in 5.2. The SAR assessment methodologies described in Clause 6 are used.

The measured data from various laboratories should be compared. Also, a comparison between measurement uncertainty analyses should be performed. If the differences and discrepancies between the measured data can be attributed to differences in the measurement uncertainties, the interlaboratory comparison is deemed to be successful. If not, all sources of uncertainties should be investigated per the recommendations of Clause 7. Also, other possible sources of uncertainties different from those defined in Clause 7 should be considered.

NOTE General guidelines for accomplishing interlaboratory comparison tests are given for example in [9], [24].

E.2 Phantom set-up

The anthropomorphic phantom is described in Clause 5 and Annex A. The phantom should have a mounting structure made of a rugged material with low permittivity (less than 5) and loss tangent (less than 0,05). Metallic parts closer than 50 cm from the structure should be avoided. The phantom should be irradiated using a reference handset mounted according to the test positions described in 6.1.

E.3 Reference wireless handsets

Reference handsets are commercial wireless handsets that are maintained and distributed in accordance with [24]. The designation of the supplier is based on the agreement between the participating parties.

E.4 Power set-up

The power set-up is dependent on the precision of the output power measurement of the reference device used for the interlaboratory comparison. Each device is individually checked by the participating laboratory so that the conducted output power of each device is in the range of ±0,3 dB of the reference value. The measured output power should be reported to the monitor laboratory. The device output power should be adjusted via test software to a predetermined value. The device battery must be fully charged.

Careful effort should be expended to ensure an accurate output power measurement. Some devices may allow easy and accurate output power measurements at the antenna port. The ease of output-power measurement should be considered when designating reference handsets for use in the comparison tests. If deemed necessary, the reference handsets should be returned to a monitor laboratory periodically during the comparison campaign for output power and frequency verification. The monitor laboratory shall also verify the radiated power of the reference handsets using a measurement method with good repeatability. Also, the battery condition should be checked by the monitor laboratory, to ensure uniform power output at all laboratories.

E.5 Interlaboratory comparison – Procedure

Measurement procedures for SAR assessment used in the interlaboratory comparison are the same as those used for compliance testing in accordance with Clause 6. The interlaboratory comparison should be performed with a calibrated probe and a validated system. Each laboratory should provide a full test report in accordance with the requirements of Clause 7 and Clause 8 including *system validation*, liquid measurements, system uncertainty data, and measured output power data. The results of the interlaboratory comparison should fall within the expanded uncertainty for exposure assessment of Clause 7. The reports from different laboratories are to be evaluated and compared by the designated monitor laboratory.

Annex F
(informative)

Definition of a phantom coordinate system and a device under test coordinate system

The offset and rotation between these optional reference coordinate systems can be used to provide an unambiguous description of device position relative to the phantom. A definition of the phantom coordinate system is illustrated in Figure F.1:

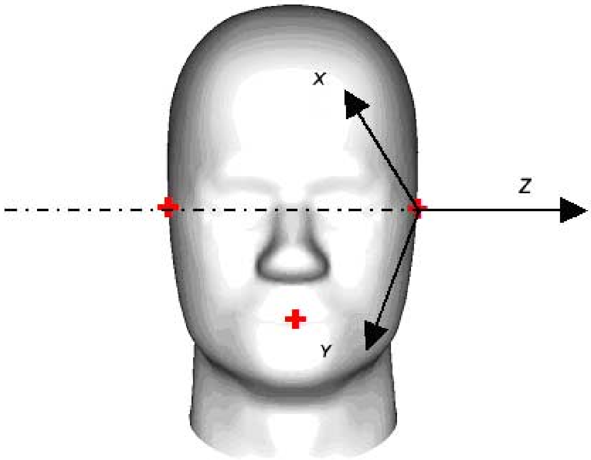

Key

x, *y*, *z*	Axes of the coordinate system relative to the phantom

Figure F.1 – Example reference coordinate system for the SAM phantom

The *x*-, *y*- and *z*-axes should form a right-handed coordinate system. The axes are defined as follows.

- The *z*-axis is defined by a connecting line between the left and the right ear reference points, and points from left to right. The $z = 0$ origin is at the left ear reference point.
- The *y*-axis is in the reference plane and is perpendicular to the *z*-axis.
- The *x*-axis is normal to the reference plane and cuts the reference plane at the ear reference point.

A definition of a device under test (DUT) coordinate system is shown in Figure F.2:

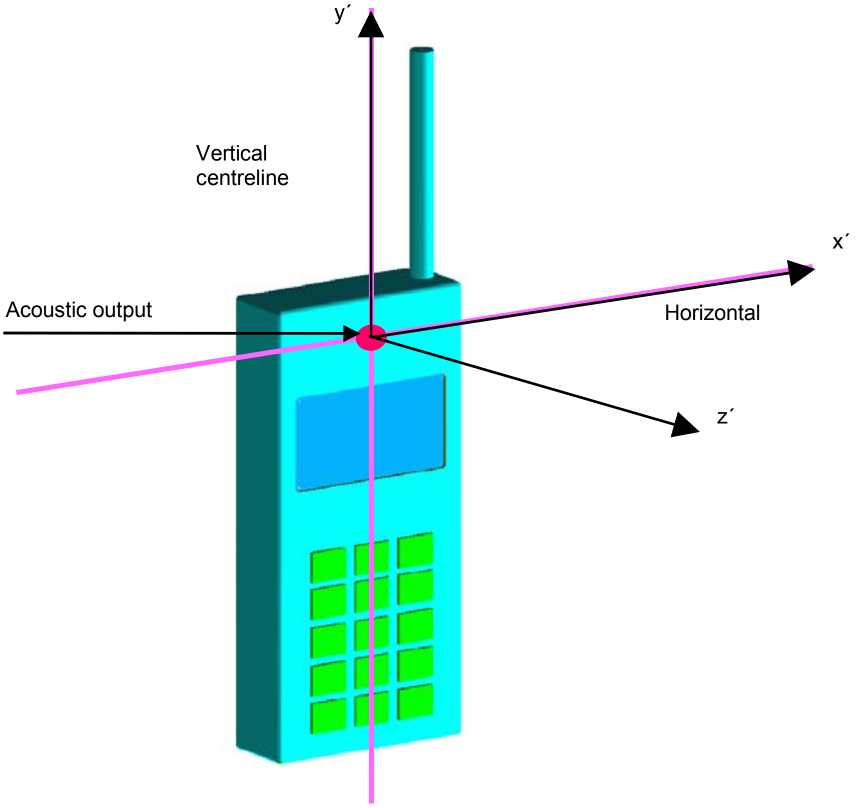

Key

x’,y’,z’ Axes of the coordinate system relative to the handset

Figure F.2 – Example coordinate system on the device under test

Annex G
(informative)

Validation dipoles

As specified in Annex D a flat phantom should be irradiated using a reference dipole for the required frequency. The reference dipoles are defined for the specific dielectric parameters and thickness of the phantom shell indicated in Table G.1. The reference dipole should be positioned below the bottom of the phantom and centred with its axis parallel to the longest dimension of the phantom. A low loss and low dielectric constant spacer can be used to establish the correct distance between the top surface of the reference dipole and the bottom surface of the phantom. The spacer should not change the measured 1 g and 10 g averaged SAR values more than 1 %. The distance between the liquid filled phantom bottom surface and the reference dipole centre (designated *s*) is specified within 0,2 mm for each test frequency. The reference dipole should have a return loss better than –20 dB (measured in the test system) at the test frequency to reduce the uncertainty in the power measurement. To meet this requirement, it is acceptable to fine-tune the reference dipoles by using low-loss dielectric or metal tuning elements at the ends of the dipole (see Figure D.1).

Table G.1 – Mechanical dimensions of the reference dipoles

Frequency MHz	***L*** mm	***h*** mm	***d*** mm
300	396,0	250,0	6,35
450	270,0	166,7	6,35
835	161,0	89,8	3,6
900	149,0	83,3	3,6
1 450	89,1	51,7	3,6
1 800	72,0	41,7	3,6
1 900	68,0	39,5	3,6
1 950	66,3	38,5	3,6
2 000	64,5	37,5	3,6
2 450	51,5	30,4	3,6
3 000	41,5	25,0	3,6

NOTE The values for 300 MHz and 450 MHz are valid for phantom shell thickness of 6,3 mm; the values for 835 MHz to 3 000 MHz are valid for a shell thickness of 2 mm. The tolerance on *L*, *h* and *d* should be better than ±2 %.

For the reference dipoles described in Annex D, the spacing distance *s* is given by:

a) s = 15 mm ± 0,2 mm for 300 MHz $\leq f \leq$ 1 000 MHz

b) s = 10 mm ± 0,2 mm for 1 000 MHz $< f \leq$ 3 000 MHz

The reference dipole arms should be parallel to the flat surface of the phantom within a tolerance of ±2° or less (see Figure D.1). This can be assured by carefully positioning the empty phantom and the reference dipole to horizontal level using a spirit level.

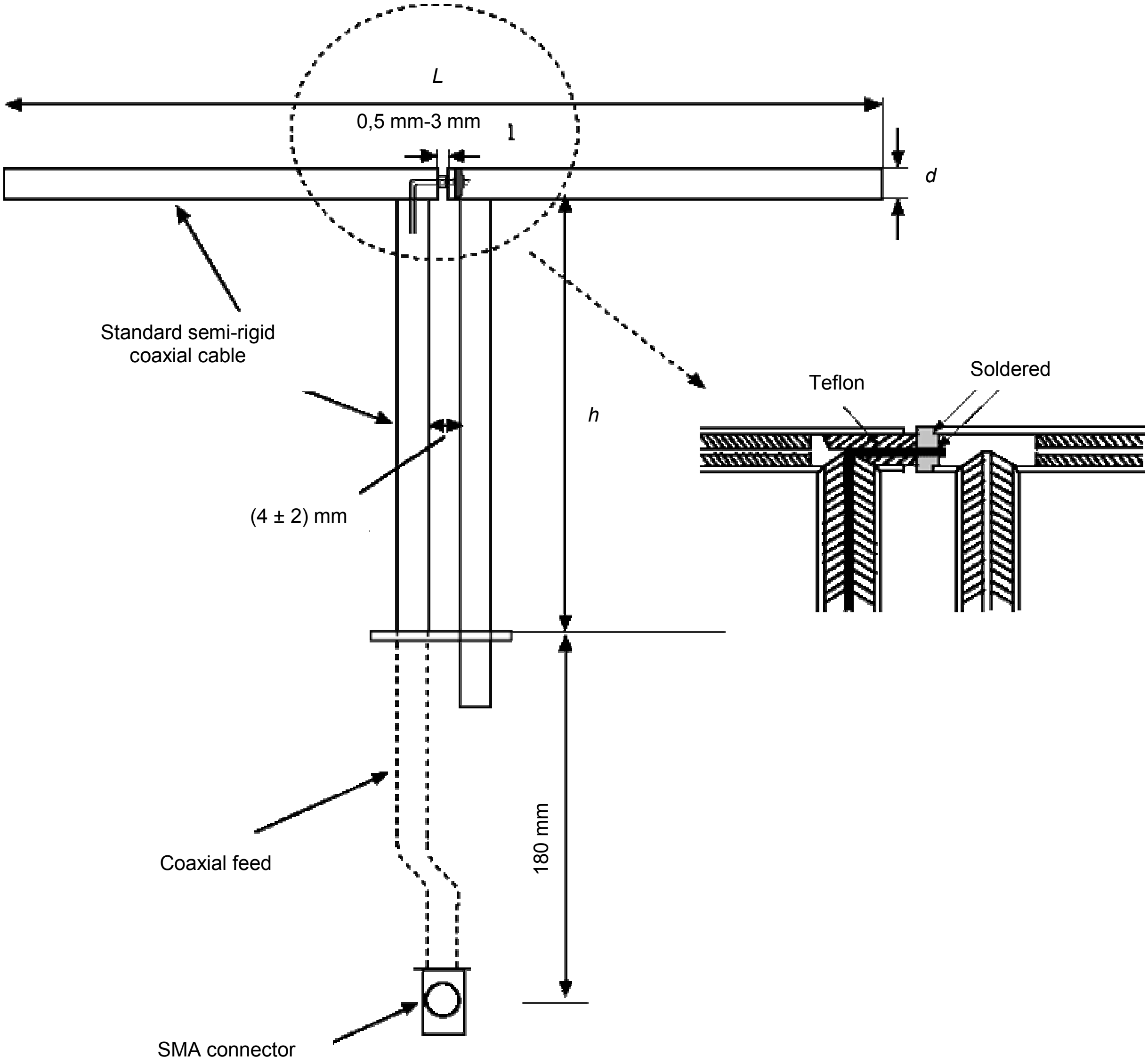

Key

L	Length of the dipole
d	Diameter of the dipole
h	Length of the balun choke section

Figure G.1 – Mechanical details of the reference dipole

Annex H
(informative)

Flat phantom

The influence of the dimensions of the flat phantom (see Figure H.1) on the absorbed energy in a 10 g cube inside the liquid-only phantom (without box) was assessed numerically using a commercial FDTD code. The phantom was illuminated with a matched dipole antenna at a distance of 15 mm (0,042 λ at 840 MHz). The dimensions of the phantom (*W* and *L*) were varied between 0,4 λ and 3 λ. The power absorbed in the cube was alternately normalized to a feedpoint current of 1 A or a feedpoint power of 1 W. Although deviations occur in the absorbed power in the cube when normalized either to the feedpoint power or the feedpoint current, the minimum dimensions necessary to keep the uncertainty below 1 % were determined for both methods of normalization. The above conditions are met for dimensions of the flat phantom larger than 0,6 λ in length and larger than 0,4 λ in width, as shown by Figure H.2. The influence of the width of the phantom is not very large. However, the width should not be less than 0,4 λ to keep the deviation of the absorbed power within the limit of 1 %. The dimensions of the phantom set-up can be scaled in terms of the free-space wavelength. The dependence on the liquid properties is not very critical as long as it is relatively lossy.

NOTE Because of its larger size, a 10 g averaging cube will be more sensitive to dimension changes, i.e., the uncertainty associated with the 1 g average will be smaller than that of the 10 g average.

The effects resulting in differences depend on perturbations of the dipole current magnitude and spatial distribution. Since the dipole dimensions are large compared with the SAR averaging volumes, the perturbations will increase with volume size. Although the depth used in this study was 10 cm, instead of the 15 cm required for the flat phantom in Annex D, it is 2,57 times the penetration depth at 840 MHz, and therefore the power reflection at the liquid surface is negligible (less than 1 %).

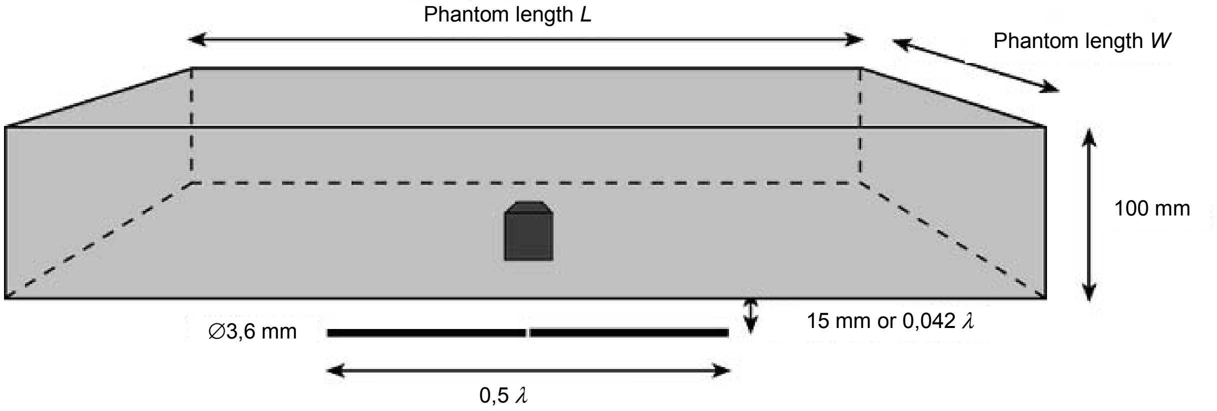

Key

λ free-space wavelength

NOTE A 10 g cube is shown at the bottom centre of the flat phantom.

Figure H.1 – Dimensions of the flat phantom set-up used for deriving the minimal dimensions for W and *L*

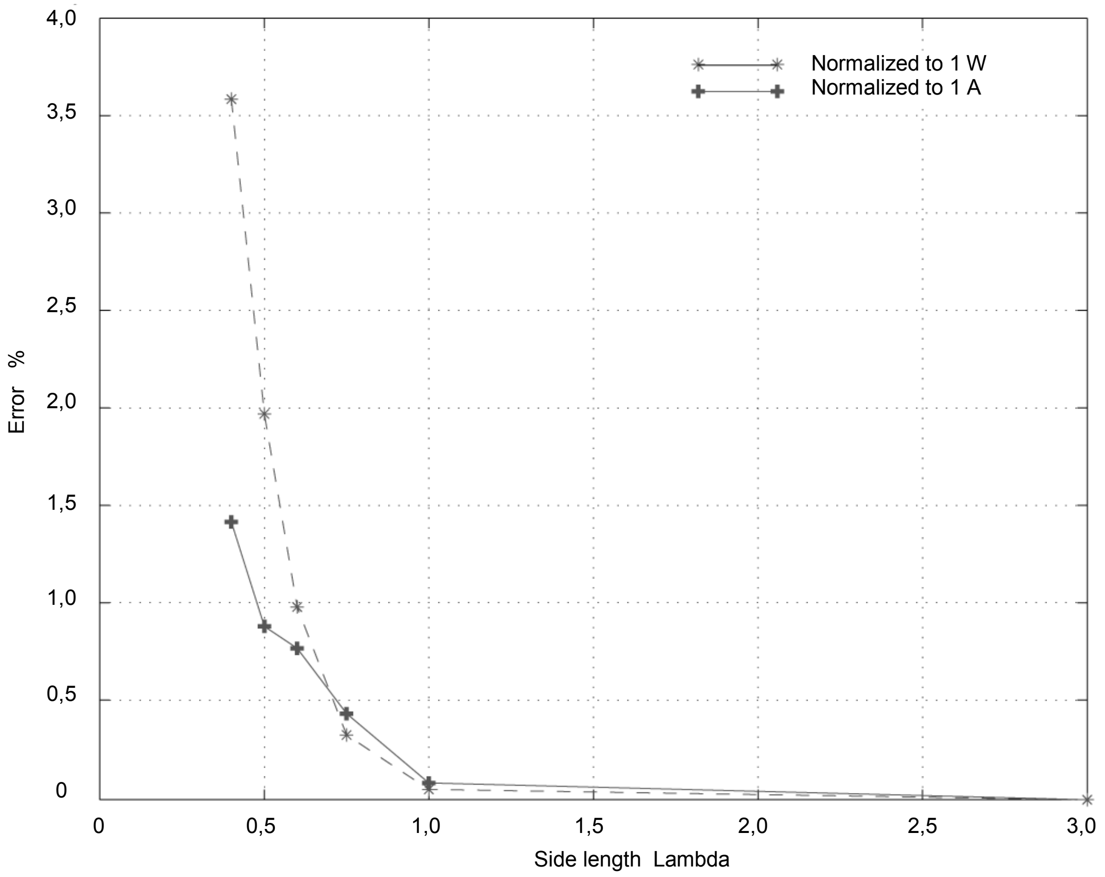

Figure H.2 – FDTD predicted uncertainty in the 10 g peak spatial-average SAR as a function of the dimensions of the flat phantom compared with an infinite flat phantom

Table H.1 – Parameters used for calculation of reference SAR values in Table D.1

Frequency MHz	**Phantom shell thickness** mm	**Phantom shell permittivity**	**Phantom dimensions used for FDTD models** mm **x, y, z**	**Reference dipole distance *s* from the liquid** mm
300	6,3	3,7	1 000, 800, 170	15
450	6,3	3,7	700, 600, 170	15
835	2,0	3,7	360, 300, 150	15
900	2,0	3,7	360, 300, 150	15
1 450	2,0	3,7	240, 200, 150	10
1 800	2,0	3,7	220, 160, 150	10
1 900	2,0	3,7	220, 160, 150	10
1 950	2,0	3,7	220, 160, 150	10
2 000	2,0	3,7	160, 140, 150	10
2 450	2,0	3,7	180, 120, 150	10
3 000	2,0	3,7	220, 160, 150	10
This table represents parameters used for the numerical FDTD modelling.				

Annex I
(informative)

Recommended recipes for phantom head tissue-equivalent liquids

I.1 Introduction

The dielectric properties of the liquid material used in the phantom should be those listed in Table 1. For dielectric properties of head tissue-equivalent liquid at other frequencies within the frequency range, a linear interpolation method should be used. Table I.1 suggests examples of recipes for liquids having parameters as defined in Table 1.

WARNING

To ensure personnel safety, the users must follow the instructions provided in the Material Safety Data Sheet (MSDS) for any material, and/or any local regulations.

I.2 Ingredients

The following ingredients are used for producing the head tissue-equivalent liquids:

a) Sucrose (sugar) (>98 % pure)
b) Sodium Chloride (salt) (>99 % pure)
c) De-ionised water (16 MΩ resistivity minimum)
d) Hydroxyethyl Cellulose (HEC)
e) Bactericide
f) Diethylene Glycol Butyl Ether (DGBE) (>99 % pure)
g) Polyethylene glycol mono [4-(1,1,3,3-tetramethylbutyl) phenyl ether]. This is available as (Triton X-100). The quality of the Triton X-100 must be ultra pure to match the composition of salt.[2)]
h) Diacetin
i) 1,2-Propanediol

NOTE 1 Viscosity of HEC-based tissue-equivalent liquids should be low enough to not affect *E*-field probe movement.

NOTE 2 Add salt to water first to make a saline solution, then add the Triton X-100.

NOTE 3 Actual results and mixture percentages may vary from those shown depending on grade and type of components used.

[2)] The formulas containing Triton X-100 are under review and verification.

I.3 Tissue-equivalent liquid formulas (permittivity/conductivity)

Table I.1 – Suggested recipes for achieving target dielectric parameters

Frequency (MHz)	**300**	**450**		**835**	**900**			**1 450**	**1 800**				**1 900**		**1 950**	**2 000**	**2 100**		**2 450**		**3 000**
Recipe No.	1	1	3	1	1	2	3	1	1	2	2	3	1	2	4	1	1	2	2	3	2
Ingredients (% by weight)																					
1,2-Propanediol						64,81															
Diacetin			48,9				49,2					49,43								49,75	
Bactericide	0,19	0,19	0,5	0,10	0,10		0,5					0,50								0,50	
DGBE								45,51	47,00	13,84	44,92		44,92	13,84	45,0	50,0	50,0	7,99	7,99		7,99
HEC	0,98	0,98		1,00	1,00																
NaCl	5,95	3,95	1,7	1,45	1,48	0,79	1,1	0,67	0,36	0,35	0,18	0,64	0,18	0,35				0,16	0,16		0,16
Sucrose	55,32	56,32		57,00	56,50																
Triton X-100										30,45				30,45				19,97	19,97		19,97
Water	37,56	38,56	48,9	40,45	40,92	34,40	49,2	53,82	52,64	55,36	54,90	49,43	54,90	55,36	55,0	50,0	50,0	71,88	71,88	49,75	71,88
Measured dielectric parameters																					
ε_r'	46,0	43,4	44,3	41,6	41,2	41,8	42,7	40,9	39,3	41,0	40,4	39,2	39,9	41,0	40,1	37,0	36,8	41,1	40,3	39,2	37,9
σ (S/m)	0,86	0,85	0,90	0,90	0,98	0,97	0,99	1,21	1,39	1,38	1,40	1,40	1,42	1,38	1,41	1,40	1,51	1,55	1,88	1,82	2,46
Temp. (°C)	22	22	20	22	22	22	20	22	22	21	22	20	21	21	20	22	22	20	20	20	20
Target values (from Table 1)																					
ε_r'	45,3	43,5		41,5	41,5			40,5	40,0								39,8		39,2		38,5
σ (S/m)	0,87	0,87		0,90	0,97			1,20	1,40								1,49		1,80		2,40

NOTE 1 Multiple columns under a single frequency indicates optional recipes.

NOTE 2 Recipe number, reference: 1 [30], 2 [64], 3 [50], 4 [15].

Annex J
(informative)

Measurement of the dielectric properties of liquids and uncertainty estimation

J.1 Introduction

Clause J.2 describes the measurement of the dielectric properties of tissue-equivalent liquid as part of the SAR characterization procedure. It is intended to provide sufficient details to enable users to select a measurement procedure on the basis of convenience and performance. The dielectric properties of some reference liquids are provided in Clause J.6 to be used for assessing the performance of the measurement procedures. General procedures to evaluate dielectric parameter measurement uncertainties are provided in Clause J.7.

J.2 Measurement techniques

The dielectric parameters required are the complex relative permittivity $\varepsilon_r = \varepsilon_r' - j\sigma/\omega\varepsilon_0$ of the tissue-equivalent liquid at specific test frequencies and temperature. Several well-established techniques can be used for dielectric property measurements of tissue-equivalent liquid.

J.2.1 Instrumentation

The following or equivalent instrumentation is required:

a) Vector network analyser and *S*-parameter test set
b) Sample holder, also known as a dielectric test cell or dielectric probe
c) Test procedures and application software to extract sample dielectric properties from *S*-parameter measurements

Three sample holders and the corresponding test methodologies are described in Clauses J.3 to J.5. The accuracy achievable depends on the manufacturing precision of the test cells – the dimensions of the test cells are commensurate with measurement frequency ranges. The procedures are validated by measurements of reference liquids.

J.2.2 General principles

The following general principles should be applied for all the procedures.

a) Ensure that the sample holder is thoroughly clean.
b) Ensure that all cell, probes, cables and connectors are undamaged.
c) Ensure that the procedure for filling the sample holder with the liquid sample fills the volume completely without trapping air bubbles.
d) Ensure that the temperature of the sample is recorded, and report that the dielectric properties are applicable at that temperature only.
e) Ensure that measurement personnel are acquainted with the nature of the measurement and what to expect at each stage of the procedure.

f) Ensure that after calibration, a measurement is made on a reference liquid to validate the system prior to measuring the sample. Data for several recommended reference liquids are given in Clause J.6.

g) Ensure that data reduction methods for relating complex reflection coefficient and complex permittivity are accurate and appropriate for the sample-holder geometry being used.

J.3 Slotted line

A terminated slotted coaxial line with a moveable probe can be used as a sample holder [4]. A network analyser provides the RF signal at the input of the slotted line and enables the magnitude and phase of the signal transmitted into the sample to be determined as a function of position along the line by means of the moveable probe.

The test procedure should specify the network analyser calibration and settings for the required frequency range, the starting measurement position, step size along the slot, and total number of subsequent measurement positions. The application software should interpret the measured data to yield the dielectric properties of the sample. An example procedure is given in the next paragraph.

J.3.1 Equipment set-up

The test equipment consists of a slotted coaxial transmission line with a probe connected to a vector network analyser, as shown in Figure J.1. The log-magnitude and phase of S_{21} should be displayed simultaneously. Source power should be set to a level high enough to provide good signal-to-noise ratio. Periodically (annually or whenever the measuring scale along the line length is changed) a measurement is made on a reference liquid to validate the system. Since the measured quantities are magnitude and phase changes versus distance, the accuracy of the scale is very critical.

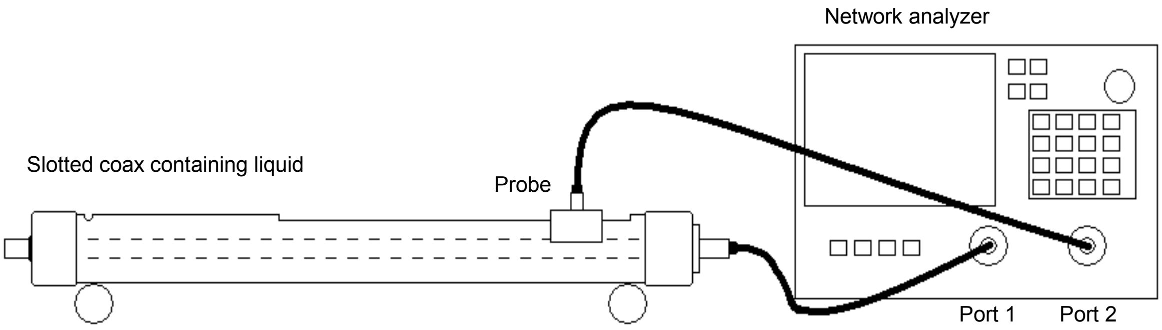

NOTE Although not shown, equipment for sample temperature monitoring is recommended.

Figure J.1 – Slotted line set-up

The network analyser injects a signal into one end of the slotted coaxial transmission line. The probe inserted through the slot into the tissue-equivalent liquid detects the RF amplitude and phase for each measurement position along the length of the line. A full two-port calibration of the network analyser should be carried out prior to connecting the sample holder, and the following precautions should be observed:

a) Fill the dried slotted line carefully to avoid trapping air bubbles. This operation should be performed while the slotted line is horizontal.

b) The probe should be inserted into the slot at the end nearest to the input connector of the slotted line, ensuring that the tissue-equivalent liquid is flush with the inside surface of the line, and aligned with a well-defined position on the distance scale of the slotted line.

c) The probe should be inserted perpendicular to the slotted–line longitudinal axis until a stable and adequate amplitude response is achieved. Do not insert the probe too deeply into the coaxial line, because it can overly perturb the field distribution.

J.3.2 Measurement procedure

a) Configure and calibrate the network analyser.

b) Measure 10 to 20 log-magnitude and phase data points along the slotted line corresponding to about a 30 dB change in magnitude.

c) Plot S_{21} log-magnitude and phase vs. measurement distance.

d) Determine if the graphed points closely follow a straight-line approximation, based on the correlation coefficient or a similar statistical measure. The data should produce a good linear curve fit (expected correlation coefficient $r^2 > 0{,}99$ for lossy materials). If not, re-measure the liquid by increasing the sample points to extend the magnitude change from 30 dB to 40 dB.

NOTE For low loss materials, ensure that the slotted line is long enough to avoid reflections from the load-terminated end.

e) Calculate the conductivity and relative permittivity of the tissue-equivalent liquid using the following equations derived from [56], [65].

$$\bar{\alpha} = \frac{m_\mathrm{m} \ln(10)}{20} \qquad \text{Np/cm}$$

$$\bar{\beta} = \frac{m_\mathrm{p} \pi}{180} \qquad \text{rad/cm}$$

$$\varepsilon'_\mathrm{r} = \frac{(\bar{\beta})^2 - (\bar{\alpha})^2}{\omega^2 \mu_0 \varepsilon_0}$$

$$\sigma = \frac{2\bar{\alpha}\bar{\beta}}{\omega\varepsilon_0}\left(\frac{100\ \text{cm}}{\text{m}}\right) \qquad \text{S/m}$$

where

m_m and m_p	are the slopes of the least-squares linear fits of the log-magnitude and phase plots, respectively;
$\bar{\alpha}$ and $\bar{\beta}$	are the average attenuation and propagation coefficients along the line.

J.4 Contact probe

Contact probes are open-ended coaxial transmission line sections, usually with an end flange serving as a ground plane for fringing fields. Measurements are made by placing the probe in contact with the sample and measuring the admittance or reflection coefficient with respect to the open-circuit end, using a network analyser or equivalent instrumentation [3], [16], [54]. Coaxial probes can also be used to test solid dielectrics, for example bulk samples of the materials used to construct the device holder or phantom. To minimize errors with contact probes, solid surfaces should be highly polished [1].

Test procedures should specify the network analyser calibration and settings for the required frequency range. The application software should interpret the measured data to yield the dielectric properties of the sample as a function of frequency. To use this technique, a probe and a software package for the network analyser has to be developed, or obtained from a commercial source. The methodology should specify the probe size and applicable frequency range. An example procedure is given in the following clauses.

J.4.1 Equipment set-up

The equipment consists of a probe connected to one port of a vector network analyser. The probe is an open-ended coaxial line, as shown in Figure J.2. Cylindrical coordinates (ρ, ϕ, z) are used where ρ is the radial distance from the axis, ϕ is the angular displacement around the axis, z is the displacement along the axis, a is the inner conductor radius, and b is the outer conductor inner radius.

The sample holder is a non-metallic container that is large compared with the size of the probe immersed in it. A probe with an outer diameter b of 2 mm to 4 mm is suitable for the measurement of tissue-equivalent liquids in the 300 MHz to 3 GHz frequency range. This probe size is commensurate with sample volumes of 50 cc or higher. Larger probes of up to 7 mm outer diameter b may be used with larger sample volumes. A flange is typically included to better represent the infinite ground-plane assumption used in admittance calculations.

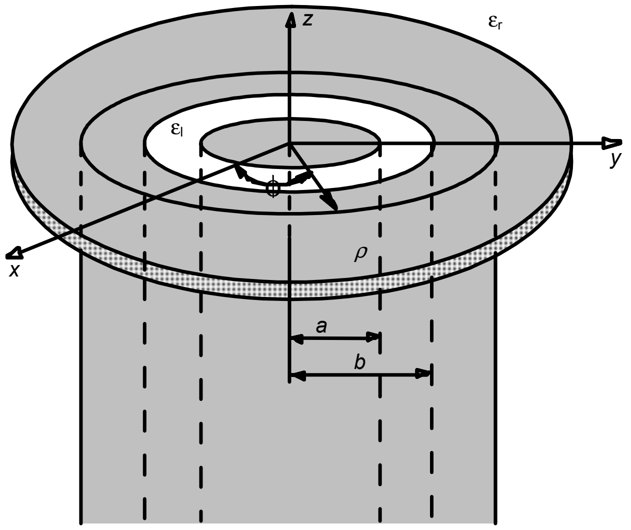

Key

a	is the inner conductor radius
z	is the displacement along the axis
b	is the outer conductor inner radius ε_r
ρ	is the radial distance from the axis
ϕ	is the angular displacement around the axis
(x, y, z)	are the Cartesian coordinates

Figure J.2 – An open-ended coaxial probe with inner and outer radii *a* and *b*, respectively

The accuracy of the short-circuit measurement should be verified for each calibration at a number of frequencies. A short circuit can be achieved by gently pressing a piece of aluminium foil against the open end. For best electrical contact, the probe end should be flat and free of oxidation [2]. Larger sensors generally have better foil short-circuit repeatability. It is possible to obtain good contact with some commercial 4,6 mm probes using the metal-disk short-circuit supplied with the kit. For best repeatability, it may be necessary to press the disk by hand.

Large measurement errors due to “flange resonances” can occur when the diameter of the flange is approximately equal to half a wavelength in the dielectric medium [6]. Such effects are most pronounced for high-permittivity liquids that have a loss tangent less than approximately 0,25 (at mobile phone frequencies these include water, methanol, and dimethyl sulfoxide). Therefore, calibration with a liquid having a high loss tangent, e.g., ethanol, is strongly recommended for larger sensors. There could be problems calibrating 7 mm flanged coaxial sensors with water at some frequencies. Tissue-equivalent liquids have a loss tangent of about 0,5, which is high enough to ensure that resonance effects are practically invisible no matter what size of sensor is used.

The network analyser is configured to measure the magnitude and phase of the admittance. A one-port reflection calibration is performed at the plane of the probe by placing liquids for which the reflection coefficient can be calculated in contact with the probe. Three standards are needed for the calibration, typically a short circuit, air, and de-ionised water at a well-defined temperature (other reference liquids such as methanol or ethanol may be used for calibration). The calibration is a key part of the measurement procedure, and it is therefore important to ensure that it has been performed correctly. It can be checked by re-measuring the short circuit to ensure that a reflection coefficient of $\Gamma = -1{,}0$ (linear units) is obtained consistently.

J.4.2 Measurement procedure

a) Configure and calibrate the network analyser and probe system.

b) Place the sample in a non-metallic container and immerse the probe. A fixture or clamp is recommended to stabilize the probe, mounted such that the probe face is at an angle with respect to the liquid surface to minimize trapped air bubbles beneath the flange.

c) Measure the complex admittance with respect to the probe aperture.

d) Compute the complex relative permittivity $\varepsilon_r = \varepsilon_r' - j\sigma/\omega\varepsilon_0$, for example from the equation [54]

$$Y = \frac{j2\omega\varepsilon'_r\,\varepsilon_0}{[\ln(b/a)]^2}\int_a^b\int_a^b\int_0^\pi \cos\phi'\,\frac{\exp\left[-j\omega(\mu_0\varepsilon'_r\,\varepsilon_0)^{1/2}r\right]}{r}\,d\phi' d\rho' d\rho$$

The last expression can be computed numerically, or expanded into a series and simplified [16], [40], [41], [42]. The equation is first solved for the sample wave number *k* then the sample complex permittivity, using Newton-Raphson or other iterative approximations. Other numerical approaches may be used, e.g., [43], [45], provided the applications software has been thoroughly tested and checked via measurements of reference liquids. Commercial open-ended coaxial probe kits typically use versions of this theory and method.

J.5 TEM transmission line

This method is based on the measurement of the complex transmission coefficient of a TEM-mode coaxial transmission line filled with the test liquid [60]. A transmission measurement carried out using a vector network analyser to determine the magnitude and phase of the scattering coefficient S_{21}, from which the complex permittivity is calculated. Test procedures should specify the network analyser settings and calibration for the required frequency range. The application software should interpret the measured data to yield the dielectric properties of the sample as a function of frequency.

J.5.1 Equipment set-up

The measurement set-up is shown in Figure J.3. The sample holder is an open-wall stripline consisting of a circular centre-conductor, two planar vertical (side) ground conductors, one optically transparent plastic bottom wall, top open, and a temperature sensor. The length *d* is chosen for a given frequency range so that the effect of multiple reflections inside the sensor is small, and the total attenuation does not exceed the dynamic range of the network analyser. For example, two sensors with different lengths can cover the frequency range of 800 MHz to 2 000 MHz. The sample is carefully syringed or poured into the holder, inspecting for air bubbles through the clear walls.

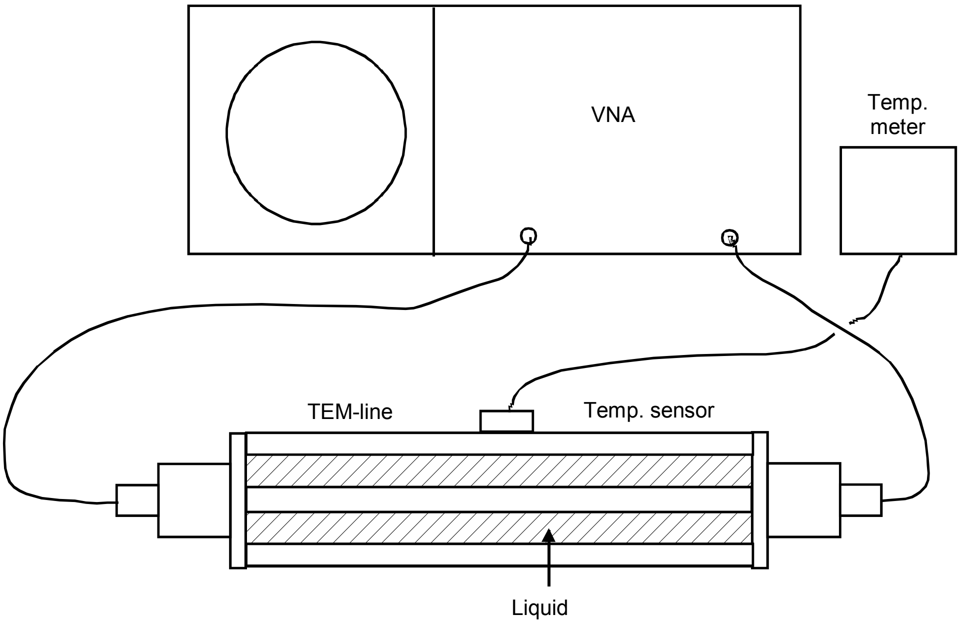

Figure J.3 – TEM line dielectric test set-up [60]

J.5.2 Measurement procedure

a) Configure and calibrate the network analyser.

b) Record the magnitude and phase of S_{21}^{0} of the empty cell at the desired frequencies.

c) Inject sample liquid into the cell, and repeat the measurement to obtain the transmission coefficient with the sample S_{21}^{S}.

d) Remove the liquid from the TEM line, thoroughly rinse the inside with water, and dry carefully.

e) Reconnect the coaxial line to the network analyser. Make sure that the magnitude and phase of S_{21}^{0} are unchanged (deviation less than 0,1 dB in magnitude and 0,5° in phase). This step is needed only if multiple samples are to be measured.

f) Calculate the complex permittivity of the liquid from the magnitude and phase of S_{21}^{S}/S_{21}^{0} by a numerical solution of the equations.

$$\frac{S_{21}^{S}}{S_{21}^{0}} = \frac{\left(1-\Gamma^2\right)\exp\left[-j(k-k_0)d\right]}{1-\Gamma^2\exp\left(-j2kd\right)},$$

$$\Gamma = \frac{1-\sqrt{\varepsilon_\mathrm{r}}}{1+\sqrt{\varepsilon_\mathrm{r}}},$$

$$k = \frac{2\pi f}{c_0}\sqrt{\varepsilon_\mathrm{r}},$$

$$k_0 = \text{free space propagation factor}$$

where

Γ	is the reflection coefficient at either end of the TEM line;
k	is the wave number in the liquid;
k_0	is the free-space wave number;
d	is the length of the sample holder (TEM line);
f	is the frequency;
c_0	is the free-space speed of light;

$\varepsilon_r = \varepsilon_r' - j\,\sigma/\omega\varepsilon_0$ is the complex relative permittivity of the sample.

J.6 Dielectric properties of reference liquids

The procedures in Clause J.2 recommend measurements of reference liquids that have well-established dielectric properties in order to validate the system. Two reference liquids are required, one for calibration, and one for checking the calibration. A general equation for calculating frequency-dependent dielectric properties is

$$\varepsilon_\mathrm{r} = \varepsilon_\infty + \frac{\varepsilon_\mathrm{s}-\varepsilon_\infty}{\left(1+(j\omega\tau)^{1-\alpha}\right)^{\beta}} + \frac{\sigma_i}{j\omega\varepsilon_0},$$

which corresponds to the Debye equation for $\alpha = 0$ and $\beta = 1$, to the Cole-Cole equation for $\beta = 1$ and $0 < \alpha < 1$, and to the Cole-Davidson relationship for $\alpha = 0$ and $0 < \beta < 1$ [20]. Here

ε_s	is the static or low frequency permittivity;
ε_∞	is the asymptotic high-frequency permittivity;
τ	is the relaxation time;
σ_i	is the ionic conductivity.

The parameters for calculating the properties of several reference liquids using this equation are given in Table J.1. These liquids are dimethyl sulfoxide, methanol, ethanediol, de-ionized water. The parameters α and σ_i are zero for all liquids listed in Table J.1. The model parameters were obtained using various test methods described in the literature. In general, results obtained with two-port closed-transmission-line cells are generally expected to be the most accurate, but results from all sources listed in the table agree relatively well. Table J.2 contains target 20 °C relative permittivity and conductivity values. If other reference liquids are used, target values and literature references should be provided in the test report.

It is a good practice to choose reference liquids with dielectric properties similar to tissue-equivalent liquids. Any reference liquid mixture recipes must be followed exactly, and dielectric properties must be measured at the specified temperatures. In order to avoid contamination and evaporation, mixtures should not be left exposed to air. Reference liquids must be high-purity grade, e.g., analytical grade or better. After opening, reagent bottles must be stored in accordance with the manufacturer's recommendation for the duration of the recommended shelf life.

NOTE All personnel should be familiar with and apply any special handling procedures according to the Material Safety Data Sheet (MSDS) for each particular liquid.

Table J.1 – Parameters for calculating the dielectric properties of various reference liquids

Reference Liquid	Temperature °C	Ref.	Model	ε_s	ε_∞	τ (ps)	β
DI water	20	[28]	Debye	80,21	5,6	9,36	1
DI water	25	[28]	Debye	78,36	5,2	8,27	1
DMS	20	[19]*	Debye	47,13	7,13	21,27	1
DMS	25	[19]*	Debye	46,48	6,63	19,18	1
DMS	25	[29]	Cole-Davidson	47,0	3,9	21,1	0,878
Ethanediol	20	[37]	Cole-Davidson	41,4	3,7	164	0,8
Methanol	20	[16]	Debye	33,7	4,8	53,8	0
Methanol	20	[19]*	Debye	33,64	5,68	56,6	0
Methanol	25	[19]*	Debye	32,67	5,58	50,8	0
*Data derived from measurements to 5 GHz only.							

Table J.2 – Dielectric properties of reference liquids at 20 °C

Frequency	Methanol [16]		DMS [19]		DI water [28]		Ethanediol [37]	
MHz	ε_r'	σ	ε_r'	σ	ε_r'	σ	ε_r'	σ
300	33,33	0,05	47,07	0,03	80,19	0,02	39,01	0,14
450	32,94	0,11	46,99	0,06	80,16	0,05	34,49	0,30
835	31,37	0,35	46,64	0,20	80,03	0,17	29,15	0,75
900	31,04	0,41	46,56	0,24	80,00	0,20	28,00	0,83
1 450	27,77	0,92	45,68	0,60	79,67	0,51	20,38	1,34
1 800	25,51	1,27	44,94	0,91	79,38	0,78	17,23	1,58
1 900	24,88	1,37	44,71	1,01	79,29	0,87	16,51	1,63
2 000	24,25	1,47	44,46	1,11	79,19	0,96	15,85	1,69
2 450	21,57	1,89	43,25	1,61	78,69	1,44	13,49	1,89
3 000	18,76	2,33	41,59	2,31	77,96	2,13	11,56	2,07

J.7 Estimation of liquid dielectric parameter measurement uncertainties

The measurement procedures described in this annex use vector network analysers for dielectric property measurements. Network analysers require calibration in order to account for and remove inherent losses and reflections. The uncertainty budget for dielectric measurement derives from inaccuracies in the calibration data, analyser drift, and random errors. Other sources of errors are the tolerances on the sample holder hardware, and deviations from the optimal dimensions for the specified frequencies, and sample properties. This applies regardless of the type of sample holder and the nature of the scattering parameters being measured. Uncertainties due to the straight-line fit in the slotted-line method can be evaluated using a least-squares analysis [59].

An example uncertainty template is shown in Table J.3. All influence quantities may or may not apply to a specific test set-up or procedure, and other components not listed may be relevant in some test set-ups. Table J.3 also includes example numeric values. Depending on the test set-up, actual uncertainty estimates may and should differ from the values shown here. Measurement of well-characterized reference liquids can be used to estimate the dielectric property measurement uncertainty [10], [26], [39], [47], as described in the following procedure.

a) Configure and calibrate the network analyser in a frequency span large enough around the centre frequency of interest, for example 835 MHz ± 100 MHz at 5 or more frequencies within the device transmission band.

b) Measure a reference material at least *n* times to obtain the average and standard deviation for the relative permittivity and conductivity at each device centre-band and nearby frequencies.

c) For each of the test runs from b), to verify calibration validity versus frequency, calculate the differences between the measured and corresponding reference data (see J.6 Table J.1) at 5 or more frequencies within the device transmission band using the equations

$$\varepsilon'_{\text{r tolerance}}\ [\%] = 100 \times \left| \frac{\varepsilon'_{\text{r measured}} - \varepsilon'_{\text{r ref}}}{\varepsilon'_{\text{r ref}}} \right|$$

$$\sigma_{\text{tolerance}}\ [\%] = 100 \times \left| \frac{\sigma_{\text{measured}} - \sigma_{\text{ref}}}{\sigma_{\text{ref}}} \right|$$

d) If predetermined standard deviations (see 7.1.2) for permittivity and conductivity are available, calculate the standard deviation of the mean ($s/\sqrt{n}$), e.g., [61], using the maximum value versus frequency for the n separate permittivity and conductivity tolerances of c); alternatively use the standard deviation of the present test series in column *a* of Table J.3.

e) Estimate the Type B uncertainties for the other components of Table E.3 (and other relevant components if needed) in the frequency range under consideration.

f) The individual combined standard uncertainties for ε_r' and σ each are entered into the tolerance column and the liquid test rows of Table 3. Insert a completed version of Table J.3 into the test report, along with rationale for which influence quantities were used or omitted.

g) Measure a second reference material to verify relative calibration validity, and ascertain that the measured data agrees with the reference values (see J.6) as in step c). If equipment drift is suspected, go back to the reference liquid tests of step b).

Table J.3 – Example uncertainty template and example numerical values for dielectric constant (ε_r') and conductivity (σ) measurement

	a		***b***	***c***	$u_i = (a/b) \times (c)$	
Uncertainty component	**Tolerance/ Uncertainty value (± %)**	**Probability distribution**	**Divisor**	c_i	**Standard uncertainty (± %)**	v_i **or** v_{eff}
Repeatability (*n* repeats, mid-band)		N	1	1		*n*-1
Reference liquid ε_r' or σ		R	√3	1		∞
Network analyser-drift, linearity, etc.		R	√3	1		∞
Test-port cable variations		U	√2	1		∞
Combined standard uncertainty						

NOTE Column headings *a*, *b*, *c* are given for reference. Separate tables are usually needed for each ε_r' and σ.

Bibliography

[1] ARAI, M.J., BINNER, G.P., and CROSS, T.E. Estimating errors due to sample surface roughness in microwave complex permittivity measurements obtained using a coaxial probe. *Electron. Lett.*, Jan. 19, 1995, vol. 32, no. 2, pp. 115-117.

[2] BAO, J.Z., SWICORD, M.L., and DAVIS, C.C. Microwave dielectric characterization of binary mixtures of water, methanol, and ethanol*. J. Chem. Phys.*, Mar. 12, 1996, vol. 104, no. 12, pp. 4441-4450.

[3] BLACKHAM, D.V. and POLLARD, R.D. An improved technique for permittivity measurements using a coaxial probe. *IEEE Trans. Instrumen. Meas.*, Oct. 1997, vol. 46, no. 5, pp. 1093-1099.

[4] CHOU, C.K., CHEN, G.W., GUY, A.W. and LUK, K.H., Formulas for preparing phantom muscle tissue at various radiofrequencies. *Bioelectromag.*, 1984, vol.5, pp. 435-441.

[5] CHRIST, A., CHAVANNES, N., POKOVIC, K, GERBER, H.U. and KUSTER, N. Numerical and Experimental Comparison of Human Head Models for SAR Assessment. *Proceedings of Millennium Workshop on Biological Effects of Electromagnetic Fields*, Heraklion, Kreta, Greece, Oct. 2000, pp. 234-240.

[6] CLARKE, R.N., GREGORY, A.P., HODGETTS, T.E., and SYMM, G.T. Improvements in coaxial sensor dielectric measurement: relevance to aqueous dielectrics and biological tissue. in *Microwave Aquametry: Electromagnetic Wave Interaction With Water-containing Materials*, A. Kraszewski, ed., New York: IEEE Press, 1996, pp. 279-297.

[7] DIECK, R.H. *Measurement Uncertainty: Methods and Applications*. North Carolina, Research Triangle Park: Instrument Society of America, 1992.

[8] DROSSOS, A., SANTOMAA, V. and KUSTER, N. The dependence of electromagnetic energy absorption upon human head tissue composition in the frequency range of 300-3000 MHz. *IEEE Trans. Microwave Theory Tech.*, Nov. 2000, vol. 48, no. 11, pp. 1988-1995.

[9] EA-2/07 (rev.01) *EAL Strategy to Achieve Comparability of Results in Calibration and Testing*, Mar. 1997.

[10] EVANS, S. and MICHELSON, S.C. Intercomparison of dielectric reference materials available for the calibration of an open-ended probe at different temperatures*. Meas. Sci. Tech.*, Dec. 1995, vol. 6, no. 12, pp. 1721-1732.

[11] FARAONE, A., McCOY, D. O., CHOU, C. K., and BALZANO, Q. Characterization of miniaturized E-field probes for SAR measurements. *IEEE Intl. Symp. Electromag. Compat.*, Washington, DC, 2000, pp. 749-754.

[12] FERREIRA P.J.S.G. Non-iterative and fast iterative methods for interpolation and extrapolation. *IEEE Trans. Sig. Proc.*, Nov 1994, vol. 41, pp. 3278-3282.

[13] FIEGUTH, P.W., KARL, W.C., WILLSKY, A.S. and WUNSCH, C. Multi-resolution optimal interpolation and statistical analysis of TOPEX/POSEIDON satellite altimetry. *IEEE Trans. Geosci. Remote Sens.*, Mar. 1995, vol. 33, pp. 280-292.

[14] FORD, C and ETTER, D.M. Wavelet basis reconstruction of non uniform sampled data. *IEEE Trans. Circuits Sys. II: Analog Dig. Sig. Proc.*, Aug. 1998, vol. 45, no. 8, pp. 1165-1168.

[15] FUKUNAGA, K., WATANABE, S., WAKE, K., and YAMANAKA, Y. Time dependence of tissue-equivalent dielectric liquid materials and its effect on SAR. *EMC Europe Symp.*, Sorrento, Italy, Sep. 2002.

[16] GABRIEL, C., CHAN, T.Y.A., and GRANT, E.H. Admittance models for open ended coaxial probes and their place in dielectric spectroscopy. *Phys. Med. Biol.*, 1994. vol. 39, no.12, pp. 2183-2200.

[17] GABRIEL, S., LAU, R.W. and GABRIEL, C. The dielectric properties of biological tissues: 3. Parametric models for the dielectric spectrum of tissues. *Phys. Med. Bio.*, 1996, vol. 41, no. 11, pp. 2271-2293.

[18] GORDON, C.C., CHURCHILL, T., CLAUSER, C.E., BRADTMILLER, B., McCONVILLE, J.T., TEBBETTS I. and WALKER, R.A., 1988 *Anthropometric Survey of U.S. Army Personnel: Methods and Summary Statistics*. Technical Report NATICK/TR-89/044, U.S. Army Natick Research, Development and Engineering Center, Massachusetts: Natick, Sep. 1989.

[19] GREGORY, A.P. and CLARKE, R.N. *Tables of the Complex Permittivity of Dielectric Reference Liquids at Frequencies up to 5 GHz*. NPL Report CETM 33, Centre for Electromagnetic and Time Metrology. Teddington, England: National Physical Laboratory, 2001.

[20] HILL, N.E., VAUGHAN, W.E., PRICE, A.H., and DAVIES, M. *Dielectric Properties and Molecular Behaviour*. London: Van Nostrand Reinhold, 1969.

[21] IEC 60050, *International Electrotechnical Vocabulary*

[22] IEEE Std 1528, *Recommended Practice for Determining the Peak Spatial-Average Specific Absorption Rate (SAR) in the Human Head from Wireless Communications Devices*: *Measurement Techniques*, New York: Institute Electrical and Electronics Engineers, Dec. 2003.

[23] ISO/IEC DIR-2 (2001-7), *IEC Directives – Part 2: Rules for the structure and drafting of International Standards*. Geneva: International Electrotechnical Commission.

[24] ISO/IEC Guide 43-1:1997, *Proficiency testing by interlaboratory comparisons–Part 1: Development and operation of proficiency testing schemes*. Geneva: International Organization for Standardization.

[25] ISO/IEC *Guide to the Expression of Uncertainty in Measurement*. Geneva: International Organization for Standardization, 1995.

[26] JENKINS, S., HODGETTS, T.E., CLARKE, R.N., and PREECE, A.W. Dielectric measurements on reference liquids using automatic network analysers and calculable geometries. *Meas. Sci. Tech.*, July 1990, vol. 1, no. 7, pp. 691-702.

[27] JOKELA, K., HYYSALO, P. and PURANEN, L. Calibration of specific absorption rate (SAR) probes in waveguide at 900 MHz. *IEEE Trans. Instrumen. Meas.*, Apr. 1998, vol. 47, no. 2, pp. 432-438.

[28] KAATZE, U. Complex permittivity of water as function of frequency and temperature. *J. Chem. Engin. Data*, 1989, vol. 34, no. 4, pp. 371–374.

[29] KAATZE, U., POTTEL R., and SCHAFER M. Dielectric spectrum of dimethyl sulfoxide/water mixtures as a function of composition. *J. Phys. Chem.*, 1989, vol. 93, pp. 5623-5627.

[30] KANDA, M.Y., BALLEN, M., CHOU, C.K. Formulation and characterization of tissue simulating liquids used for SAR measurement (500-2000 MHz)*. Asia-Pacific Radio Science Conference*, Tokyo, Japan, Aug. 1-4, 2001, pp. 274.

[31] KUSTER N., KÄSTLE, R., and SCHMID, T. Dosimetric evaluation of mobile communications equipment with known precision (invited paper). *IEICE Trans. Commun.*, May 1997, vol. E80-B, no. 5, pp. 645-652.

[32] KUSTER, N., BALZANO, Q. and LIN, J.C., Eds. *Mobile Communications Safety.* London: Chapman & Hall, 1997.

[33] LANCASTER, P. and SALKAUSKA, K. *Curve and Surface Fitting: An Introduction*. New York: Academic Press, 1986.

[34] LEE, A.K., and PACK, J.K. Effect of head size for cellular telephone exposure on EM absorption. *IEICE Trans. Commun*., Mar. 2002, vol. E85-B, no. 3, pp. 698-701.

[35] LEE, A.K., CHOI, H.D., LEE, H.S., and PACK, J.K. Human head size and SAR characteristics for handset exposure. *ETRI J.*, Apr. 2002, vol. 24, no. 2, pp. 176-179.

[36] LEISTEN, O., VARDAXAGLOU, Y., SCHMID, T., ROSENBERGER, B., AGBORAW, E., KUSTER, N., and NICOLAIDIS, G. Miniature dielectric-loaded personal telephone antennas with low user exposure. *Electron. Lett.*, Aug. 20, 1998, vol. 34, no. 17, pp. 1628-1629.

[37] LEVIN, V.V. and PODLOVCHENKO, T.L. Dispersion of the dielectric permittivity of ethylene glycol. *Zhurnal Strukturnoi Khimii*, 1970, vol. 11, pp. 766-767.

[38] MEIER, K., BURKHARDT, M., SCHMID, T. and KUSTER, N. Broadband calibration of E-field probes in lossy media. *IEEE Trans. Microwave Theory Tech.*, Oct. 1996, vol. 44, no. 10, pp. 1954-1962.

[39] MIGLIORE, M.D. Partial self-calibration method for permittivity measurement using truncated coaxial cable. *Electron. Lett.*, July 20, 2000, vol. 36, no. 15, pp. 1275-1277.

[40] MISRA, D. A quasi-static analysis of open-ended coaxial lines. *IEEE Trans. Microwave Theory Tech.*, Oct. 1987, vol. 35, no. 10, pp. 925-928.

[41] MISRA, D., CHABBRA, M., EPSTEIN, B.R., MIROTZNIK, M., and FOSTER, K.R. Noninvasive electrical characterization of materials at microwave frequencies using an open-ended coaxial line: test of an improved calibration technique. *IEEE Trans. Microwave Theory Tech.*, Jan. 1990, vol. 38, no. 1, pp. 8-14.

[42] MISRA, D. On the measurement of the complex permittivity of materials by an open-ended coaxial probe. *IEEE Microwave Guided Wave Lett.*, May 1995, vol. 5, no. 5, pp. 161-163.

[43] MOSIG, J.R, BESSON, J.C.E, GEX-FABRY, M. and GARDIOL, F.E. Reflection of an open-ended coaxial line and application to non-destructive measurement of materials. *IEEE Trans. Instrumen. Meas.*, 1981, IM-30, pp 46-51.

[44] NAHMAN, N.S., KANDA, M., LARSEN, E.B. and CRAWFORD, M.L. Methodology for standard electromagnetic field measurements. *IEEE Trans. Instrumen. Meas.*, Dec. 1985, vol. IM-34, no. 4, pp. 490-503.

[45] NEVELS, R.D., BUTLER, C.M. and YABLON, W. The annular slot antenna in a lossy biological medium. *IEEE Trans. Microwave Theory Tech.*, 1985, MTT-30, pp 314-319.

[46] NIST TN1297, *Guidelines for Evaluating and Expressing the Uncertainty of NIST Measurement Results*. Gaithersburg, MD: National Institute of Standards and Technology, 1994.

[47] NYSHADHAM, A., SIBBALD, C.L., and STUCHLY, S.S. Permittivity measurements using open-ended sensors and reference liquid calibration – an uncertainty analysis. *IEEE Trans. Microwave Theory Tech.*, Feb. 1992, vol. 40, no. 2, pp. 305-314.

[48] PERSON C., AHLONSOU, L.N. and GRANGEAT, C. New test bench for the characterization of SAR measurement probes used in tissue equivalent liquids, *Bioelectromagnetics Society 22nd Annual Meeting*, Munich Germany, June 11-16, 2000.

[49] PERSON, C., TANNÉ, G., AHLONSOU, L.N., NGOUNOU, C. and GRANGEAT C. New reference antennas for SAR probe calibration in tissue equivalent liquid. *Millennium Conference on Antennas and Propagation, AP2000*, Davos, Switzerland: April 9-14, 2000.

[50] PEYMAN, A. and GABRIEL, C. Tissue equivalent liquids for SAR measurement at microwave frequencies. *Bioelectromagnetics Society 24th Annual Meeting*, Quebec, Canada, June 2002, poster P-53.

[51] POKOVIC, K. *Advanced Electromagnetic Probes for Near Field Evaluation*. Doc. Tech. Sci. Diss. ETH Nr. 13334. Switzerland, Zurich: Swiss Federal Institute of Technology, 1999.

[52] POKOVIC, K., SCHMID, T. and KUSTER, N. Robust setup for precise calibration of E-field probes in tissue simulating liquids at mobile communication frequencies. In *Proceedings ICECOM'97*. Dubrovnik, Croatia, Oct. 12-17, 1997, pp. 120-124.

[53] POKOVIC, K., SCHMID, T., CHRIST, A. and KUSTER, N. Design and characterization of E-field probes for lossy media. Submitted to *IEEE Trans. Microwave Theory Tech.*, 1999.

[54] POURNAROPOULOS, C.L. and MISRA, D.K. The co-axial aperture electromagnetic sensor and its application in material characterization. *Meas. Sci. Tech.*, 1997, vol. 8, pp. 1191-1202.

[55] PRESS, W.H., FLANNERY, B.P., TEUKOLSKY, S.A. and VETTERLING, W.T. *Numerical Recipes in FORTRAN 77: The Art of Scientific Computing*. New York: Cambridge University Press, 1992.

[56] RAMO, S., WHINNERY, J.R. and VAN DUZER, T. *Fields and Waves in Communication Electronics*. New York, Wiley, 1993.

[57] SCHMID, T., EGGER O. and KUSTER, N. Automated E-field scanning system for dosimetric assessments. *IEEE Trans. Microwave Theory Tech.*, Jan. 1996, vol. 44, no. 1, pp. 105-113.

[58] SCHÖNBORN, F., BURKHARDT, M. and KUSTER, N. The difference of EM energy absorption between adults and children. *Health Phys.*, Feb. 1998, vol. 74, no. 2, pp. 160-168.

[59] TAYLOR, J.R. *An Introduction to Error Analysis: The Study of Uncertainties In Physical Measurements*. 2nd ed. Sausalito, CA: University Science Books, 1997.

[60] TOROPAINEN, A., VAINIKAINEN, P., and DROSSOS, A. Method for accurate measurement of complex permittivity of tissue equivalent liquids. *Electron. Lett.*, 2000, vol. 36, no. 1, pp. 32-34.

[61] UKAS LAB34, *The Expression of Uncertainty in EMC Testing*. Feltham, Middlesex, England: United Kingdom Accreditation Service, 2002.

[62] UKAS M3003, *The Expression of Uncertainty and Confidence in Measurement.* Feltham, Middlesex, England: United Kingdom Accreditation Service, 1997.

[63] USTUNER, K.F. and FERRAI, L.A. Discrete splines and spline filters. *IEEE Trans. Circuits Sys.*, July 1991, vol. 39, no. 7, pp 417-422.

[64] VIGNERAS, V. *Elaboration and characterization of biological tissues equivalent liquids in the frequency range 0.9-3 GHz, final report*. France: PIOM Laboratory, University of Bordeaux, Nov. 2001.

[65] VON HIPPEL, A. *Dielectric Materials and Applications*. Cambridge: MA: MIT Press, 1954.

Bureau of Indian Standards

BIS is a statutory institution established under the *Bureau of Indian Standards Act*, 1986 to promote harmonious development of the activities of standardization, marking and quality certification of goods and attending to connected matters in the country.

Copyright

BIS has the copyright of all its publications. No part of these publications may be reproduced in any form without the prior permission in writing of BIS. This does not preclude the free use, in course of implementing the standard, of necessary details, such as symbols and sizes, type or grade designations. Enquiries relating to copyright be addressed to the Director (Publications), BIS.

Review of Indian Standards

Amendments are issued to standards as the need arises on the basis of comments. Standards are also reviewed periodically; a standard along with amendments is reaffirmed when such review indicates that no changes are needed; if the review indicates that changes are needed, it is taken up for revision. Users of Indian Standards should ascertain that they are in possession of the latest amendments or edition by referring to the latest issue of 'BIS Catalogue' and 'Standards: Monthly Additions'.

This Indian Standard has been developed from Doc No.: LITD 9 (3066).

Amendments Issued Since Publication

Amendment No.	Date of Issue	Text Affected

BUREAU OF INDIAN STANDARDS

Headquarters:

Manak Bhavan, 9 Bahadur Shah Zafar Marg, New Delhi 110002
Telephones: 2323 0131, 2323 3375, 2323 9402 *Website*: www.bis.org.in

Regional Offices: *Telephones*

Central : Manak Bhavan, 9 Bahadur Shah Zafar Marg
NEW DELHI 110002 — 2323 7617, 2323 3841

Eastern : 1/14, C.I.T. Scheme VII M, V.I.P. Road, Kankurgachi
KOLKATA 700054 — 2337 8499, 2337 8561, 2337 8626, 2337 9120

Northern : SCO 335-336, Sector 34-A, CHANDIGARH 160022 — 260 3843, 260 9285

Southern : C.I.T. Campus, IV Cross Road, CHENNAI 600113 — 2254 1216, 2254 1442, 2254 2519, 2254 2315

Western : Manakalaya, E9 MIDC, Marol, Andheri (East)
MUMBAI 400093 — 2832 9295, 2832 7858, 2832 7891, 2832 7892

Branches: AHMEDABAD. BANGALORE. BHOPAL. BHUBANESHWAR. COIMBATORE. DEHRADUN. FARIDABAD. GHAZIABAD. GUWAHATI. HYDERABAD. JAIPUR. KANPUR. LUCKNOW. NAGPUR. PARWANOO. PATNA. PUNE. RAJKOT. THIRUVANATHAPURAM. VISAKHAPATNAM.

Published by BIS, New Delhi